Title
Degradation of mRNAs in budding yeast by novel decay pathways involving the REX exonucleases

Author
Hodko, Domagoj

Publication Date
2015

Peer reviewed|Thesis/dissertation

UNIVERSITY OF CALIFORNIA

Los Angeles

Degradation of mRNAs in budding yeast by novel decay pathways involving the REX exonucleases

A dissertation submitted in the partial satisfaction of the

requirements for the Degree Doctor of Philosophy

in Biochemistry and Molecular Biology

by

Domagoj Hodko

2015

ABSTRACT OF THE DISSERTATION

Degradation of mRNAs in budding yeast by novel decay pathways involving the REX exonucleases

By

Domagoj Hodko

Doctor of Philosophy in Biochemistry and Molecular Biology

University of California, Los Angeles, 2015

Professor Guillaume Chanfreau, Chair

We searched through gene expression databases for long 3' UTR mRNAs that are targeted for degradation by the cytoplasmic mRNA degradation pathway, nonsense-mediated mRNA decay (NMD) (Sayani et al., 2008). This pathway, known for degrading mRNAs containing premature translation termination codons, also targets mRNAs with long 3'UTRs. We focused on the *RTR1* locus which produces mRNAs with two prominent 3'UTR isoforms; the longer of which is targeted by the NMD system. We found from an RNA-seq data set that the *RTR1* locus also produces a long non-coding RNA, known as a XUT, which is overlapping and antisense to the 3'UTR (van Dijk et al., 2011). We hypothesized that the XUT may form double-stranded RNA segments with the target mRNA 3'UTR and thus may stabilize the target mRNA. Our pursuit of this hypothesis was spurred by the result that early termination

of the 3'UTR antisense XUT, which eliminates overlap between the *RTR1* 3'UTR and the antisense XUT, decreased the overall *RTR1* mRNA steady-state abundance. We pursued a model for the regulation of target mRNAs by 3'UTR antisense XUTs whereby the XUT may compete with an RNA binding protein (RBP) that binds the 3'UTR and facilitates degradation of the mRNA. Ultimately, we invalidated this model by showing that the early termination of the antisense XUT does not result in a change in the half-life of *RTR1* mRNAs compared to the wildtype strain upon transcription shut-off, and thus, the mutation must affect the mRNA abundance through changing the rate of transcription. In testing this model, however, we found an RBP site in the 3'UTR of *RTR1* revealed by previously published genome-wide PAR-CLIP analysis of all RBP sites in the yeast genome (Freeberg et al., 2013). Deletion of this 3'UTR cis element led to an overall increase in abundance and stability of the *RTR1* mRNAs. While deletion of known and well-characterized RBPs did not show an increase in *RTR1* mRNA abundance, deletion of the *RTR1* gene resulted in an increase in the abundance of an mRNA containing the *RTR1* 3'UTR that was also epistatic to the deletion of the cis element. This result led to the undertaking of a new study into the role of Rtr1p in mRNA decay that culminated in the manuscript presented in the second chapter of this dissertation. A key finding in this work was that mRNAs containing the Rtr1p cis element are targeted to a novel degradation pathway involving the 5'-3' RNA helicase, Dhh1p, and REX exonucleases. Because degradation of mRNAs constitutes a previously unrecognized role for the REX exonucleases, we followed up on this study by analyzing the impact of deleting the REX exonucleases on the transcriptome by RNA-seq. We present this RNA-seq analysis in Chapter 3 and further explore other cellular functions and mechanisms of Rex2p and Rex3p by performing affinity purification and mass-spectrometry sequencing of the interacting proteins. Our results show that Rex2p and Rex3p interact with the histone acetylase complex, SAGA, and this interaction may be important in the regulation of ribosomal protein genes

(RPGs). Our transcriptome analysis of the REX mutants also reveals a possible role in the quality control of splicing. Overall, this work defines new substrates for the REX exonucleases and establishes a new function for this family of exonucleases in the regulation and quality control of gene expression via mRNA degradation.

The dissertation of Domagoj Hodko is approved

Albert J. Courey

Feng Guo

Guillaume F. Chanfreau, Committee Chair

University of California, Los Angeles

2015

TABLE OF CONTENTS **PAGE**

LIST OF FIGURES **PAGE**

ACKNOWLEDGEMENTS

Professional

All experiments were designed by Guillaume Chanfreau and myself. Experiments were executed by me with the exception of GAL transcription shut-off assays in chapter 2 which were done with assistance from Taylor Ward. I also thank Willliam Munroe who advised and aided me in performing the sucrose gradient fractionations found in chapter 1 and chapter 3 and for performing the fractionation step in this protocol. Guillaume Chanfreau and I wrote the article manuscript presented in chapter 2. Ajay Vashisht from the Wohlschlegel lab performed the mass spectrometry sequencing of the Rex2-TAP and Rex3-TAP purifications. Next Generation RNA Sequencing carried out on the Illumina HiSeq2500 was done by Macrogen, Inc. and is presented in chapter 3.

Personal

First of all, I would like to profoundly thank my mentor, Guillaume Chanfreau, for all his advice and input on my projects throughout all these years. His ongoing guidance and inspiration kept me engaged and focused on finding new and interesting phenomena in RNA biology through the thick and the thin of it. I also would like to thank Marta Rivas who was our lab helper for the past few years and whose assistance in making media, buffers, plates, and washing and autoclaving glassware is invaluable to the lab. I also owe a debt of gratitude to all my lab mates (current and past) who answered so many of my questions and trained me in various protocols, particularly, Cynthia Lee, Camille Nery, and Tadashi Kawashima. I thank Shakir Sayani who trained me during my rotation and has been an amazing friend ever since. And finally, I thank my family and friends for all the love and support over the years.

VITA

2008 B.A., Biochemistry, University of San Diego

CHAPTER 1—Potential gene regulatory mechanisms by 3'UTR antisense long noncoding RNAs

INTRODUCTION

Noncoding RNAs (ncRNAs) have raised attention in biomedical research due to recent findings that they regulate genes relevant to cancer and diseases like Alzheimer's (He et al., 2004; Matick 2004; Volinia et al., 2006; Ghildiya and Zamore 2009; Wilusz et al., 2009; Kaikkonen et al., 2011; Benhamed et al., 2012; Guttman and Rinn 2012; Bao et al., 2013). Transcriptome analyses have revealed that mammalian genomes transcribe more lncRNAs than protein-coding mRNAs (Kaikkonen et al., 2011). Since the early 2000's, studies have revealed roles for these RNAs in regulating protein-coding transcripts (mRNAs) via chromatin modifications and post-transcriptional gene regulation (Pelechano and Steinmetz, 2013). While mechanisms of transcriptional gene silencing (or TGS) have been identified that implicate the roles of ncRNAs, mechanisms of posttranscriptional gene regulation have mainly focused on genes targeted by small ncRNAs (sncRNAs) like microRNAs or siRNAs. In the model eukaryote budding yeast, lncRNAs regulate transcription through various mechanisms (van Dijk et al., 2011; Toesca et al., 2011; Kim et al., 2012), but examples of posttranscriptional gene regulation by lncRNAs are few in number. One such example is the case of an antisense lncRNA found in human cells, which is transcribed from within the open reading frame of the *BACE1* gene and upregulates the downstream protein expression. This case highlights the importance of lncRNAs in gene regulation and demonstrates that *BACE1*, which forms amyloid fibers in Alzheimer's disease, is upregulated in Alzheimer's patients in correlation with the *BACE1* antisense lncRNA (Faghihi et al., 2008). This example provides a paradigm of how antisense lncRNAs may inhibit the degradation of target mRNAs. Further research led to the discovery that the *BACE1* antisense lncRNA actually competes with microRNA for binding to the *BACE1* mRNA and thus inhibits microRNA-mediated repression of the *BACE1* transcript (Faghihi et al., 2010).

Utilizing *S. cerevisiae* as a model organism, our work excludes the possibility of any RNAi based regulatory mechanisms since the budding yeast have lost the factors necessary for RNAi function (Drinnenberg et al., 2009). Any posttranscriptional decay mechanisms occurring in budding yeast take place through ordinary routes of decay involving either endonucleases or exonucleases. The major example of mRNA decay in budding yeast initiated by endonucleolytic cleavage is the Rnt1-mediated decay pathway which targets a variety of mRNAs genome-wide that have a sequence specific tetraloop (Zer and Chanfreau, 2005; Lee et al., 2005; Roy and Chanfreau 2014; Gagnon et al., 2015). The main exonucleases recognized to degrade bulk mRNA and mRNAs targeted for decay by specific degradation pathways are the nuclear exosome, the cytoplasmic exosome, the nuclear 5' to 3' exonuclease, Rat1p, and the cytoplasmic 5'-3' exonuclease, Xrn1p (Reviewed in Parker 2012). Xrn1p has been recognized as the cell's workhorse for degrading the bulk of cytoplasmic mRNA in both general and specific degradation pathways (Long and McNally 2003; van Dijk et al. 2011). 5' capped and 3' polyadenylated mRNAs typically undergo deadenylation-dependent decapping prior to processive 5'-3' degradation by Xrn1p. Another 5'-3' degradation factor, Dxo1p, performs a quality control function for aberrantly 5' capped mRNAs (Chang et al., 2012). This enzyme is unique in that it executes both the decapping function and distributive 5'-3' exoribonuclease activity, though its targets are thought to be limited to aberrant mRNAs (Chang et al., 2012). The exosome, on the other hand, is thought to be a major player in degrading bulk mRNAs as well as mRNAs targeted by quality control pathways like No-Go Decay or Non Stop Decay (Doma and Parker, 2006; Tsuboi et al., 2012). While the extent of degradation of bulk mRNA by the exosome is not clear, a deletion of the cytoplasmic exosome component, *SKI2*, in an *xrn1Δ*background is synthetic lethal, suggesting that the exosome may fulfill the function of Xrn1p in degrading cytoplasmic mRNAs in its absence (Johnson and Kolodner 1995). The alternate pathway for degradation

involves deadenylation and 3'-5' degradation by the exosome. In addition to the exosome, the RNA Exonuclease factors, or REXs, have homology to the RNase D type exonucleases from E. coli (van Hoof et al. 2000). The Rex proteins, like the exosome, are known to be involved in the 3'-end processing of ncRNAs like snRNAs, the 5S and 5.8S rRNAs, and the RNA component of RNase MRP, but have not been shown to be involved in the degradation of mRNAs (van Hoof et al. 2000).

One well-characterized mRNA surveillance pathway that also regulates gene expression is the nonsense mediated mRNA decay (NMD). The NMD system in yeast operates to degrade mRNAs by sensing the length of the distance between the stop codon and the poly (A) tail during the pioneer round of translation (Muhlrad and Parker 1999; Amrani et al. 2004; Hogg et al. 2010; for a review see Shoemaker and Green 2012). In higher eukaryotes that have an exon junction complex (EJC), another mechanism predominates that is dependent on the position of the stop codon relative to the EJC (Brogna and Wen, 2009). mRNAs targeted by the NMD system may originate from mutations that introduce premature translation termination codons (PTCs), unspliced mRNAs that contain PTCs within the introns, long 5'UTR mRNAs with uORFs, mRNAs containing programmed ribosomal frameshifts, mRNAs with naturally long 3'UTRs, or alternative polyadenylation sites in which the alternate 3'end processing site results in a long 3'UTR (Guan et al., 2006). NMD is initiated upon the binding of Upf1p to Sup35p at a stop codon recognized as "aberrant" (Czaplinski et al. 1998). The assembly of the other UPF factors, Upf2p and Upf3p, proceeds resulting in the rapid degradation of the transcript usually through deadenylation-dependant decapping followed by 5'-3' degradation by Xrn1p. As Upf1 is an ATPase-dependent DEAD-Box RNA helicase, NMD itself takes place independently of Dhh1p (Coller et al. 2002). While physiological targets of the NMD system are thought to be primarily degraded by Xrn1p, some evidence utilizing constructs demonstrates that NMD-targeted mRNAs may

also be degraded by the cytoplasmic exosome in a capping-independent manner (Mitchell and Tollervey 2003).

Previous work from our group has revealed the importance of the NMD system in the degradation of unspliced or mispliced mRNAs genome-wide (Sayani et al., 2008; Kawashima et al., 2009; Kawashima et al. 2014). Since the NMD system is known to target mRNAs with long 3'UTRs, we used our NMD mutant tilling arrays and RNA-seq data sets to determine whether NMD also plays a role in degrading alternatively 3'end-processed mRNAs. Our analysis revealed numerous examples of long 3'UTR mRNAs targeted by the NMD pathway. We focused on the *RTR1* mRNA since two major 3' end processing isoforms are visibly detected by northern blotting. We observed some anomalous degradation phenotypes in the *RTR1* mRNA that hinted at a second type of regulation other than NMD. We also observed these phenotypes in the *LRS4* mRNA and found that both of these mRNAs have antisense lncRNAs overlapping their 3'UTR that were previously termed XUTs (van Dijk et al., 2011). We hypothesized that these XUTs may posttranscriptionally regulate their target mRNAs in a novel manner that stabilized the cognate mRNAs. Ultimately, we invalidated this hypothesis, but our findings suggest a function for antisense lncRNAs in transcription gene regulation and the cyclization of their cognate mRNAs in the cell-cycle. Moreover, we established here a basis for the investigation of the turnover mechanisms of the *RTR1* mRNAs , which led us to the discovery of a novel mRNA degradation pathway discussed in Chapter 2.

RESULTS

Deletion of any of the Upf factors (*upf1Δ*, *upf2Δ*, or *upf3Δ*) entirely inactivates NMD and results in the distinct accumulation of NMD targets visible by an increased abundance of the mRNA by northern blotting. Further, the 5' to 3' cytoplasmic exonuclease, Xrn1p, plays a general role in the degradation of mRNAs globally and also specifically degrades NMD targets downstream of binding by the Upf factors (van Dijk et al., 2012; Brogna and Wen, 2009). We tested deletions of Xrn1p and Upf1p for their effect on long 3'UTR mRNAs. Upf1p acts upstream of Xrn1p in the NMD pathway, and thus, a deletion of UPF1 in an xrn1Δ background should be epistatic. However, we encountered a surprising result when we observed a synergistic increase in *RTR1* and *LRS4* mRNA abundance in a double mutant, *upf1Δxrn1Δ*, as compared to the single *xrn1Δ* mutant (Figure 1.1.A). Further, we tested whether this increase in steady-state abundance of the *RTR1* mRNAs was due to an increased stability in the double *upf1Δxrn1Δ* mutant over the *xrn1Δ* single mutant. We did so by replacing the endogenous *RTR1* promoter with the galactose-driven *GAL1* promoter. By switching from galactose containing media to dextrose, we shut-off transcription from GAL promoters. *GAL-RTR1* strains were generated in the *upf1Δ*, *xrn1Δ*, and *upf1Δxrn1Δ* backgrounds. The transcription shut-off assay showed that the half-life of mRNAs increased in the *upf1Δxrn1Δ* double mutant over the *xrn1Δ* mutant (Figure 1.1.B). Together, these results suggested to us that Upf1p may affect the stability of the *RTR1* mRNA in an NMD-independent manner.

From previously published RNA-seq databases of the *XRN1* deletion (*xrn1Δ*) strain we discovered that both *RTR1* and *LRS4* have lncRNAs transcribed antisense to their 3'UTRs (van Dijk et al., 2011). These lncRNAs comprise the XUT class of lncRNAs in *S. cerevisiae* (van Dijk et al., 2011). We confirmed the presence of the *RTR1* antisense XUT (*RTR1-aXUT*)

(Figure 2A) and the *LRS4-aXUT* (Figure 1.2.B) and their sensitivity to Xrn1p. The *RTR1* mRNAs and the *RTR1-aXUT* are both polyadenylated suggesting that the *RTR1-aXUT* is transcribed and processed similarly to a normal mRNA (Figure 1.2.A). Because XUTs are subject to degradation by Xrn1p, their abundance is higher in the *xrn1Δ* mutant. This suggested to us that in presence of higher levels of this antisense XUT, the *RTR1* mRNA could become stabilized perhaps through formation of duplex RNA. Potentially, the 5'-3' ATP-dependent helicase function of Upf1p could antagonize the formation of double stranded RNAs as Upf1p has previously been shown to prefer double-stranded RNA as a substrate *in vitro* (see Figure 1.2.C) (Weng et al., 1996). In support of this hypothesis, a global study of 3'end isoform half-lives in yeast found that double-stranded structures within 3'UTRs are a major determinant in mRNA stability (Geisberg et al., 2014). This Upf1p-dependent regulation model would explain the phenotype that we observed for the *upf1Δxrn1Δ* double mutant.

If our hypothesis were correct, then in absence of the antisense XUT, we would see a corresponding decrease in *RTR1* abundance. To test this hypothesis, we inserted the *ADH1* terminator downstream of the transcription start site of the *RTR1* antisense XUT (*RTR1-aXUT*) and downstream of the poly(A) site of the long *RTR1* mRNA (Figure 1.2.D). This early termination of the XUT eliminates the overlap between the *RTR1* 3'UTR and the XUT allowing us to test the mRNA steady-state levels in absence of any potential base-pairing between the two RNAs. Early termination of the *RTR1-aXUT* results in a decrease in the amount of *RTR1* noticeable by northern blotting (Figure 1.2.E). This result thus provided evidence to support the model.

Based on the steady-state abundance of mRNAs in the WT and *RTR1-aXUT*::T_{ADH1} strains as determined by northern blotting, we concluded that the effect of the insertion of the

terminator was detected to the highest extent in the *xrn1Δ* background. We explored possible conditions that might lead to an increase in the *RTR1-aXUT* in the wildtype background, which might in turn impact the expression of *RTR1*.. We found two conditions, cycloheximide treatment and amino acid starvation, that lead to an increase in both the *RTR1* mRNA levels and the *RTR1-aXUT* levels (Figure 1.3.A,B). Furthermore, early termination of the XUT resulted in an apparent decrease in the response to both cycloheximide treatment and amino acid starvation thus providing a physiological importance of the *RTR1-aXUT* in regulating the cognate mRNA. Since Gcn4p is a transcription factor known to upregulate genes in response to amino acid starvation, we looked for Gcn4p binding sites at the *RTR1* locus and found the presence of Gcn4p binding sites at the promoters of both *RTR1* and *RTR1-aXUT (*Hinnebusch and Fink, 1983). However, deletion of *GCN4* did not alter the amino acid response at the *RTR1* locus as the *RTR1* mRNAs increased in abundance regardless of *GCN4* deletion (Figure 1.3.C).

Both of the conditions that we found to upregulate *RTR1* and *RTR1-aXUT* are known to result in an abrogation of translation. We thus wondered if the *RTR1-aXUT* only affects mRNAs that are not being actively translated. This would provide evidence for a novel role for long noncoding RNAs in regulating the degradation of mRNAs that are not undergoing active translation. To test this, we performed polysome fractionation analysis of the *RTR1* mRNAs to determine whether mRNAs not associated with the ribosome are more affected by the absence of the overlapping, antisense XUT. The polysome profile of *RTR1* mRNAs revealed however that a vast majority of the mRNAs are bound to ribosomes with or without the XUT terminator (Figure 1.4.A). The profiles in the *xrn1Δ* background did not reveal any major differences in the free mRNPs either when differences in total RNA content in each fraction are taken into account (Figure 1.4.B). We also did not see a major effect of the *RTR1-aXUT* on translation of *RTR1* mRNAs since the distribution of mRNAs in the

polyribosomal fractions did not shift much between the wildtype and XUT terminator mutant profiles.

We observed that early termination of the *RTR1-aXUT* had the largest impact in the *xrn1Δ* background; thus, if the XUT actually mediates *RTR1* stability and impairs its degradation, then exonucleases other than Xrn1p would have to be responsible for the degradation. Since Xrn1p is the major cytoplasmic exonuclease, we reasoned that the 3'-5' degradation pathway may be a plausible alternative. To this end, we tested the deletion of *SKI2*, an auxiliary component of the cytoplasmic 3'-5' exosome, which normally impairs exosome activity to a large degree (Jacobs et al., 1998). However, *SKI2* deletion does not result in an increase in steady-state mRNA levels (Figure 1.5.A), suggesting that Ski2p does not likely participate in the degradation of *RTR1*. The deletion of *SKI2* also did not restore *RTR1* mRNA abundance in the *RTR1-aXUT* terminator background strain as would be expected if Ski2p participated in the degradation of *RTR1* in the absence of the XUT (Figure 1.5.A). We also tested whether the exosome may in this case be responsible for the degradation of *RTR1* in a manner independent of *SKI2*. *DIS3* is an essential component of both the cytoplasmic and nuclear exosome and its deletion is lethal (Mitchell et al., 1997). We utilized a *DIS3-dAMP* strain which adds a long 3'UTR to the transcript and decreases overall gene expression by targeting the transcript for degradation by the NMD pathway. Since we still see a decrease in *RTR1* steady-state levels in the *DIS3-dAMP, RTR1-aXUT*::T_{ADH1} strain compared to the *DIS3-dAMP* strain, we conclude that neither the cytoplasmic nor nuclear exosome degrades *RTR1* mRNA in absence of the XUT (Figure 1.5.B). Additionally, the 5'-3' decapping exonuclease, Dxo1p, also did not show any restoration of *RTR1* transcript abundance in the *RTR1-aXUT*::T_{ADH1} background (Figure 1.5.C). Finally, we tested the REX exonucleases, Rex1p, Rex2p, and Rex3p, for their potential involvement in the degradation of *RTR1* in absence of the XUT, and surprisingly,

we detected an increase in *RTR1* mRNA levels in the *rex2Δrex3Δ* background with no further concomitant increase in the *rex1Δrex2Δrex3Δ* strain (Figure 1.5.D). This suggested that Rex2p and Rex3p participate in the degradation of *RTR1* mRNAs which for the first time suggested a role for the REX exonucleases in the degradation of mRNA (van Hoof et al., 2000). Unfortunately, Rex2p and Rex3p could not be assigned as the exonucleases responsible for degrading *RTR1* in absence of the *RTR1-aXUT* since early termination of the XUT in the *rex2Δrex3Δ* background did not restore *RTR1* mRNA abundance to wildtype levels (Figure 1.5.D). However, we continued to search for the pathway responsible for targeting *RTR1* transcripts to degradation by Rex2p/Rex3p and present these findings in Chapter 2 of this Dissertation.

Unable to identify a nuclease responsible for degrading the *RTR1* mRNAs in absence of the *RTR1-aXUT*, we tested the stability of the *RTR1* mRNA in *RTR1-aXUT* terminator strain compared to the wildtype, using a strain in which expression of *RTR1* is driven by the GAL promoter (*GAL-RTR1*). Using the galactose to dextrose shift to shut-off transcription, we measured the half-lives of *RTR1* mRNAs. Based on this assay, we found that the stability of the *RTR1* mRNAs, does not change between the wildtype and XUT terminator strains (Figure 1.6.A). This suggested that the effect of the terminator insertion may somehow be altering the transcription rate at the *RTR1* promoter. We had originally tested the insertion of the *ADH1* terminator sequence at two different sites downstream of the *RTR1* terminator and observed similar effects. We then tested a third site which then resulted in no effect on the *RTR1* mRNA in either the wildtype or the *xrn1Δ* background (Figure 1.6.B). Thus, the insertion mutation used to assay the effect of the absence of the XUT most likely altered the chromatin structure at the *RTR1* locus so that an overall decrease in the *RTR1* mRNAs was observed whenever the transcripts were more abundant. We then conclude from these results that the *RTR1-aXUT* had no effect on the posttranscriptional stability of the RTR1 mRNAs.

The antisense XUT does not appear to affect the stability of the *RTR1* mRNA; however, we still wished to test the hypothesis that the XUT may impact the expression of Rtr1p through an effect at the translational level. Thus, a 3X-FLAG-RTR1 strain was used to test the overall protein abundance in the XUT terminator strain. Insertion of the terminator at the new site also did not negatively impact the protein abundance (Figure 1.6.C). If anything, a slight increase is observed in the XUT terminator strain. From this, we conclude that the *RTR1-aXUT* does not drastically affect the gene expression of *RTR1*.

Though our analysis of the *RTR1-aXUT* and its effect on *RTR1* did not reveal a post-transcriptional regulatory role, we did observe that the *RTR1* and *LRS4* antisense XUTs may play roles in transcriptional gene regulation. Previously published tilling array analysis of *cdc28-1* and *bar1Δ* arrested cell cycle synchronization experiments revealed that several intergenic noncoding RNAs were cell cycle regulated (Granovskaia et al., 2010). The most prominent of these intergenic noncoding RNAs in terms of the extent to which the expression fluctuated throughout the cell cycle was the *LRS4* 3'UTR antisense XUT. This data set revealed that *RTR1* is cell cycle regulated as well. Mat-haploid yeast arrest their cell cycles at G1 upon exposure to alpha factor mating pheromone in the media (Breeden 1997). We synchronized the Mat-a strain, BY4741, by exposure to alpha factor and took time points every 10 minutes for 2 hours. Northern blotting for the *LRS4* and antisense *LRS4-aXUT* revealed that these RNAs are indeed cell-cycle synchronized and peak in abundance at opposite times during the cell cycle (Figure 1.7.A,B). The *LRS4-aXUT* peaks with the *CLN2* transcript, known to be expressed during G1 and peak in late G1 (Hadwiger et al., 1989). *LRS4*, then, appears to peak between G2/M phase. This anti-correlation between the mRNA expression levels throughout the cell-cycle is also observed with *RTR1* and *RTR1-aXUT*, but to a lesser extent (Figure 1.7.C,D). These results are reminiscent of previous findings that convergent genes (those whose 3' termini face each other) are also anti-correlated throughout

the cell cycle and the expression of one gene represses transcription of the other (Wang et al., 2014). Our results suggest that long noncoding RNAs may act in a similar manner to repress the transcription of genes with which they converge.

DISCUSSION

Our work presented in this chapter explores the possibility of posttranscriptional gene regulation of antisense lncRNAs in stabilizing target mRNAs. This hypothesis was initiated by the observation that *RTR1, LRS4,* and other NMD-targeted mRNAs accumulate to higher amounts in a *upf1Δxrn1Δ* strain. We show that the *RTR1-a*XUT does not appear to have a stabilizing effect on the *RTR1* mRNA and thus cannot be the cause of this increased stability observed in the *upf1Δxrn1Δ* strain.

While we focused on the *RTR1* mRNA here, we also surveyed the effect of XUT termination in other loci with 3'UTR antisense XUTs and found little overall effect on the target mRNAs (not shown). Our results seem to suggest that overall, long noncoding RNAs that may potentially form double-stranded regions with cognate mRNAs have little impact on posttranscriptional gene expression. Though it is feasible that antisense and cognate RNAs could base-pair *in vivo* forming double-stranded RNA, budding yeast may have evolved highly efficient mechanisms for unwinding double-stranded RNAs. One potential mechanism that may suppress the formation of dsRNA is the activity of RNA helicases. Indeed, ATPase-dependent RNA helicase activity is present in at least 30 known factors in *S. cerevisiae* (Saccharomyces Genome Database). mRNP complexes undergo many transitions and rearrangements when transiting from the cytoplasm to the nucleus. Rearrangements during export, for example, require the essential DEAD-Box RNA helicase, Dbp5p, which complexes with the nuclear pore complex and the polyribosomes (Tseng et al., 1998; Snay-

Hodge et al., 1998; Gross et al., 2007; Noble et al., 2011). The ribosome itself is an efficient RNA helicase that unwinds double-stranded structures and expels proteins lying in its path (Takyar et al., 2005). Since the ribosome typically stops at the stop codon, unless the cell may be impaired in efficient ribosome recycling, 3'UTR regions are largely devoid of ribosomes and thus special mechanisms may have evolved to limit the formation of dsRNA within 3'UTR regions (Guydosh and Green, 2014). One potential factor that may perform this function could be Upf1p, as previous studies have reported the enrichment of Upf1p in 3'UTRs due to displacement of Upf1p from ORFs during translation (Hurt et al., 2013; Kurosaki and Maquat, 2013). Our results suggest that the absence of Upf1p may result in the stabilization of the *RTR1* mRNA, though this increased stability did not depend on the antisense XUT. We have not formally ruled out the possibility that Upf1p does indeed displace antisense lncRNAs binding to 3'UTRs but that this binding does not affect the *RTR1* mRNA stability. The Struhl lab, however, has shown that double-stranded RNA formation within 3'UTRs typically stabilizes mRNAs (Geisberg et al., 2014). A distinct possibility is that another RNA helicase may function in lieu of Upf1p upon *UPF1* deletion or that another RNA helicase altogether fulfills this function.

Our finding that the LRS4-aXUT is anti-correlated with the LRS4 transcript throughout the cell-cycle suggests a transcriptional gene regulation model whereby the XUT represses the transcription of the mRNA (Figure 7A,B). To some extent, we also see an anti-correlation in expression between *RTR1* and the *RTR1-aXUT* in alpha factor synchronized cells. These observations seem to contradict the finding that both the *RTR1 and RTR1-aXUT* transcripts are upregulated in amino acid starvation conditions (Figure 1.3). However, translation is abruptly abrogated in this condition and thus, it is possible that turnover pathways that depend on translation may also be blocked. This effect would be independent of the effect of transcription of the XUT and its impact on the transcription of *RTR1*.The anti-

correlation of *RTR1* and the *RTR1-aXUT* in the cell cycle is likely due to an effect at the transcriptional level. An attractive hypothesis is that the XUT aids in cyclization of the 3'UTR-overlapping transcript during the cell-cycle and this effect may be similar to that seen in a previous study that examined convergent pairs of genes (Wang et al., 2014). Interestingly, it was found that this repression of overlapping 3'UTR genes could also be replicated in trans (Wang et al., 2014). In other eukaryotes, like fission yeast, active RNAi pathways act to degrade and transcriptionally silence overlapping mRNAs and noncoding RNAs; and further, this mechanism is responsible for the cyclization of convergent pairs of genes which form heterochromatin at alternating points in the cell-cycle (Gullerova et al., 2008; Gullerova et al., 2011).Though the phenomenon of repression of convergent pairs of genes throughout the cell-cycle is conserved between budding and fission yeasts, the mechanism must be distinct since RNAi is lacking in budding yeast. This repression could be mediated by DNA-RNA hybrids rather than dsRNA. Work from the Heiter group revealed the importance of DNA-RNA hybrid formation in the regulation of gene expression by antisense transcripts (Chan et al., 2014). The accumulation of antisense RNAs in budding yeast could also potentially impact DNA-RNA hybrid formation in the nucleus, though the formation of DNA-RNA hybrids is also suppressed by three independent mechanisms comprising of the RNase H nuclease, Rnh1p, the Sen1p helicase, and the THO complex (Chan et al., 2014).

Lastly, our results, shown in Figure 5D, indicated to us that *RTR1* transcripts may be degraded by the REX exonucleases. Though the *RTR1-aXUT* did not block degradation of *RTR1* by the REX exonucleases, we expanded upon these results and found that the REX exonucleases participate in a novel mRNA degradation pathway. Our study of the *RTR1* mRNAs and their degradation continued and we present the article manuscript describing our findings in Chapter 2.

FIGURES

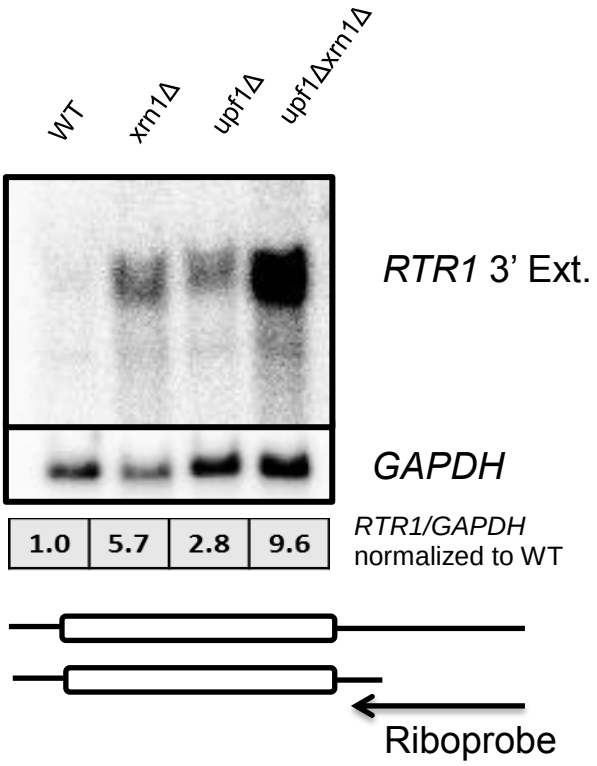

Figure 1.1.A. Northern blot showing steady-state levels of the *RTR1* long 3'UTR isoform transcript ($RTR1_L$). The quantitation of the bands relative to GAPDH and normalized to the WT lane is shown below the blot. The schematic below shows the location of the antisense 32P-labled Riboprobe used for detection.

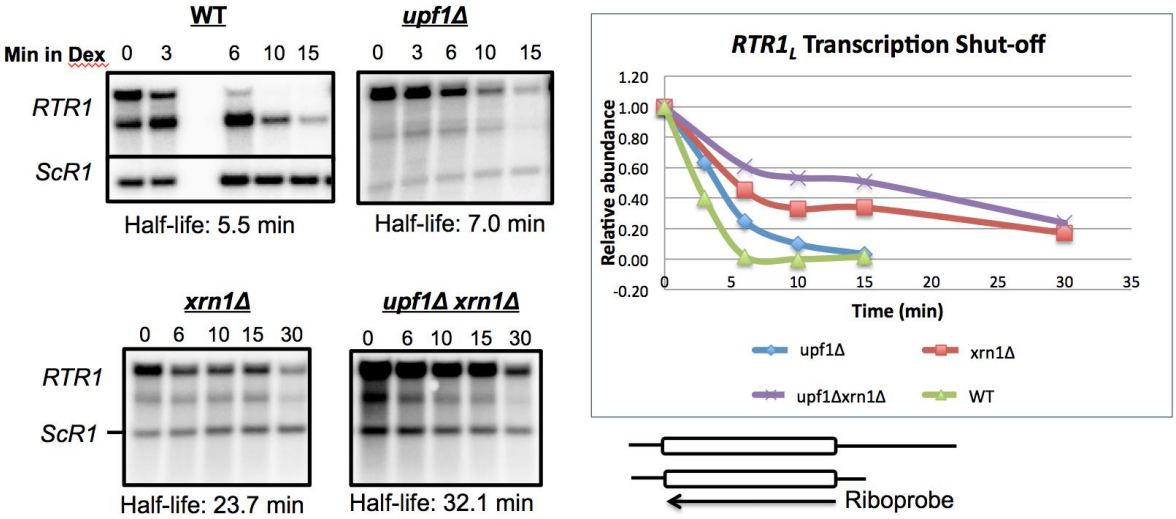

Figure 1.1.B. Northern blot showing transcription shut-off analysis of the *RTR1* mRNAs. The native *RTR1* promoter was replaced with the Gal promoter for inducible expression of *RTR1*. Cells were grown in galactose containing medium and switched to dextrose at OD=0.6 to shut off transcription from the Gal promoter. The indicated time points were taken. The chart to the right of the blot shows the normalized quantitation of the bands in the blot relative to the scR1 signal at each time point and normalized to the zero minute time point. The half-life beneath each blot is calculated for the $RTR1_L$ transcript.

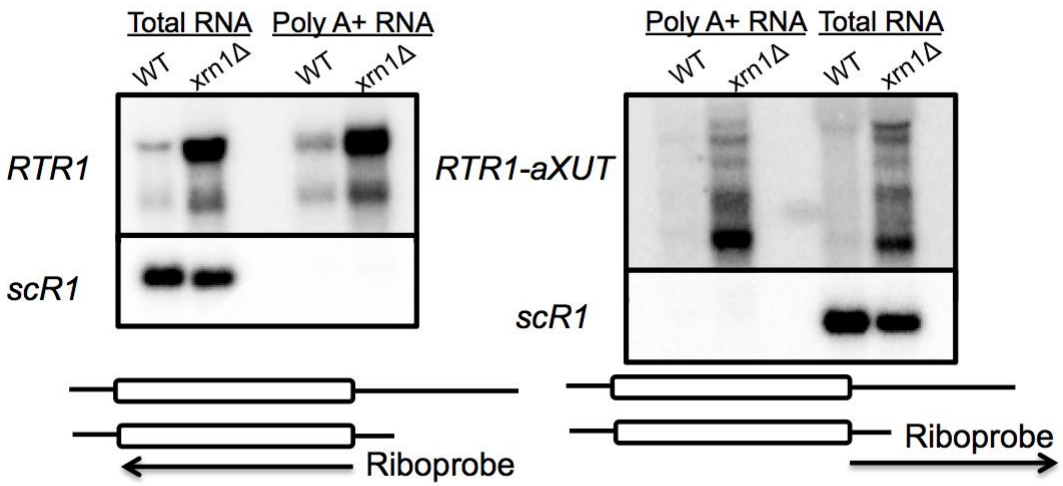

Figure 1.2.A. Northern blot total RNA and poly(A) selected RNAs for the *RTR1* and *RTR1-aXUT* transcripts. Poly(A) selection was performed using the Promega PolyA Tract mRNA Isolation System. The scR1 control below shows the efficiency of the poly(A) selection since this Pol III transcribed RNA is not polyadenylated.

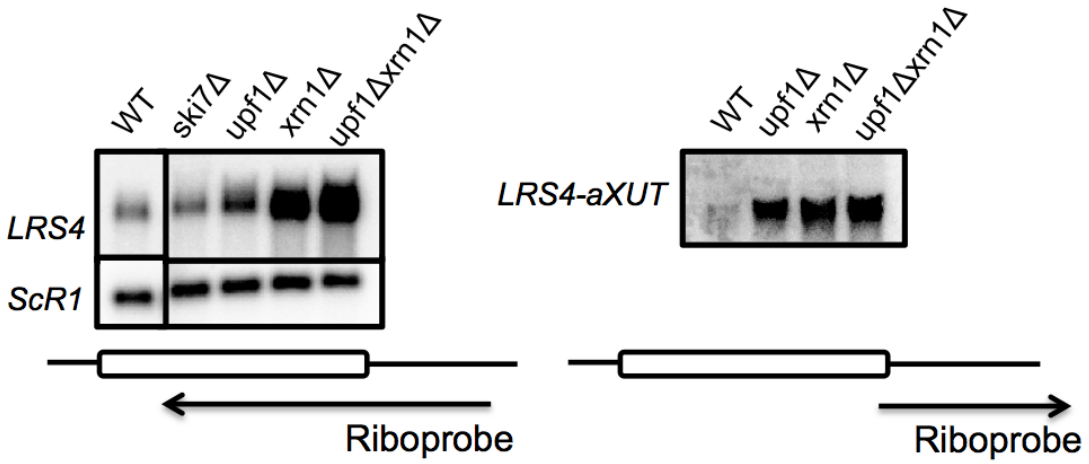

Figure 1.2.B. Northern blot showing steady-state levels of the *LRS41* and *LRS4-aXUT* transcripts in various mutants

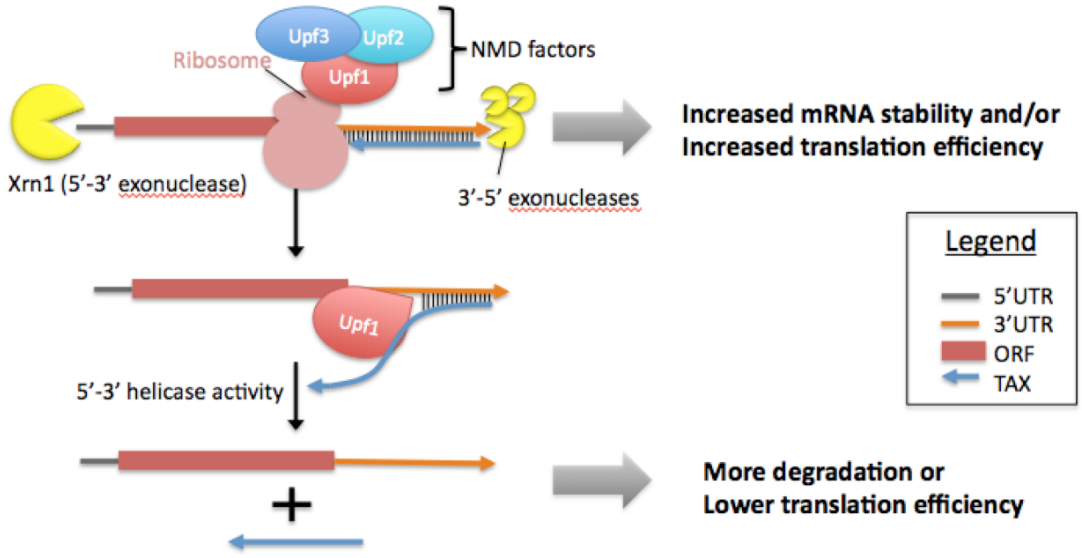

Figure 1.2.C. Hypothetical model of a role for Upf1p in regulating dsRNA formation and target mRNA stability

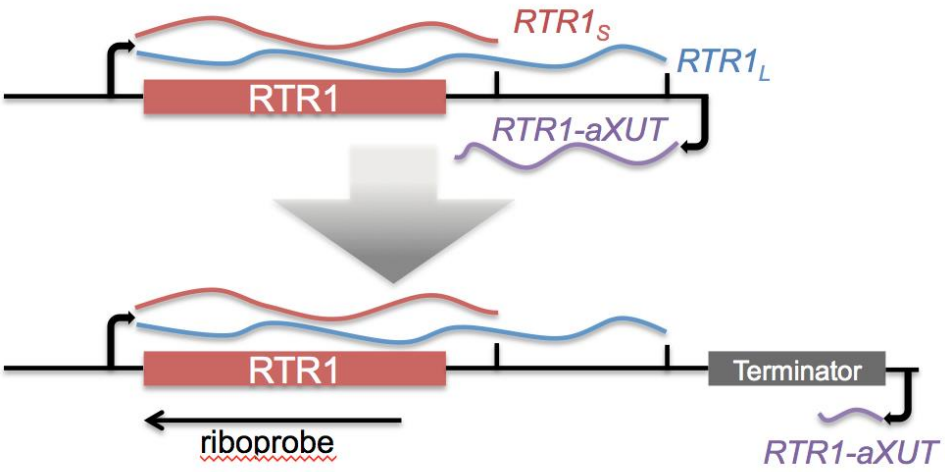

Figure 1.2.D. Schematic representation of the genomic insertion of the *ADH1* terminator which terminates transcription of the *RTR1-aXUT* early so that it no longer overlaps with the *RTR1* 3'UTR

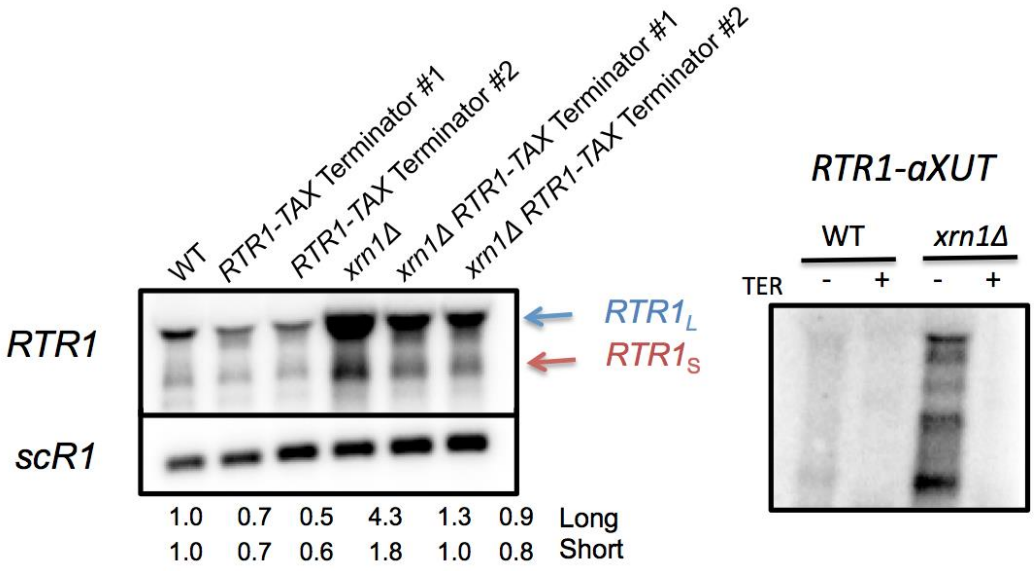

Figure 1.2.E. Northern blot showing steady-state levels of the *RTR1* and *RTR1-aXUT* transcripts in the absence or presence of the XUT terminator. The quantitation of the bands relative to scR1 and normalized to the WT lane is shown below the blot.

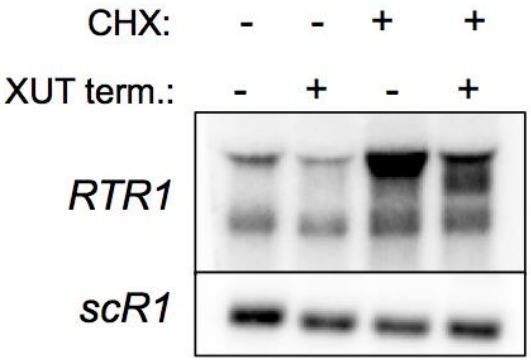

Figure 1.3.A. Northern blot showing steady-state levels of the *RTR1* transcripts in log phase or in log phase after 20 minutes of 100ug/mL cycloheximide (CHX) addition to the media.

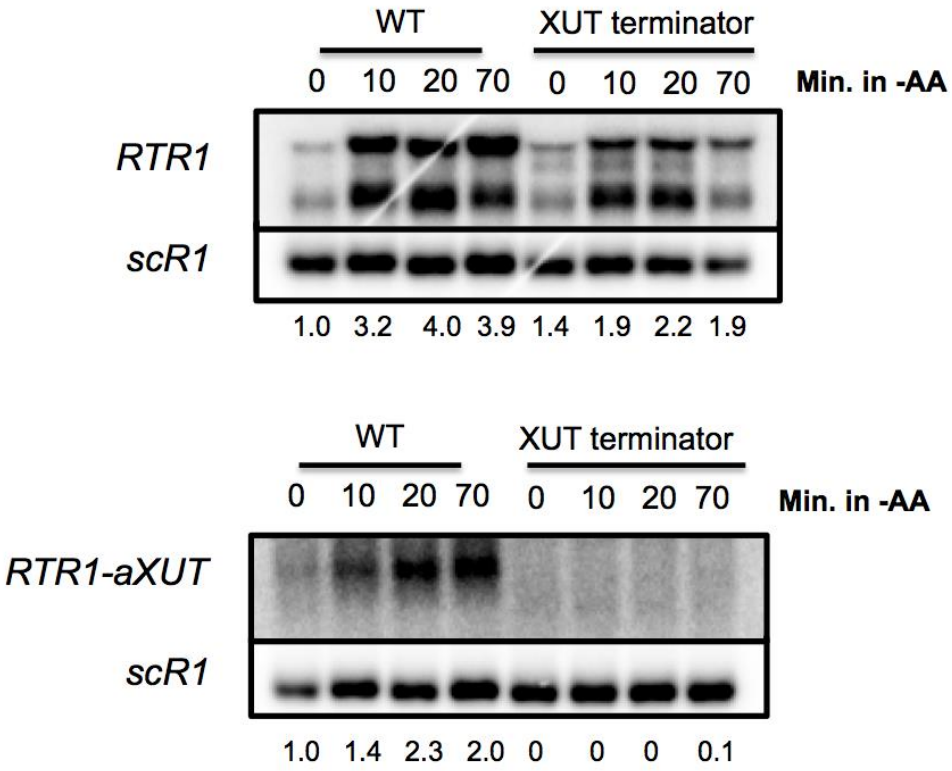

Figure 1.3.B. Northern blot showing the response of the *RTR1* and *RTR1-aXUT* transcripts to amino acid starvation conditions (-AA). Cells were grown to log phase and shifted from YPD to YP media lacking amino acids. Cells were harvested at the indicated time points.

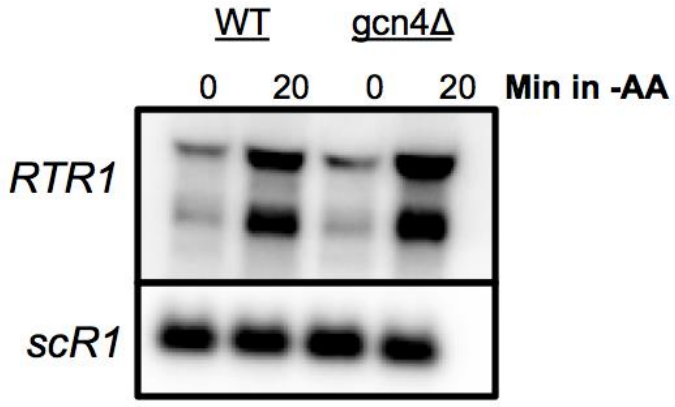

Figure 1.3.C. Northern blot showing the response of the *RTR1* mRNA to amino acid starvation in either wildtype or *gcn4Δ* cells.

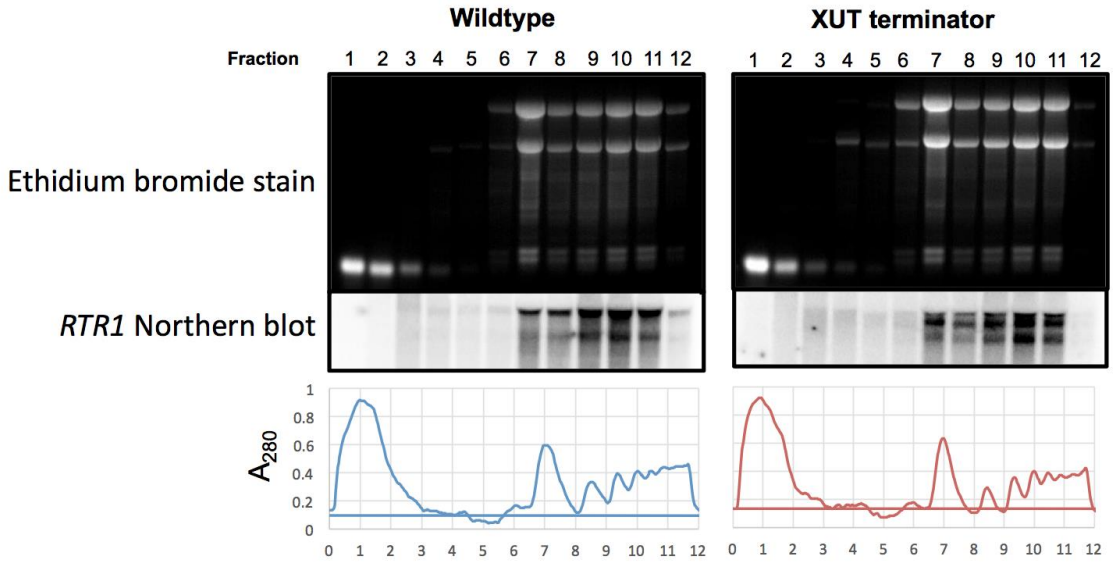

Figure 1.4.A. Sucrose fractionation and northern blot for *RTR1* in the wildtype or XUT terminator strain

After harvesting and lysing cells, 10 OD units of the soluble fraction of the lysate was applied to a 15-50% sucrose gradient and the gradient was ulta-centrifuged at 37,000 RPM for 3.5 hours. Fractions were collected and the A280 trace during the fractionator run is shown below the northern blots. The ethidium bromide stained gels are provided for referencing the polysomal fractions.

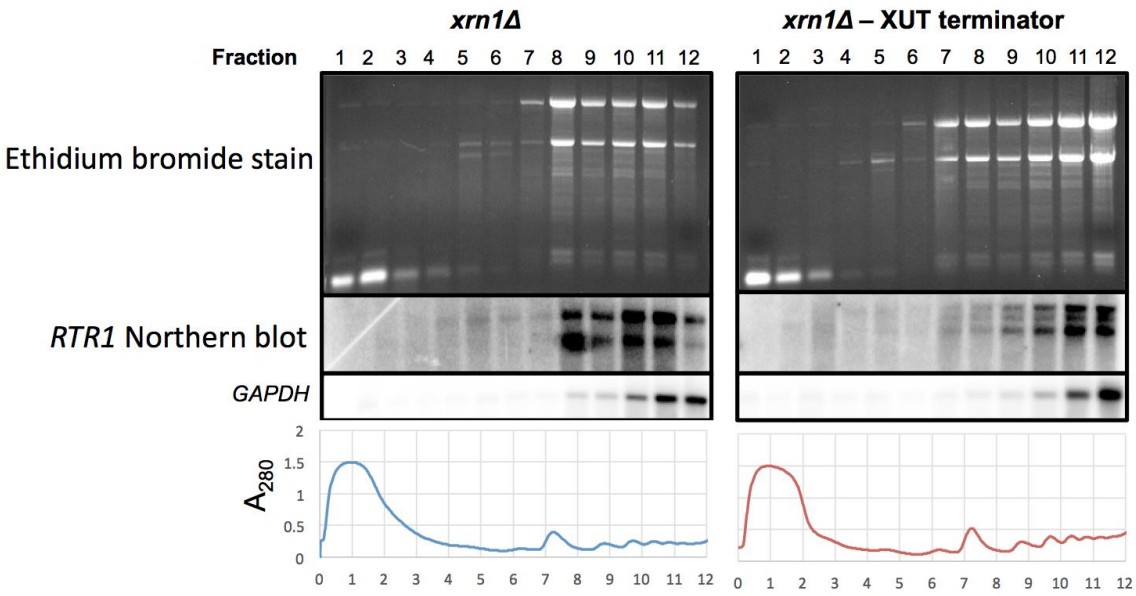

Figure 1.4.B. Sucrose fractionation and northern blot for *RTR1* in the xrn1Δ or XUT terminator strain in the xrn1Δ background

After harvesting and lysing cells, 10 OD units of the soluble fraction of the lysate was applied to a 15-50% sucrose gradient and the gradient was ulta-centrifuged at 37,000 RPM for 3.5 hours. Fractions were collected and the A280 trace during the fractionator run is shown below the northern blots. The ethidium bromide stained gels are provided for referencing the polysomal fractions.

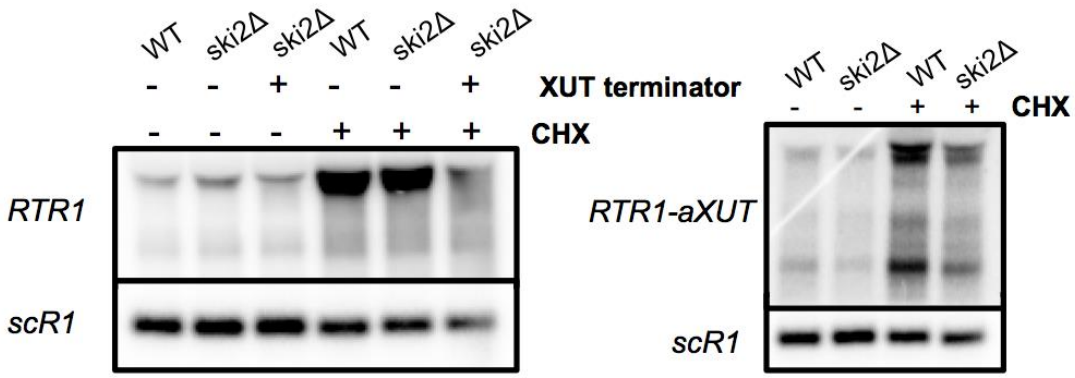

Figure 1.5.A. Northern blot showing steady-state levels of the *RTR1* and *RTR1-aXUT* in the indicated mutants

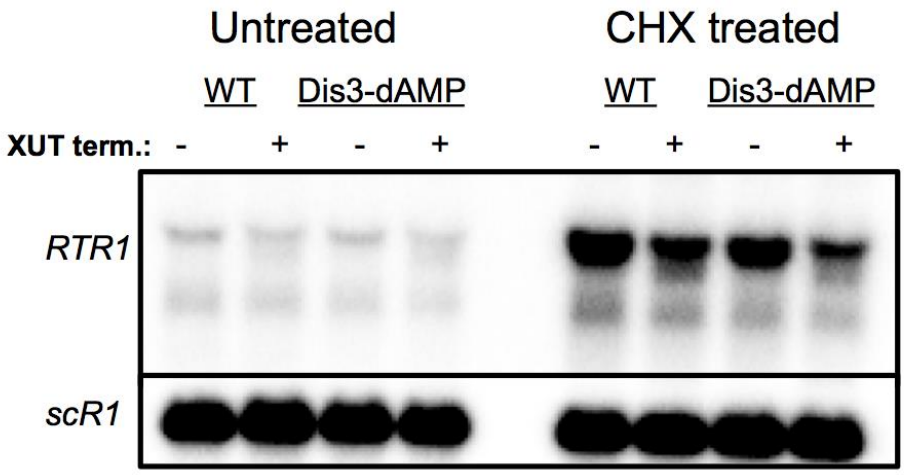

Figure 1.5.B. Effect of Dis3 downregulation on the *RTR1* mRNAs in the XUT terminator background or wildtype context. The four right lanes consist of cells harvested after a 20 minute 100ug/mL cycloheximide treatment.

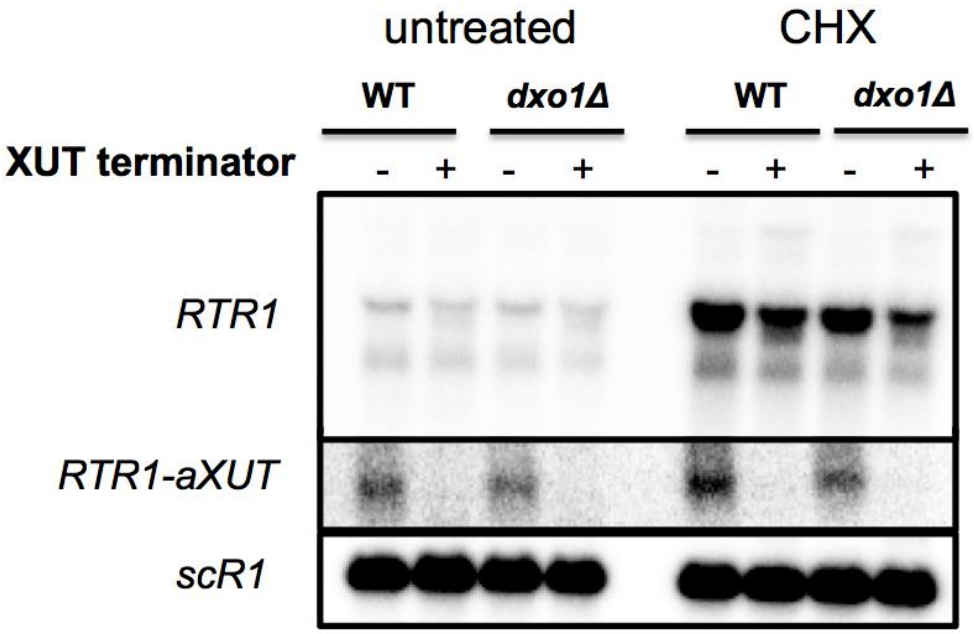

Figure 1.5.C. Effect of *DXO1* deletion on the *RTR1* mRNAs in the XUT terminator background or wildtype context. The four right lanes consist of cells harvested after a 20 minute 100ug/mL cycloheximide treatment.

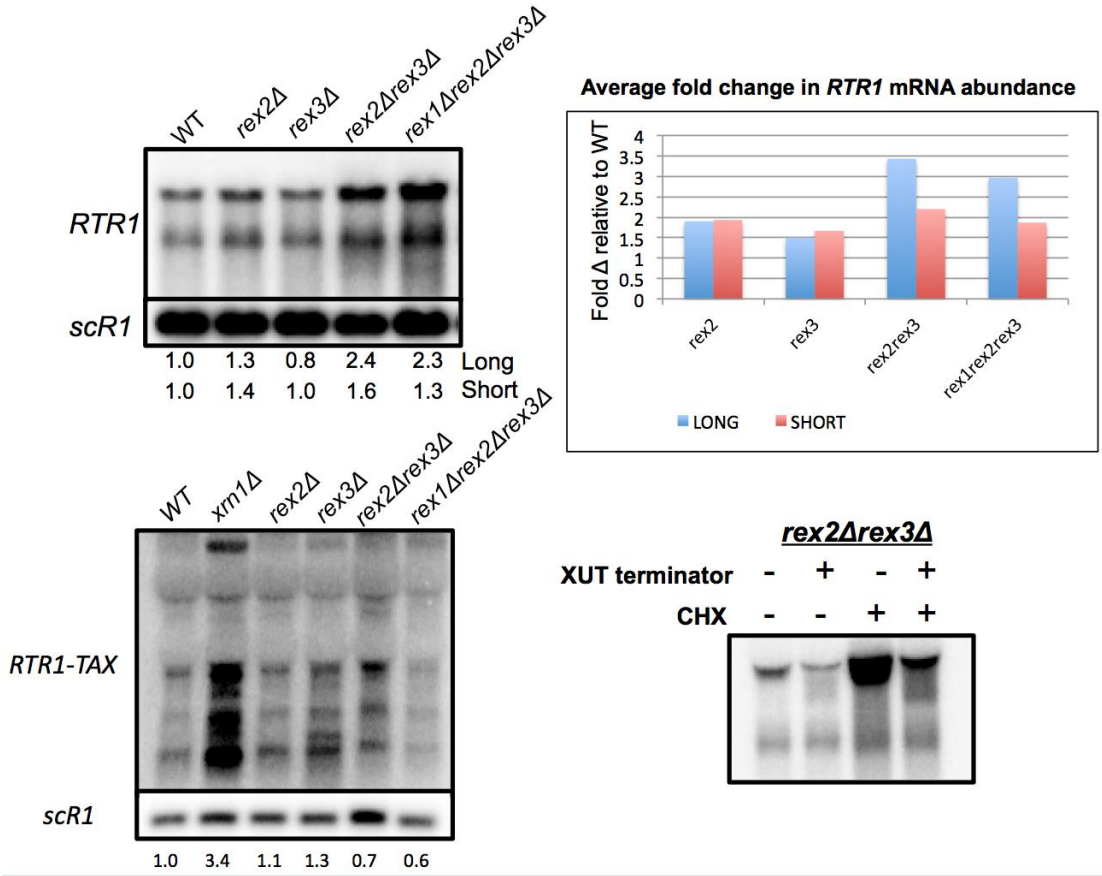

Figure 1.5.D. Northern blot showing steady-state levels of the *RTR1* and *RTR1-aXUT* in the REX mutant backgrounds. The quantitation of the bands relative to scR1 and normalized to the WT lane is shown below the blot. The graph to the right of the blot shows the quantitation. The lower right panel is a northern showing the effect of CHX treatment of *RTR1* mRNAs in the *rex2Δrex3Δ* background.

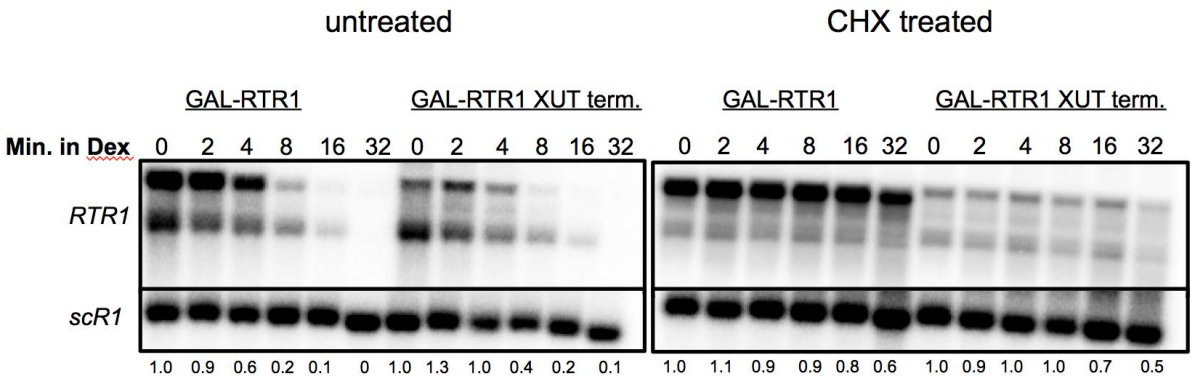

Figure 1.6.A. *RTR1* Transcription shut-off assay of the WT and XUT terminator strain). The shut-off at the Gal driven promoter was performed as before except that half of the culture for each strain was transferred to a separate flask and treated with 100ug/mL CHX for 20 min. prior to shifting to a CHX-supplemented dextrose media.

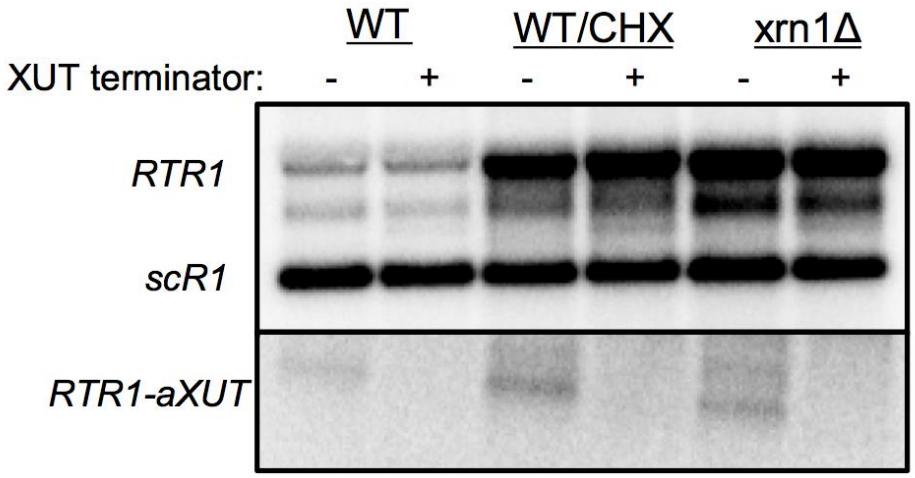

Figure 1.6.B. Effect of inserting the XUT terminator at a third site downstream of the two previously tested insertion sites.

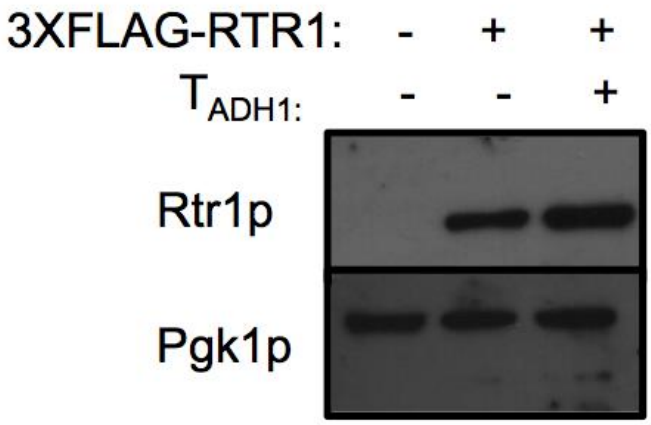

Figure 1.6.C. Western blot analysis of the N-terminally 3X-FLAG tagged Rtr1p in an *xrn1Δ* background. The new XUT terminator insertion site was used for making the XUT terminator strain.

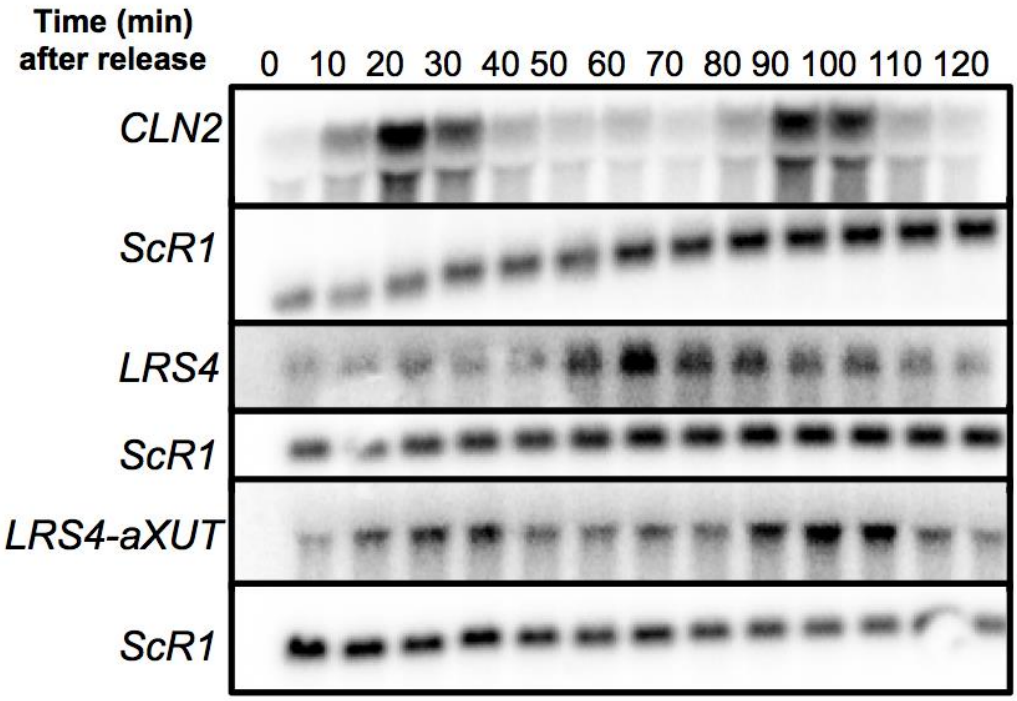

Figure 1.7.A. Northern blots showing *CLN2*, *LRS4*, and *LRS4-aXUT* RNAs harvested from alpha-factor synchronized cells at the indicated time points. The cells were grown in YPD media pH 3.9 to inactivate Bar1p protease and allow for more efficient release from alpha-factor arrest (Elledge lab protocol). CLN2 is provided as a control for synchrony.

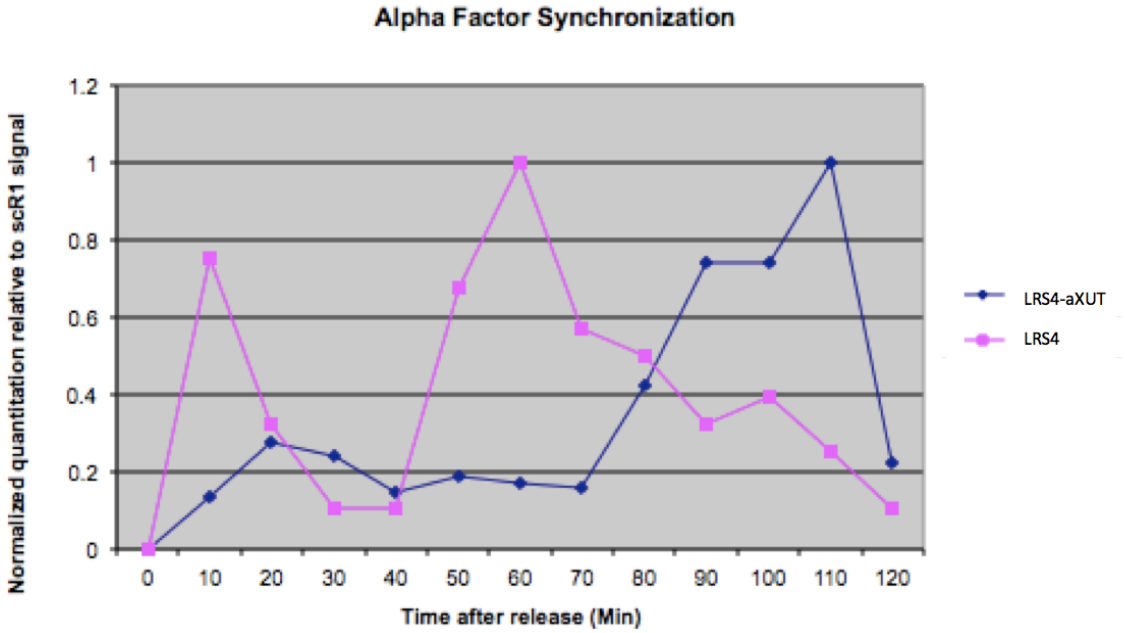

Figure 1.7.B. Chart displaying quantitated values from the northern blot performed in 1.7.A Bands were quantitated relative to scR1 and normalized to the 0 minute time point.

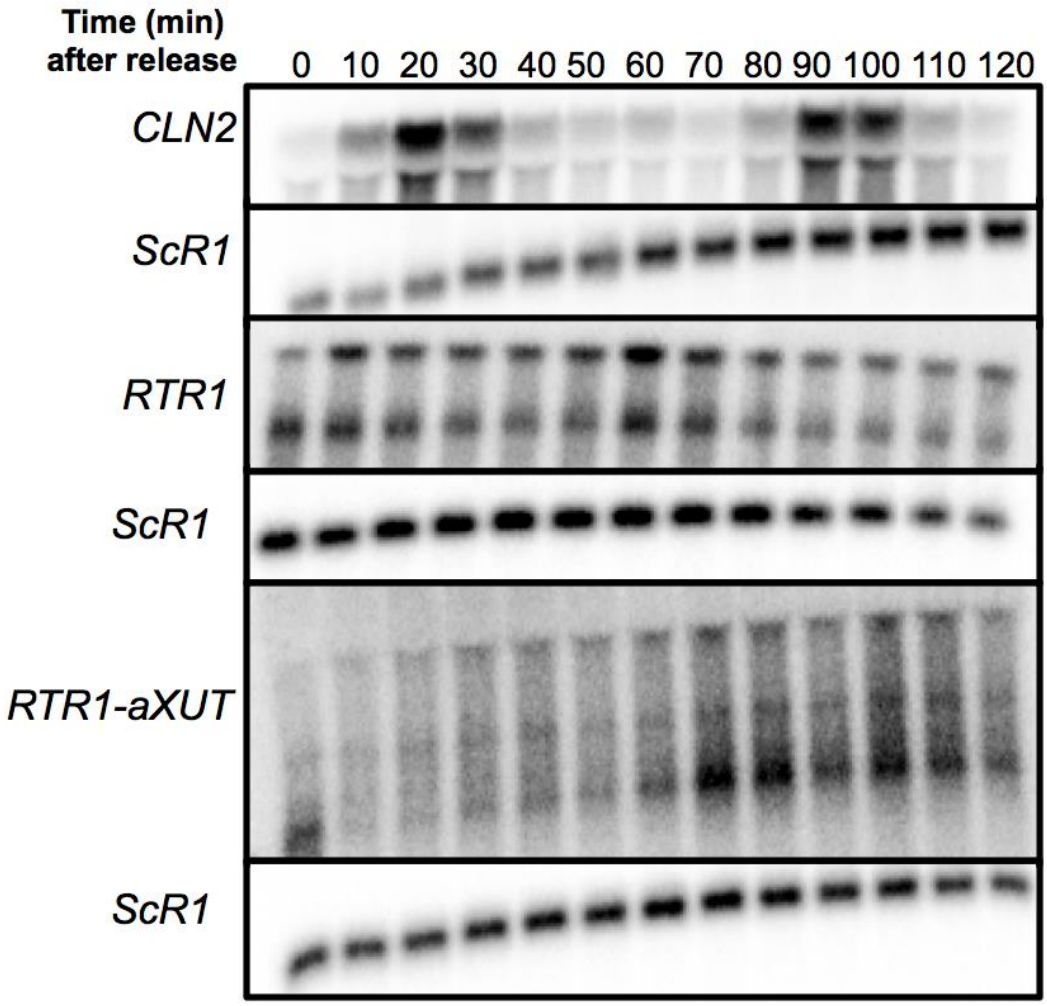

Figure 1.7.C. Northern blots showing *CLN2*, *RTR1*, and *RTR1-aXUT* RNAs harvested from alpha-factor synchronized cells at the indicated time points. The cells were grown in YPD media pH 3.9 to inactivate Bar1p protease and allow for more efficient release from alpha-factor arrest (Elledge lab protocol). CLN2 is provided as a control for synchrony.

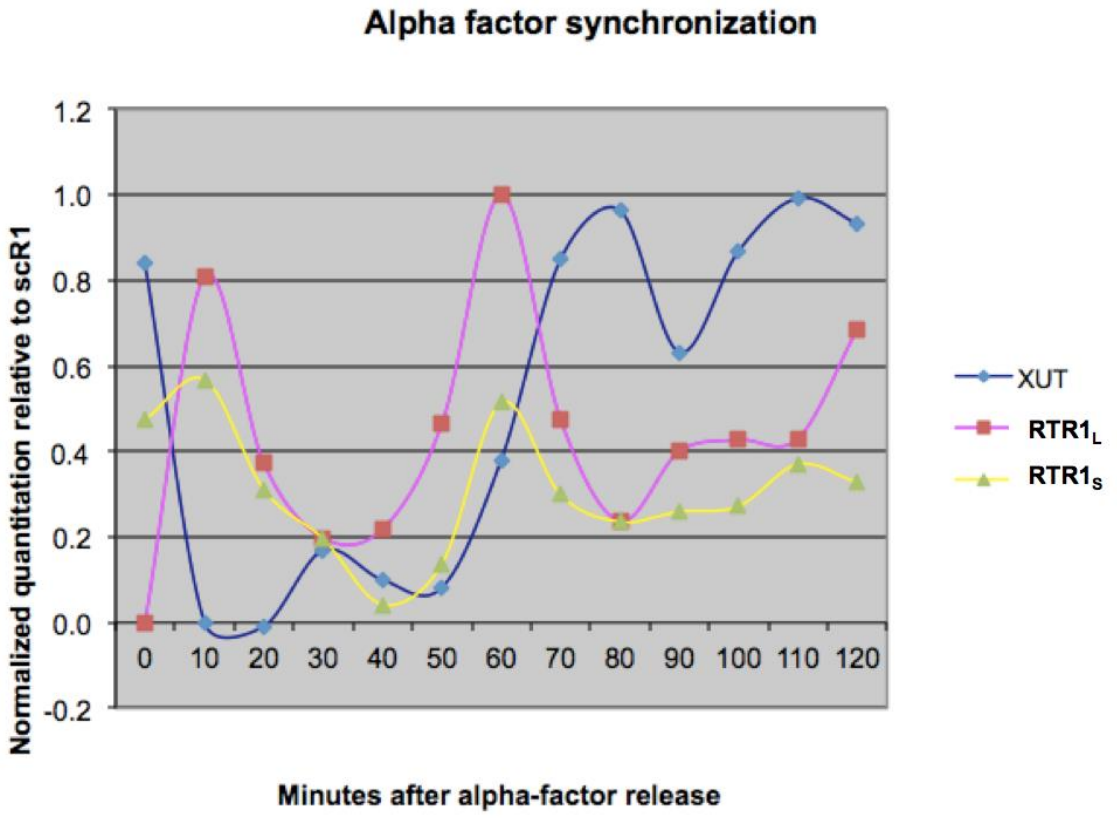

Figure 1.7.D. Chart displaying quantitated values from the northern blot performed in 1.7.C Bands were quantitated relative to scR1 and normalized to the 0 minute time point.

REFERENCES

Amrani, N., R. Ganesan, S. Kervestin, D.A. Mangus, S. Ghosh, and A. Jacobson, A faux 3'-UTR promotes aberrant termination and triggers nonsense-mediated mRNA decay. Nature, 2004. 432(7013): p. 112-8.

Bao, J. Wu, J. Schuster, A.S., Hennig, G., Yan, W. Expression profiling reveals developmentally regulated lncRNA repertoire in the mouse male germline. Biol Reprod, 2013. 89 (5): p. 1-12.

Benhamed, M., Herbig, U., Ye, T., Dejean, A., Bischof, O. Senescence is an endogenous trigger for microRNA-directed transcriptional gene silencing in human cells. Nat Cell Biol, 2012. 14 (3): p. 266-75.

Breeden, L. L. (1997). Alpha-factor synchronization of budding yeast. *Methods in enzymology*, *283*, 332-341.

Brogna, S., Wen. J. Nonsense-mediate mRNA decay (NMD) mechanisms. Nat Struct Mol Biol. 2009 (16) 2: p. 107-13.

Chang, J. H., Jiao, X., Chiba, K., Oh, C., Martin, C. E., Kiledjian, M., & Tong, L. (2012). Dxo1 is a new type of eukaryotic enzyme with both decapping and 5′-3′ exoribonuclease activity. *Nature structural & molecular biology*, *19*(10), 1011-1017.

Chan, Y. A., Aristizabal, M. J., Lu, P. Y., Luo, Z., Hamza, A., Kobor, M. S., ... & Hieter, P. (2014). Genome-wide profiling of yeast DNA: RNA hybrid prone sites with DRIP-chip. *PLoS Genet*, *10*(4), e1004288.

COLLER, J. M., TUCKER, M., SHETH, U., VALENCIA-SANCHEZ, M. A., & PARKER, R. (2001). The DEAD box helicase, Dhh1p, functions in mRNA decapping and interacts with both the decapping and deadenylase complexes.*Rna*, *7*(12), 1717-1727.

Czaplinski, K., Ruiz-Echevarria, M. J., Paushkin, S. V., Han, X., Weng, Y., Perlick, H. A., ... & Peltz, S. W. (1998). The surveillance complex interacts with the translation release factors to enhance termination and degrade aberrant mRNAs. *Genes & development*, *12*(11), 1665-1677.

Doma, M. K., & Parker, R. (2006). Endonucleolytic cleavage of eukaryotic mRNAs with stalls in translation elongation. *Nature*, *440*(7083), 561-564.

Drinnenberg, I.A., D.E. Weinberg, K.T. Xie, J.P. Mower, K.H. Wolfe, G.R. Fink, and D.P. Bartel, RNAi in budding yeast. Science, 2009. 326(5952): p. 544-50.

Faghihi, M.A., F. Modarresi, A.M. Khalil, D.E. Wood, B.G. Sahagan, T.E. Morgan, C.E. Finch, G. St Laurent, 3rd, P.J. Kenny, and C. Wahlestedt, Expression of a noncoding RNA is elevated in Alzheimer's disease and drives rapid feed-forward regulation of beta-secretase. Nat Med, 2008. 14(7): p. 723-30.

Gagnon, J., Lavoie, M., Catala, M., Malenfant, F., & Elela, S. A. (2015). Transcriptome Wide Annotation of Eukaryotic RNase III Reactivity and Degradation Signals. *PLoS genetics*, *11*(2).

Geisberg, J. V., Moqtaderi, Z., Fan, X., Ozsolak, F., & Struhl, K. (2014). Global analysis of mRNA isoform half-lives reveals stabilizing and destabilizing elements in yeast. *Cell*, *156*(4), 812-824.

Ghildiya, M., Zamore, P. Small silencing RNAs: an expanding universe. Nat Rev Genet, 2009. 10 (2): p. 94-108

Granovskaia, M. V., Jensen, L. J., Ritchie, M. E., Toedling, J., Ning, Y., Bork, P., ... & Steinmetz, L. M. (2010). High-resolution transcription atlas of the mitotic cell cycle in budding yeast. *Genome Biol*, *11*(3), R24.

Gross, T., Siepmann, A., Sturm, D., Windgassen, M., Scarcelli, J. J., Seedorf, M., ... & Krebber, H. (2007). The DEAD-box RNA helicase Dbp5 functions in translation termination. *Science*, *315*(5812), 646-649.

Gullerova, M., & Proudfoot, N. J. (2008). Cohesin complex promotes transcriptional termination between convergent genes in S. pombe. *Cell*, *132*(6), 983-995.

Gullerova, M., Moazed, D., & Proudfoot, N. J. (2011). Autoregulation of convergent RNAi genes in fission yeast. *Genes & development*, *25*(6), 556-568.

Guttman, M., Rinn, J. Modular regulatory principles of large non-coding RNAs. Nature, 2012. 482 (7385): p. 339-46.

Guydosh, N. R., & Green, R. (2014). Dom34 rescues ribosomes in 3′ untranslated regions. *Cell*, *156*(5), 950-962.

He, L., Hannon, G., MicroRNAs: small RNAs with a big role in gene regulation. Nat Rev Genet, 2004. 5 (7): p. 522-31

Hinnebusch, A. G., & Fink, G. R. (1983). Positive regulation in the general amino acid control of Saccharomyces cerevisiae. *Proceedings of the National Academy of Sciences*, *80*(17), 5374-5378.

Hurt, J. A., Robertson, A. D., & Burge, C. B. (2013). Global analyses of UPF1 binding and function reveal expanded scope of nonsense-mediated mRNA decay. *Genome research*, *23*(10), 1636-1650.

Hogg, J. R., & Goff, S. P. (2010). Upf1 senses 3′ UTR length to potentiate mRNA decay. *Cell*, *143*(3), 379-389.

Johnson, A. W., & Kolodner, R. D. (1995). Synthetic lethality of sep1 (xrn1) ski2 and sep1 (xrn1) ski3 mutants of Saccharomyces cerevisiae is independent of killer virus and suggests a general role for these genes in translation control.*Molecular and cellular biology*, *15*(5), 2719-2727.

Kaikkonen, M., Lam, M., Glass, C., Non-coding RNAs as regulators of gene expression and epigenetics. Cardiovasc Res, 2011. 90(3): p.430-40

Kawashima, T., Pellegrini, M., & Chanfreau, G. F. (2009). Nonsense-mediated mRNA decay mutes the splicing defects of spliceosome component mutations.*Rna*, *15*(12), 2236-2247.

Kawashima, T., Douglass, S., Gabunilas, J., Pellegrini, M., & Chanfreau, G. F. (2014). Widespread use of non-productive alternative splice sites in Saccharomyces cerevisiae. *PLoS Genet*, *10*(4), e1004249.

Kim, T., Xu, Z., Clauder-Muster, S., Steinmetz, L., Buratowski, S. Set3 HDAC mediates effects of overlapping noncoding transcription on gene induction kinetics. Cell, 2012. 150 (6): p.1158-69.

Kurosaki, T., Li, W., Hoque, M., Popp, M. W. L., Ermolenko, D. N., Tian, B., & Maquat, L. E. (2014). A post-translational regulatory switch on UPF1 controls targeted mRNA degradation. *Genes & development*, *28*(17), 1900-1916.

Lee, A., Henras, A. K., & Chanfreau, G. (2005). Multiple RNA surveillance pathways limit aberrant expression of iron uptake mRNAs and prevent iron toxicity in S. cerevisiae. *Molecular cell*, *19*(1), 39-51.

Long, R. M., & McNally, M. T. (2003). mRNA decay: x (XRN1) marks the spot.*Molecular cell*, *11*(5), 1126-1128.

Mattick J. RNA regulation: A new genetics? Nat Rev Genet, 2004. **5**:316–323.

Mitchell, P. and D. Tollervey, An NMD pathway in yeast involving accelerated deadenylation and exosome-mediated 3'-->5' degradation. Mol Cell, 2003. 11(5): p. 1405-13.

Muhlrad, D., & Parker, R. (1999). Aberrant mRNAs with extended 3′ UTRs are substrates or rapid degradation by mRNA surveillance. *Rna*, *5*(10), 1299-1307.

Mosley, A., Pattenden, S., Carey, M., Venkatesh, S., Gilmore, J., Florens, L., Workman, J., Washburn, M. Rtr1 is a CTD phosphatase that regulates RNA polymerase II during the transition from serine 5 to serine 2 phosphorylation. Mol Cell, 2009. 34 (2): p.168-78

Noble, K. N., Tran, E. J., Alcázar-Román, A. R., Hodge, C. A., Cole, C. N., & Wente, S. R. (2011). The Dbp5 cycle at the nuclear pore complex during mRNA export II: nucleotide cycling and mRNP remodeling by Dbp5 are controlled by Nup159 and Gle1. *Genes & development*, *25*(10), 1065-1077.

Parker, R. (2012). RNA degradation in Saccharomyces cerevisae. *Genetics*,*191*(3), 671-702.

Pelechano, V., Steinmetz, L. Gene regulation by antisense transcription. Nat Rev Genet, 2013. 14 (12): p.880-93.

Roy, K., & Chanfreau, G. (2014). Stress-Induced Nuclear RNA Degradation Pathways Regulate Yeast Bromodomain Factor 2 to Promote Cell Survival. PLOS Genetics.

Sayani, S., Janis, M., Lee, C. Y., Toesca, I., & Chanfreau, G. F. (2008). Widespread impact of nonsense-mediated mRNA decay on the yeast intronome. *Molecular cell*, *31*(3), 360-370.

Sayani, S. and G.F. Chanfreau, Sequential RNA degradation pathways provide a fail-safe mechanism to limit the accumulation of unspliced transcripts in Saccharomyces cerevisiae. RNA, 2012. 18(8): p. 1563-72.

Shoemaker, C. J., & Green, R. (2012). Translation drives mRNA quality control.*Nature structural & molecular biology*, *19*(6), 594-601.

Snay-Hodge, C. A., Colot, H. V., Goldstein, A. L., & Cole, C. N. (1998). Dbp5p/Rat8p is a yeast nuclear pore-associated DEAD-box protein essential for RNA export. *The EMBO Journal*, *17*(9), 2663-2676.

Takahashi S., Araki Y., Sakuno, T., Kateda T. Interaction between Ski7p and Upf1p is required for nonsense-mediate 3'-5' mRNA decay in yeast. EMBO J, 2003. 22 (15): p. 3951-9

Takyar, S., Hickerson, R. P., & Noller, H. F. (2005). mRNA helicase activity of the ribosome. *Cell*, *120*(1), 49-58.

Toesca, I., C.R. Nery, C.F. Fernandez, S. Sayani, and G.F. Chanfreau, Cryptic transcription mediates repression of subtelomeric metal homeostasis genes. PLoS Genet, 2011. 7(6): p. e1002163.

Tseng, S. S. I., Weaver, P. L., Liu, Y., Hitomi, M., Tartakoff, A. M., & Chang, T. H. (1998). Dbp5p, a cytosolic RNA helicase, is required for poly (A)+ RNA export. *The EMBO Journal*, *17*(9), 2651-2662.

Tsuboi, T., Kuroha, K., Kudo, K., Makino, S., Inoue, E., Kashima, I., & Inada, T. (2012). Dom34: hbs1 plays a general role in quality-control systems by dissociation of a stalled ribosome at the 3′ end of aberrant mRNA. *Molecular cell*, *46*(4), 518-529.

van Dijk, E.L., C.L. Chen, Y. d'Aubenton-Carafa, S. Gourvennec, M. Kwapisz, V. Roche, C. Bertrand, M. Silvain, P. Legoix-Ne, S. Loeillet, A. Nicolas, C. Thermes, and A. Morillon, XUTs are a class of Xrn1-sensitive antisense regulatory non-coding RNA in yeast. Nature, 2011. 475(7354): p. 114-7.

van Hoof, A., Lennertz, P., & Parker, R. (2000). Three conserved members of the RNase D family have unique and overlapping functions in the processing of 5S, 5.8 S, U4, U5, RNase MRP and RNase P RNAs in yeast. *The EMBO journal*, *19*(6), 1357-1365.

Volinia S., Calin G., Liu C., Ambs S., Cimmino A., Petrocca F., Visone R., Iorio M., Roldo C., Ferracin M., Prueitt R., Yanaihara N., Lanza G., Scarpa A., Vecchione A., Negrini M., Harris C., Croce C. A microRNA expression signature of human solid tumors defines cancer gene targets. Proc Natl Acad Sci USA, 2006. 103 (7): p. 2257-61.

Wang, L., Jiang, N., Wang, L., Fang, O., Leach, L. J., Hu, X., & Luo, Z. (2014). 3′ untranslated regions mediate transcriptional interference between convergent genes both locally and ectopically in Saccharomyces cerevisiae. *PLoS genetics*, *10*(1).

Weng, Y. Czaplinski, K., Peltz, S. Genetic and biochemical characterization of mutations in the ATPase and helicase regions of the Upf1 protein. Mol Cell Biol, 1996. 16 (10): 5477-90

Wilusz, J. Sunwoo, H., Spector, D. Long noncoding RNAs: functional surprises from the RNA world. Genes & Dev, 2009. 23: p. 1494-1504

Zer, C., & Chanfreau, G. (2005). Regulation and surveillance of normal and 3′-extended forms of the yeast aci-reductone dioxygenase mRNA by RNase III cleavage and exonucleolytic degradation. *Journal of Biological Chemistry*,*280*(32), 28997-29003.

Chapter 2—The Rtr1p CTD phosphatase stimulates mRNA decay through a degradation pathway involving Dhh1p and the Rex exonucleases

Domi Hodko[1] , Taylor Ward[1] and Guillaume Chanfreau[1,2]*

[1] Department of Chemistry and Biochemistry, University of California, Los Angeles, Los Angeles, California 90095,USA

[2] Molecular Biology Institute, University of California, Los Angeles, Los Angeles, California 90095,USA

* To whom correspondence should be addressed. Email: guillom@chem.ucla.edu

ABSTRACT

Rtr1p is a phosphatase that impacts gene expression by modulating the phosphorylation status of the C-terminal domain of the large subunit of RNA polymerase II. Here, we show that Rtr1p is a component of a novel mRNA degradation pathway that promotes its autoregulation by turnover of its own mRNA. We show that the 3'UTR of the *RTR1* mRNA contains a cis element that destabilizes this mRNA. *RTR1* mRNA turnover is achieved through binding of Rtr1p to the 3'UTR *cis*-element and by recruitment of the 5'-3' DExD/H-box RNA helicase, Dhh1p by Rtr1p. Rtr1p-mediated turnover of *RTR1* mRNAs also involve the 3'-5' exonuclease, Rex3p, which interacts with Dhh1p. This novel degradation pathway potentially impacts multiple transcripts, including the unspliced BMH1 pre-mRNA. We propose that Rtr1p may imprint its RNA targets cotranscriptionally and determine their downstream degradation mechanism by directing these transcripts to a novel turnover pathway that requires Rtr1, Dhh1 and the Rex family of exonucleases.

INTRODUCTION

Messenger RNA (mRNA) degradation in eukaryotes is a critical part of gene expression control. A single mRNA in a yeast cell may produce thousands of proteins, as on average, there are 4,000 proteins per cognate mRNA (Garcia-Martinez et al. 2007). Cellular mRNA concentrations are thus tightly regulated at both the level of transcription and degradation since even just one fully processed and exported mRNA molecule may drastically impact protein expression. Proteins that bind to specific cis regulatory elements within 3'UTRs play a major role in post-transcriptional regulatory mechanisms (for a review see Glisovic et. al 2008). These RNA binding proteins (RBPs) that bind 3'UTRs play an important role in modulating gene expression through their impact at various steps in the mRNA lifetime including mRNA processing, export, localization, turnover, and translation. Genome-wide targets of the well-characterized PUF proteins and other RPBs have been identified through the use of either affinity purification or UV cross-linking of RNA-protein complexes in vivo (Hogan et al. 2008; Freeburg et al. 2013; Wilinski et al. 2015). These studies have aided in determining the genome-wide impact of RBPs.

RBPs affecting target mRNAs through decay processes normally enhance the degradation of the target mRNA by recruitment of degradation machineries. RBPs have previously been reported to interact with factors involved in various steps in the degradation pathway. Prior to degradation by exonucleases, mRNAs must undergo deadenylation and decapping. As the first step of mRNA decay, deadenylation is first carried out by the Pan2-Pan3 complex and further digested by the Ccr4-Not complex (reviewed in Norbury 2013). Some RBPs, like the PUFs, are known to activate degradation of target mRNAs through their interaction with Pop2p, a member of the Ccr4-Not complex (Goldstruhm et al. 2006; Hyun-Jun et al. 2014). After deadenylation, mRNA may be degraded by the exosome or decapped by Dcp1p/Dcp2p, which are recruited by the Pat1-Lsm1-Lsm7 complex (Tharun et al. 2000;

Bouveret et al. 2000; Coller and Parker 2004). In addition, the cytoplasmic DExD/H-box helicase, Dhh1p, plays a central role in in linking deadenylation and decapping. Many studies have demonstrated the interaction between Dhh1p and components of the Ccr4-Not complex, Pop2p, and the Pat-Lsm1-Lsm7 complex and its role in stimulating decapping (Hata et al. 1998; Coller et al. 2001; Fischer and Weis 2002; Maillet and Collart 2002; Caroll et al. 2011; Sweet et al. 2012). Dhh1p has also been shown to interact specifically with the RBP, Rbp1, to stimulate decay of the *POR1* mRNA suggesting that in some cases, Dhh1p may be a determinant in mRNA decay (Chang and Lee 2011). This is consistent with the observation that tethering Dhh1p to an mRNA is sufficient to target the mRNA for degradation (Carroll et al. 2011).

The main exonucleases recognized to degrade bulk mRNA and mRNAs targeted for decay by specific degradation pathways are the nuclear exosome, the cytoplasmic exosome, the nuclear 5' to 3' exonuclease, Rat1p, and the cytoplasmic 5'-3' exonuclease, Xrn1p (Reviewed in Parker 2012). Xrn1p has been recognized as the cell's workhorse for degrading the bulk of cytoplasmic mRNA in both general and specific degradation pathways (Long and McNally 2003; van Dijk et al. 2011). 5' capped and 3' polyadenylated mRNAs typically undergo deadenylation-dependent decapping prior to processive 5'-3' degradation by Xrn1p. The alternate pathway for degradation involves deadenylation and 3'-5' degradation by the exosome. In addition to the exosome, the RNA Exonuclease factors, or REXs, have homology to the RNase D type exonucleases from E. coli (van Hoof et al. 2000). The Rex proteins, like the exosome, are known to be involved in the 3'-end processing of ncRNAs like snRNAs, the 5S and 5.8S rRNAs, and the RNA component of RNase MRP, but not in the degradation of mRNAs (van Hoof et al. 2000).

In addition to general degradation pathways, mRNA surveillance pathways such as the nonsense mediated mRNA decay (NMD) also regulate gene expression. NMD is initiated

upon the binding of Upf1p to Sup35p at a stop codon recognized as “aberrant” (Czaplinski et al. 1998). The assembly of the other UPF factors, Upf2p and Upf3p, proceeds resulting in the rapid degradation of the transcript usually through deadenylation-dependant decapping followed by 5’-3’ degradation by Xrn1p. NMD takes place independently of Dhh1p (Coller et al. 2001; Fischer and Weis 2002).

Recent research suggests that RNA turnover is tightly connected to transcription, and that mRNA degradation factors influence the rate of transcription and vice versa (Sun et al. 2012; Sun et al. 2013; Haimovich et al. 2014; Braun and Young 2014). Particularly, Xrn1p appears to play an important role in “buffering” mRNA levels by increasing transcription rate, for example, when mRNA degradation rates are slowed (Sun et al. 2013; Medina et al. 2014). Conversely, the transcriptional machinery may “imprint” a transcript with transcription factors that determine the downstream translation or decay rates (Reviewed in Dahan and Choder 2013).

The present study identifies a novel role for the Rtr1p transcription factor in mediating mRNA degradation. Rtr1p, (Regulator of transcription 1), was previously identified as a phosphatase that dephosphorylates Ser5 and Tyr1 of the RNA polymerase II CTD tail, thus establishing a role for this protein in regulating transcription elongation and termination (Gibney et al. 2008; Mosley et al. 2009; Hsu et al. 2014). In this work we show that Rtr1p autoregulates its own mRNA post-transcriptionally and that this degradation pathway involves the 3’ to 5’ exonucleases Rex2p and Rex3p and the Dhh1p helicase. Rtr1p-mediated mRNA decay is a novel mRNA degradation pathway that contributes to the autoregulation of *RTR1* by its own protein product and that also targets unspliced BMH2 pre-mRNAs, and potentially other transcripts genome-wide. We propose that Rtr1p may imprint its mRNA cotranscriptionally and determine its downstream degradation rate by targeting the transcript to this specific turnover pathway. These results identify a novel function for Rtr1p

in controlling gene expression and provide evidence that mRNA decay may take place using non-classical exonucleases.

RESULTS

Rtr1p autoregulates *RTR1* mRNA levels through the use of an element in the 3'UTR

Inspection of data obtained by previous tiling arrays and RNA-Seq analysis of NMD mutants revealed an upregulation of the RTR1 mRNA in these mutants (Sayani et al. 2008; Kawashima et al. 2009). Our initial survey of *RTR1* mRNAs by northern blotting and 3' RACE revealed two major 3' end processing isoforms, $RTR1_L$ and $RTR1_S$. As expected from the faux 3'UTR NMD model, only the longer *RTR1* mRNA isoform with a 3'UTR length of 726 nt. is targeted by the NMD system (Fig. 1a), based on increased accumulation upon deletion of the NMD component Upf1p. We analysed the expression of *RTR1* in the deletion of the nuclear exosome component, *rrp6*Δ, or the double mutant *rrp6*Δ*upf1*Δ because previous work showed the cooperative degradation by the NMD system and the nuclear exosome of certain unspliced mRNAs (Sayani and Chanfreau 2012); however, based solely on these steady-state analyses, *RTR1* mRNAs are targeted only by the NMD system and the nuclear and cytoplasmic exosomes both do not appear to degrade *RTR1* mRNAs (Fig. 1a).

Due to Rtr1p's role in altering the phosphorylation status of Ser5 and Tyr1 of the RNAP II CTD heptad repeat, and given the importance of these residues in the recruitment of transcription termination factors, we explored the possibility that Rtr1p may affect its own 3' end processing site selection. This would impact the size of the 3'UTR, and potentially the susceptibility of the *RTR1* transcripts to NMD. To test this hypothesis, we cloned the *RTR1* 3'UTR and terminator region into a plasmid (pRS404) downstream from the *GFP* ORF expressed from the *TEF1* promoter (Fig. 1b). This construct, GFP-$RTR1_{3'UTR/TER}$,

successfully expresses the *GFP* mRNA with two 3'UTR isoforms, recapitulating the *RTR1* isoforms expressed from the endogenous locus (Fig. 1c). Surprisingly, expressing the *GFP-RTR1*$_{3'UTR}$ mRNA in the *rtr1Δ* strain resulted in an increase in the steady-state abundance of both *RTR1*$_S$ (~5-fold) and *RTR1*$_L$ (~3-fold) in comparison to the wild-type strain (Fig. 1d). Since deletion of Rtr1p affected the overall abundance of both 3'end processing isoforms, we hypothesized that there may be a feature present in the 3'UTR affecting the overall expression or stability of these transcripts. Previous gPAR-CLIP data (Freeberg et al. 2013) had revealed crosslinking sites for cellular RNA binding proteins located 64 to 78 residues downstream of the stop codon within the 3'UTR of *RTR1*. We thus examined the effect of deleting this potential binding site (BS) to determine if RNA binding proteins (RBPs) may affect the posttranscriptional stability of the *RTR1* mRNAs through NMD or another pathway. Strikingly, deletion of the 3'UTR binding site (ΔBS) resulted in an increase in *RTR1* isoform levels that was comparable to the increase observed in the *rtr1Δ* strain (Fig. 1d). Moreover, no further increase in the abundance of these forms was detected in the ΔBS construct expressed in the *rtr1Δ* strain, suggesting that the regulation of *RTR1* mRNA levels through the RBP site depends on Rtr1p. This effect of the 3'UTR binding site on *RTR1* expression was also detected on the endogenous *RTR1* locus as we found that deletion of the binding site (ΔBS) within the 3'UTR of the chromosomal *RTR1* locus using the *delitto perfetto* approach resulted in an increase in the overall abundance of the *RTR1* mRNAs expressed from the endogenous locus (Fig. 1e).

To rule out that the changes in mRNA levels were due to changes in transcriptional output as a result of the absence of Rtr1p, we measured mRNA stability through the use of the transcriptional inhibitor, Thiolutin. In these experiments, a large increase in half-life was observed for the *GFP-RTR1*$_S$ mRNA when either *RTR1*, the 3'UTR binding site, or both the binding site and *RTR1* are deleted, while a more modest increase in half-life is observed for

the *GFP -RTR1*$_{L}$ mRNA (Fig. 2a). As described previously with steady state assays, the effect of deleting *RTR1* appears to be epistatic to deleting the binding site within the plasmid-borne mRNA. This result provides genetic evidence that Rtr1p participates in the auto-regulation of its own mRNAs via modulation of posttranscriptional stability of *RTR1* through its 3'UTR sequence. The effect of the 3'UTR element on *RTR1* stability was also detected on *RTR1* transcripts expressed from the endogenous locus. Utilizing a galactose driven promoter to shut-off transcription of the *RTR1* chromosomal copy, we detected an increase in the half-life of both the long and short *RTR1* isoforms in the ΔBS mutant as compared to the wildtype 3'UTR (Fig. 2b).

Because gPAR-CLIP unambiguously defines crosslinking sites of all RBPs genome-wide, we aimed to determine the identity of the RBP that contributes to degradation of the *RTR1* mRNAs by binding to this 3'UTR element. Since the sequence of the *RTR1* 3'UTR BS closely resembles the consensus element for Puf1p and Puf2p binding sites, we tested the deletion of the individual *PUF* genes, *puf1Δ puf2Δ*, as well as a deletion mutant of five *PUF* genes, *5Δ pufs (*Hogan et al. 2008). None of these mutants showed substantial changes in steady-state mRNA abundance as compared to the isogenic WT strain (Fig. 3a). Additionally, deletion mutants of several other characterized RBPs, including *rbp1Δ,* likewise resulted in a lack of increase in the steady-state abundance of *RTR1* mRNAs (Fig. 3b). Based on these results and on the epistatic effects of the *RTR1* and 3'UTR element deletions, we hypothesized that Rtr1p might bind this 3'UTR element to regulate the stability of its mRNAs. We thus investigated the ability of Rtr1p to associate with *RTR1* 3'UTR-containing mRNAs by testing the association of an N-terminally tagged 3X-FLAG-Rtr1p with the *GFP-RTR1*$_{3'UTR}$ mRNA *in vivo* using RNA immunoprecipitation (RIP). Because the Rtr1p phosphatase associates with the large subunit of RNA polymerase II, we controlled for the possibility that Rtr1p may associate with any mRNAs in complex with RNAPII at the site of

transcription by also determining the association of FLAG-Rtr1p with a GFP mRNA containing the *TEF1* 3'UTR, or the *RTR1* 3'UTR lacking the 3'UTR binding site (ΔBS). As determined by RT-qPCR (see materials and methods), FLAG-tagged Rtr1p showed an approximately 8-fold increase in association with *GFP-RTR1*$_{3'UTR}$ over the "no-tag" control and a two- to three-fold increase in association over the *GFP-TEF1*$_{3'UTR}$ or *GFP-RTR1*$_{3'UTR,\ \Delta BS}$ (Fig. 4a). We thus conclude from these results that Rtr1p autoregulates its mRNA abundance through physical association with its mRNA, which is strongly dependent on the presence of the 15 nt. binding site in the 3'UTR. Whether or not this RNA element corresponds to a direct binding site for Rtr1p remains to be determined.

Dhh1p interacts with Rtr1p and facilitates decay of *RTR1* mRNAs

We gained insight into potential degradation factors that may participate in the Rtr1p-mediated decay of its own mRNAs through a previous study that performed mass-spectrometry analysis of proteins associated with Rtr1p (Smith-Kinnaman et al. 2014). In that study, Rtr1p was found to associate with the DEAD-box helicase, Dhh1p. Additionally, tethering Dhh1p to various mRNAs has been shown to result in an increase in their turnover and also decreased protein levels (Carroll et al. 2011). Based on these observations we hypothesized that Dhh1p could facilitate degradation of the *RTR1* mRNA through its interaction with Rtr1p. Indeed, we detected the association of Rtr1p with Dhh1p by coimmunoprecipitation using tagged strains (3X-FLAG-RTR1 and HA-tagged Dhh1p (Fig. 4b). Furthermore, we show that Rtr1p interacts with Dhh1p independently of any RNAs that may link the association since its association with Dhh1p was unaffected by RNase A treatment (Fig. 4c).

To further demonstrate the impact of Dhh1p on *RTR1* decay, we analysed the effect of Dhh1p absence on *RTR1* mRNA levels. Deletion of *DHH1* resulted in a two-fold or more increase in the *RTR1* mRNA levels; this increased accumulation was not the result of Dhh1p's general role in mRNA decay (Fig. 5a) because Dhh1p inactivation had no effect on transcripts bearing the *RTR1* 3'UTR lacking the binding site. In addition, deletion of *RTR1* in the *dhh1Δ* strain does not result in a further increase in accumulation of either the WT *RTR1* 3' UTR mRNAs or the ΔBS mRNAs. Additionally, a transcription shut-off assay with the Gal system in the *dhh1Δ* strain demonstrates similar half-lives for the decay of the WT and ΔBS *RTR1* mRNAs, further evidencing that deletion of *DHH1* negates the effect of the deletion of the binding site (Fig. 5b). Taken together, these data demonstrate that Dhh1p is involved in the Rtr1p-dependent turnover pathway of *RTR1* mRNAs.

The Rtr1p binding element is required for degradation of *RTR1* mRNAs by Rex2p and Rex3p

To determine the downstream factors that are responsible for degrading the *RTR1* mRNAs through the 3'UTR binding site, we tested several exonuclease mutant strains. Inactivating exonucleases specifically involved in *RTR1* decay through its 3'UTR binding site element should result in an increase in steady-state abundance of the WT *GFP-RTR1*$_{3'UTR}$ mRNA but not the *GFP-RTR1*$_{3'UTR,\ \Delta BS}$ mRNA. We found that deletion of the *XRN1* gene coding for the major cytoplasmic 5'-3' exonuclease Xrn1p, resulted in a large synergetic increase in steady-state abundance when combined with the deletion of the binding site (Fig. 6a). This results showed that the Rtr1p-dependent degradation pathway is not epistatic to the deletion of *XRN1* and that another exonuclease is responsible for the Rtr1p-mediated turnover pathway. Because the steady-state abundance of endogenous *RTR1* mRNAs does not increase in either deletions of the nuclear exosome component, Rrp6, or the cytoplasmic exosome component,

Ski2, (Fig. 1a), we tested other exonucleases and focused on the Rex family of exonucleases. Implicated in the processing of 3' ends of noncoding RNAs and having purported 3'-5' exonuclease activity (van Hoof et al. 2000), we postulated that the Rex factors could also participate in the degradation of mRNAs. To our surprise, deletion of *REX2* in combination with *REX3* resulted in an increased abundance of the *GFP-RTR1*$_{3'UTR}$ (Fig. 6b) and the endogenous *RTR1* mRNAs, while a triple deletion mutant, *rex1Δ rex2Δ rex3Δ*, did not exhibit further accumulation (Fig. 6b). Furthermore, the *GFP-RTR1*$_{3'UTR}$ and *GFP-RTR1*$_{3'UTR,\ \Delta BS}$ mRNAs accumulated to the same degree in the *rex2Δ rex3Δ* strain indicating that Rex2p and Rex3p are most likely responsible for the degradation of Rtr1p-targeted mRNAs through their 3'UTR. To ensure that the effects detected in the rex mutants were due to turnover defects, we demonstrated an increase in the half-life of the *RTR1* mRNAs in the *rex2Δ rex3Δ* strain as determined by a transcription shut-off assay with the Gal system controlling transcription of the endogenous *RTR1* gene (Fig. 6c). Overall these results demonstrate that the Rex2p and Rex3p proteins contribute to the degradation of *RTR1* mRNAs through a pathway dependent on the presence of the 3'UTR binding site recognized by Rtr1p.

We also analysed the interaction of Dhh1p with the Rex2 and Rex3 exonucleases, which facilitate the degradation of *RTR1* mRNAs. We utilized TAP-tagged *REX2* and *REX3* strains to perform Calmodulin Binding Protein (CBP) pull-down of these proteins using calmodulin beads, and tested for the co-precipitation of proteinA-tagged Dhh1p. This pull-down assay showed that Dhh1p appears to interact solely with Rex3p and not Rex2p in "wildtype" cells (Fig. 6d). This result was somewhat unexpected considering the previous results, which implicated an overlapping function of Rex2p and Rex3p in the degradation of *RTR1*. However this result suggests that the main degradation factor recruited by Dhh1p might be Rex3p.

Rtr1p-mediated decay potentially targets multiple classes of RNAs

We hypothesized that Rtr1p may play a role in the degradation of other cellular RNAs and performed a blast search of the 3'UTR cis element found in the *RTR1* 3'UTR (Fig. 7a). This search identified potential Rtr1p binding sites in RNAs expressed from a variety of genetic loci (ORFs, UTRs, and ncRNAs; Fig.7A). Of the various RNAs showing a sequence resembling the Rtr1p binding site, we tested the *BMH2* 5'UTR intron for accumulation of steady-state levels in the *rtr1Δ*, *dhh1Δ*, *rtr1Δdhh1Δ* strains by northern blotting with a probe specific for the intron-containing mRNA and by realtime reverse transcriptase PCR (RT-qPCR). Our results show a moderate (~1.5 fold) increase of the *BMH2* pre-mRNA in the *rtr1Δ* strain compared to the WT. Strikingly, there was no increase in steady-state level in the *rtr1Δdhh1Δ* double mutant compared to the single *dhh1Δ* mutant (Fig. 7b). Previous tiling array and RNA-seq data shows that the *BMH2* pre-mRNA is also an NMD target (Sayani et al. 2008; Kawashima et al. 2009), suggesting that Rtr1p-mediated decay of the BMH2 unspliced pre-mRNA may cooperate with NMD to degrade these unspliced transcripts. Indeed, a much larger increase in unspliced BMH2 was detected in the *rtr1Δ* mutant compated to WT when NMD was inhibited by the translation elongation inhibitor, cyclohexamide (CHX) (Fig. 7b). This demonstrates that the impact of Rtr1p on the *BMH2* pre-mRNA is greater when the impact of NMD degradation on the unspliced species is diminished by translational inhibition. These results also show that Rtr1p-mediated decay may impact a larger number of transcripts than the Rtr1p transcripts.

DISCUSSION

In this study we report a novel role for the RNA pol II CTD Ser5 and Tyr1 phosphatase Rtr1p in an mRNA degradation pathway that autoregulates its own mRNA, and might also regulate a specific class of cellular transcripts. This pathway depends on the recognition of a cis element by Rtr1p, utilizes the Rex2p/Rex3p factors for degradation, and suggests a novel mechanism for the 5'-3' DExD/H-box RNA helicase, Dhh1p in promoting mRNA degradation through Rex proteins recruitment. Using a reporter system, we have demonstrated that the deletion of *RTR1* directly affects the degradation of a *RTR1* 3'UTR – containing mRNA. In our model, the binding of Rtr1p to the *RTR1* mRNP complex acts as a scaffold for the assembly of other mRNA degradation factors (Fig. 8). We propose that the interaction of Rtr1p with Dhh1p occurs upstream of the recruitment of Rex3p and deadenylation. Dhh1p at this stage may serve to remodel the mRNP complex to prime it for degradation. Subsequently, the interaction of Rex3p with Dhh1p serves to recruit the exonuclease to degrade the mRNA. Thereby, the binding of Rtr1p to *RTR1* mRNAs controls the overall expression by targeting a portion of the *RTR1* mRNA population for degradation in response to increasing Rtr1p protein levels. Given Rtr1p's localization to the site of transcription, an attractive hypothesis may be that Rtr1p is deposited onto the mRNA co-transcriptionally and may then potentially target the mRNP for degradation. As the binding site for Rtr1p is transcribed in the 3'UTR region, Rtr1p may then get imprinted onto the transcript thus altering its posttranscriptional stability. If this is the case, the RNAP II CTD tail may compete with the binding element for Rtr1p. For the *RTR1* transcript, an over-abundance of Rtr1p near the site of transcription would lead to a reduction of mRNA overall via the downstream degradation pathway. In other cases, this may serve as an efficient quality-control mechanism to mark unspliced mRNAs like the *BMH2* pre-mRNA for degradation.

We have shown that Rtr1p associates with the mRNP complex of this mRNA and negatively regulates its stability. Though the *in vivo* association of Rtr1p with its own 3'UTR is clear, we have not resolved whether the binding to the mRNP is due to a direct interaction with the binding element or whether the interaction takes place through the aid of an unidentified RBP. While Rtr1p does not have homology to any known RNA binding domain and an X-ray crystal structure of Rtr1p also did not necessarily reveal an RNA binding domain, it may be that the binding of Rtr1p to its target sequence, if direct, may occur in a noncanonical fashion and possibly through a disordered region (Hsu et al 2014). Recent evidence suggests that a large population of previously unrecognized RBPs exist among metabolic enzymes and other factors not specifically recognized as being involved in RNA metabolism (Scherrer et al. 2010; Tsvetanova et al. 2010). Utilizing two approaches to UV crosslinking of RBPs to RNA, over 300 new RBPs have been discovered in HeLa cells, many of which are involved in metabolic processes (Castello et al. 2012). Unusually, these proteins may interact with RNA through repetitive and disordered regions or other non-classical domain architectures (Castello et al. 2012; Neelamraju et al. 2015). Further, analysis of RIP-ChIP data sets has revealed that up to a third of known RBPs may posttranscriptionally autoregulate their own mRNAs including PUF1, PUF2, PUF3, and PUF4 (Janga and Mittal 2011). This suggests that in addition to regulating other mRNA targets, autoregulatory feedback loops may be a common way for proteins to regulate their own intracellular concentrations. Rtr1p may fall into this category as well.

Whether direct or indirect, the binding of Rtr1p to the mRNP complex containing the 3'UTR and binding site is of significance to the regulation of the *RTR1* mRNA stability. This Rtr1p-mediated decay pathway, intriguingly, does not involve the well-characterized 5'-3' cytoplasmic decay pathway nor 3'-5' decay by the cytoplasmic or nuclear exosome. Rather, we find that the degradation of *RTR1* by the Rtr1p-mediated decay pathway requires Rex2p

and Rex3p. Known for their role in trimming the 3' ends of noncoding RNAs, we find a novel role for these purported exonucleases in the degradation of mRNA. While the *RTR1* mRNA accumulates to similar abundances in the *rex2*Δ or *rex3*Δ single mutants, we find that Dhh1p interacts only with Rex3p in our pulldown assay suggesting that Rex3p may normally be the predominant exonuclease acting in this pathway. Thus it is possible that Rex2p only degrades the *RTR1* mRNA in the absence of Rex3p.

In this study we observe that Rtr1p-mediated decay of *RTR1* mRNA requires *DHH1*. The deletion of *DHH1* was epistatic to the deletion of both the binding site and *RTR1* itself. Here, and in a previous study (Smith-Kinnaman et al. 2014), it has been determined that Rtr1p interacts with Dhh1p providing biochemical evidence that Dhh1p is involved in this decay pathway. Given that Dhh1p interacts with members of the Ccr4-Not deadenylase complex, a plausible role for Dhh1p's involvement would be to stimulate deadenylation of the *RTR1* mRNA prior to degradation by Rex2p/Rex3p (Coller et al. 2001; Fischer and Weis 2002; Maillet and Collart 2002). On the other hand, previous studies based on a *PGK1* reporter mRNA have concluded that Dhh1p acts downstream of deadenylation to stimulate decapping (Fischer and Weis 2002). Another study found that the enhanced degradation of an mRNA tethered to Dhh1p was independent of *CCR4* but not *XRN1* or other factors involved in 5'-3' decay (Carroll et al. 2011). Other evidence suggests that the greatest amount of impairment in deadenylation results from deletion of both *CCR4* and *PAN2* and thus it is also possible that deadenylation may still occur in absence of *CCR4* by the *PAN2-PAN3* deadenylases (Tucker et al. 2002; reviewed in Wahle and Winkler 2013). The involvement of Dhh1p in Rtr1p-mediated decay, however, may involve a distinct mechanism, since normally, the action of Dhh1p in the degradation of mRNAs requires the 5'-3' decay machinery which we have shown is not involved to Rtr1p-mediated decay. Rtr1p-mediated decay is also distinct from the previously established decay pathway involving Rbp1p, which degrades the

POR1 mRNA and also interacts with Dhh1p, since a deletion of *RBP1* does not affect *RTR1* mRNA levels (Fig. 4) (Chang and Lee 2011). Dhh1p may alternatively stimulate the decay of the *RTR1* mRNA through its recruitment of Rex3p. Deadenylation may take place prior to this step and may be activated by another mechanism; though, we have not formally ruled out the possibility that Rex3p may digest the poly(A) tail and degrade the full-length mRNA.

In summary, Rtr1p-mediated decay is a novel mRNA degradation pathway that utilizes non-canonical exonucleases for degradation and may contribute to the stability and quality control of diverse RNAs, since the Rtr1p binding element was potentiall found in a variety of cellular RNAs. Since we do not know the precise sequence determinants for Rtr1p binding, the list presented in Fig.7A might correspond only to a small subset of the actual population of RNAs targeted by Rtr1p-mediated decay.

MATERIAL AND METHODS

Plasmid and strain construction

All strains used in this study are listed in Supplementary Table 1. All oligonucleotides utilized for plasmid and strain construction are listed in Supplementary Table 2. Strains were constructed using standard PCR-based homologous recombination in yeast as described on the Geitz lab website (http://home.cc.umanitoba.ca/~gietz/). Single gene knockouts or promoter replacements were done with cassettes amplified from the pFA6a-kanMX6 or pFA6a-kanMX6-PGal1 (Longtine et al. 1998). The *rtr1*Δ was made using the CORE cassette (Storici and Resnick 2006). The *rex2*Δ, *rex3*Δ, *rex2*Δ*rex3*Δ and *rex1*Δ*rex2*Δ*rex3*Δ strains were constructed using the delitto perfetto approach (Storici and Resnick 2006). The 3X-FLAG-RTR1 strain was constructed by inserting the CORE cassette in between the ATG and

second codon of the *RTR1* ORF. The CORE cassette was excised with complementary IROs containing the 3XFLAG sequence and sequences homologous to the region flanking the CORE insertion site. The 3' ends of the complementary IROs were extended using the Phusion High Fidelity DNA polymerase (NEB, Ipswich, MA, USA). The RTR1-3'UTR-ΔBS strain was generated by the delitto perfetto method as well (Storici and Resnick 2006).

The pRS404-GFP-RTR1$_{3'UTR/TER}$ was made using the pRS404-PTEF-AGO1 plasmid purchased from Addgene. First, the GFP ORF was amplified from pFA6a-GFP(S65T)-HIS3MX6 plasmid with oligonucleotides that have 40nt 5' overhangs homologous to the regions flanking the *RTR1* ORF. This PCR product was transformed into the *rtr1*::CORE strain by the delitto perfetto approach (Storici and Resnick 2006). The gDNA from this strain was used to amplify the *RTR1* ORF, 3'UTR, and Terminator PCR product that was inserted into the SpeI/MluI sites of pRS404-PTEF-AGO1. The pRS404-GFP-TEF1$_{3'UTR/TER}$ was constructed by amplifying the GFP ORF from pFA6a-GFP(S65T)-HIS3MX6 and inserting the PCR product into the SpeI/XhoI sites of pRS404-PTEF-AGO1.

RNA extraction and Northern blotting

All RNA extractions and northern blots were performed as described previously (Sayani and Chanfreau 2012). Oligonucleotides used to generate riboprobes are listed in Supplementary Table 2. The *scR1* ncRNA was probed for using the listed oligonucleotide, which was incubated with T4 PNK (NEB, Ipswich, MA, USA) and □-^{32}P-ATP (Perkin Elmer) prior to hybridizing to the membranes.

3'RACE and Sequencing

The 3' RLM-RACE kit (Thermo Fischer Scientific, Waltham, MA, USA) was used for determining the 3'ends of *RTR1* mRNAs. The custom forward primer contained a BamHI site

along with the provided reverse anchor primer. The 3'RACE products were ligated into the BamHI site in the pUG35 plasmid and transformed into competent DH5-α *E. coli* for sequencing.

Transcription shut-off assays

Transcription was inhibited by the transcription inhibitor, Thioloutin (Enzo Life Sciences, Farmingdale, NY, USA) at a final concentration of 3 μg/mL as described previously (Pelechano and Pérez-Ortín). We tested 3, 6, 10, and 18 μg/mL Thiolutin and saw little effect on the *RTR1* half-lives. Samples were harvested by centrifugation at 3000 RPM for 1.5 min and transferred to 2mL screw-cap tubes for RNA extraction. Samples were flash frozen in N_2 (l) and stored in -20°C prior to RNA extraction.

For measuring half-lives of the *RTR1* mRNAs with the GAL-RTR1 strains, overnight cultures were grown in YPGAL and back-diluted the next day to OD 0.05. When the cultures reached OD 0.4-0.5, the cells were spun down and resuspended in 20 mL YP media lacking sugar. A 2mL zero minute time point was taken just prior to shifting the culture to 4% dextrose. To begin transcription shut-off at the GAL promoter, the remaining 18mL of YP culture was added to a flask containing 3.6mL 20% Dextrose. Time points were taken by centrifuging 2mL samples in screw-cap tubes, removing the supernatant, and flash freezing the cells in N_2 (l). This protocol was adapted from the Coller lab protocol book (http://www.case.edu/med/coller/Coller%20Protocol%20Book.pdf).

RNA Immunoprecipitation and RT-qPCR

Overnight cultures for each sample were back diluted to 0.05 and then grown to OD 0.5. When the cultures reached OD 0.5, 20 OD units were harvested from each culture (~40mL). The samples were pelleted then washed with 10mL cold ddH_2O. Pellets were spun down and

then resuspended in 1 mL cold ddH_2O and transferred to a 2 mL eppendorf tube. The supernatant was removed and the pellet was frozen at -80°C.

The pellets were thawed resuspended in 600 µL NET-2 Buffer (40mM Tris-HCl pH 7.5, 150mM NaCl, and 0.05% IGEPAL). 12 µL of 50X protease inhibitor cocktail was added (Roche Diagnostics, F. Hoffman-La Roche Ltd, Switzerland) along with glass beads. The tubes were then vortexed 5 times at 4°C for 45s each time with 45s intervals on ice between each vortexing. The eppendorf tubes were then pierced with a 23G flamed needle at the bottom of the tube and placed into a 2mL screw cap tube. The tubes were taped together and spun down for 1 minute at 3000 rpm to allow the lysate to flow from the top to the bottom tube. Samples were then centrifuged for 20 minutes at 4°C at maximum speed to pellet the insoluble fraction. The supernatant was transferred to a clean eppendorf tube and the total protein/RNA was then quantiated by Nanodrop (Thermo Fischer Scientific, Waltham, MA, USA). 2.5 OD units of each sample was then used for immunoprecipitaiton and 2.5 OD units was also used for the input by directly extracted with Phenol/Chloroform/Isoamyl alcohol (PCA). To prepare the input total RNA, the volume of each sample was raised to 400 µL with NET-2 buffer and 40 µL 3M sodium acetate and 5 µL 20% SDS were added. 400 µL PCA was added and vortexed for 1 minute. The samples were spun for 3 minutes at maximum speed. The supernatant was transferred to a tube containing 1 mL 100% ethanol and 1 µL Glycoblue (Ambion, Carlsbad, CA, USA). The samples were precipitated overnight at -80°C, spun at maximum speed for 10 minutes, and washed with 70% ethanol prior to resupsending in 15 µL RNase-free water (Ambion, Carlsbad, CA, USA).

The immunoprecipitation was done by conjugating the FLAG antibody (M2 monoclonal antibody from Sigma) to Protein G Sepharose beads (4 Fast Flow by GE Healthcare, Piscataway, NJ, USA). The Protein G sepharose beads (20 µL per sample) were

first washed with NET-2 buffer twice and resupsended to 400 µL with NET-2 buffer. 5 µL of FLAG antibody per sample was added to the tube and the mixture was rotated for 1 hr at 4°C. After conjugation, the beads were washed twice with NET-2 buffer and aliquoted in separate tubes for each sample. 400 µL of 2.5 OD RNA/protein lysate for each sample was added to the aliquoted beads and the mixture was rotated for 1 hour at 4°C. The beads were then washed four times with 1mL cold NET-2 buffer each time and resupsended in 400 µL NET-2 buffer after the fourth wash. 400 µL PCA, 40 µL 3M sodium acetate,and 5 µL 20% SDS was then added directly to the beads/NET-2 buffer and the RNA was extracted the same as for the input RNA.

RNA was reverse transcribed with the Superscript III First-Strand synthesis kit (Life Technologies, Carlsbad, CA, USA). The cDNAs were diluted ten-fold and 1µL of each cDNA was used for qPCR. qPCR was performed using the GFP TaqMan assay and the TaqMan Universal Master Mix II, with UNG (Applied Biosystems, Foster City, CA, USA). The qPCR runs were done on the Bio-Rad CFX Connect Realtime PCR detection system. The GFP TaqMan assay was validated using serial dilutions of the pFA6a-kanMX6-GFP plasmid across six orders of magnitude. The PCR efficiency was then calculated using the CFX Manager software to be 94.6%.

Co-Immunoprecipitation and Pulldown assays

1L cultures of 3X-FLAG-RTR1 or WT strains harbouring the BG1805-DHH1 plasmid (Yeast ORF collection from Dharmacon) were grown in SGAL-URA and harvested at log phase, OD 0.6. The cultures were spun down and resuspended in 10mL cold IPP150 buffer (10mM TRIS-HCl pH8.0, 150mM NaCl, and 0.1% IGEPAL). The cells were then dripped into ~400mL N_2 (l) in a Nalgene beaker. After freezing the cell suspension, the samples were stored at -80°C. The cells were then mechanically lysed in N_2 (l) using the Retsch MM400

with 4 cycles of shaking at 12hz for 3 minutes each. Between cycles, the capsule was incubated in in N_2 (l). The powdered cells were then transferred to centrifuge tubes, allowed to thaw on ice for about 1 hour, and spun at 12,000 RPM (JA 25.50 rotor) for 10 minutes with the Beckman-Coulter centrifuge set at -8°C. After the insoluble fraction was pelleted, the supernatant was transferred to 15 mL falcon tubes and protease inhibitor was added to 1X concentration. 500 µL aliquots from each sample were precipitated with TCA for the input. Anti-FLAG conjugated to Protein G sepharose beads were added to the supernatant samples and the complexes were precipitated at 4°C overnight in the presence of Protease 3C. The next day, the beads were washed four times with cold IPP150 buffer. The beads were transferred after the last wash to a clean eppendorf tube and boiled in Thorner buffer (40mM TRIS pH 8, 5% SDS, 8M Urea, 100 µM EDTA). Western blotting was carried out using an an HA antibody.

REX2-TAP and REX3-TAP strains were purchased from GE Dharmacon (Lafayette, CO, USA). These strains or the wt strain were transformed with the BG1805-DHH1 vector. 1L cultures were grown in SGAL-URA and harvested at log phase, OD 0.6. The calmodulin pulldown assay was performed the same as the Anti-FLAG co-IP, except the lysate was applied to Calmodulin Sepharose 4B beads (GE Healthcare, Piscataway, NJ, USA) without antibodies. IPP150 Calmodulin binding buffer (10mM β-mercaptoethanol, 10 mM TRIS-HCl pH8.0, 150 mM NaCl, 1mM Mg-acetate, 1mM imidazole, 2mM $CaCl_2$, and 0.1% IGEPAL) was used in lieu of IPP150 for the pulldown. Western blotting for these experiments was done using an proteinA antibody.

ACKNOWLEDGEMENT

We thank Dr. Roy Parker and his lab for providing us with the PUF mutant strains. We also thank Dr. Isabelle Toesca for her contribution in the *rex*Δ mutant strain construction.

FIGURES AND TABLES

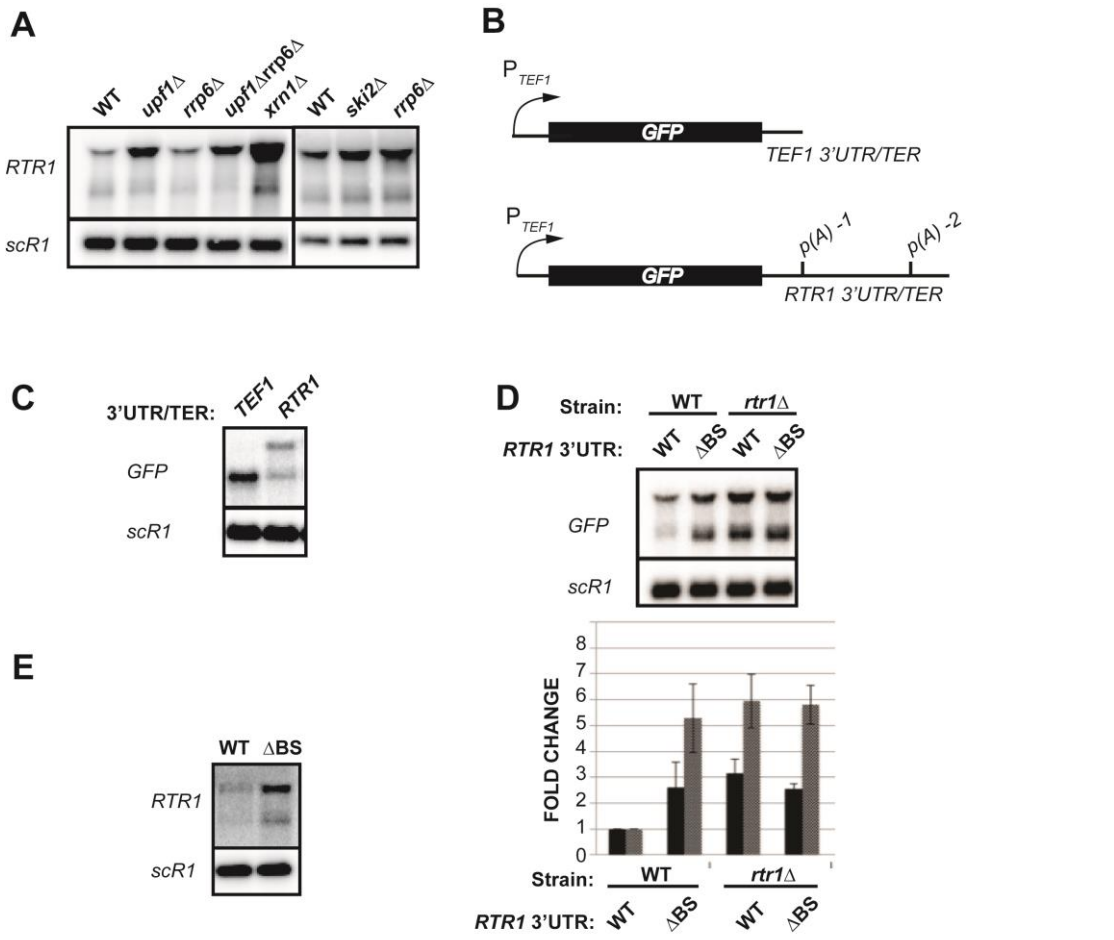

Figure 1. Analysis of *RTR1* mRNAs or *RTR1* 3'UTR-containing mRNAs in steady state conditions **(A)** Northern blot analysis of steady-state *RTR1* mRNAs in mRNA degradation mutants detected using an *in vitro* transcribed ^{32}P-radiolabeled RNA antisense to the *RTR1* ORF (riboprobe). Cultures were grown in YPD prior to harvesting during log phase at OD 0.4-0.5. A representative northern blot is shown of two independent biological replicates. **(B)** Schematic representation of the GFP-TEF1$_{3'UTR/TER}$ or the GFP-RTR1$_{3'UTR/TER}$ cloned into the pRS404 vector. **(C)** Northern blot analysis of WT BMA64-a strains harbouring the GFP-TEF1$_{3'UTR/TER}$ or the GFP-RTR1$_{3'UTR/TER}$ plasmids. Cultures were grown in SD-TRP, harvested at OD 0.4-0.5, and the northern blots were probed with an *in vitro* transcribed ^{32}P-

radiolabeled RNA antisense to the *GFP* ORF. A representative northern blot of two independent biological replicates is shown. **(D)** Northern blot analysis of WT or *rtr1*Δ cells transformed with either the GFP-RTR1$_{3'UTR/TER}$ or *GFP-RTR1*$_{3'UTR, \Delta BS}$ plasmids. The graph below plots the average values of steady state *RTR1*$_L$ (black columns) or *RTR1*$_S$ (grey columns) mRNAs with standard deviations resulting from three biological replicates. Relative intensity for each sample was normalized to the *scR1* loading control prior to normalizing the fold change to the WT/ GFP-RTR1$_{3'UTR/TER}$ sample. **(E)** Steady-state analysis of the endogenous *RTR1* 3'UTR cis element deletion (ΔBS) as compared to the WT strain. Cultures were grown in SDC, harvested at log phase at OD 0.5, and northern blotting was performed with the *RTR1* riboprobe. A representative northern blot of two independent biological replicates is shown.

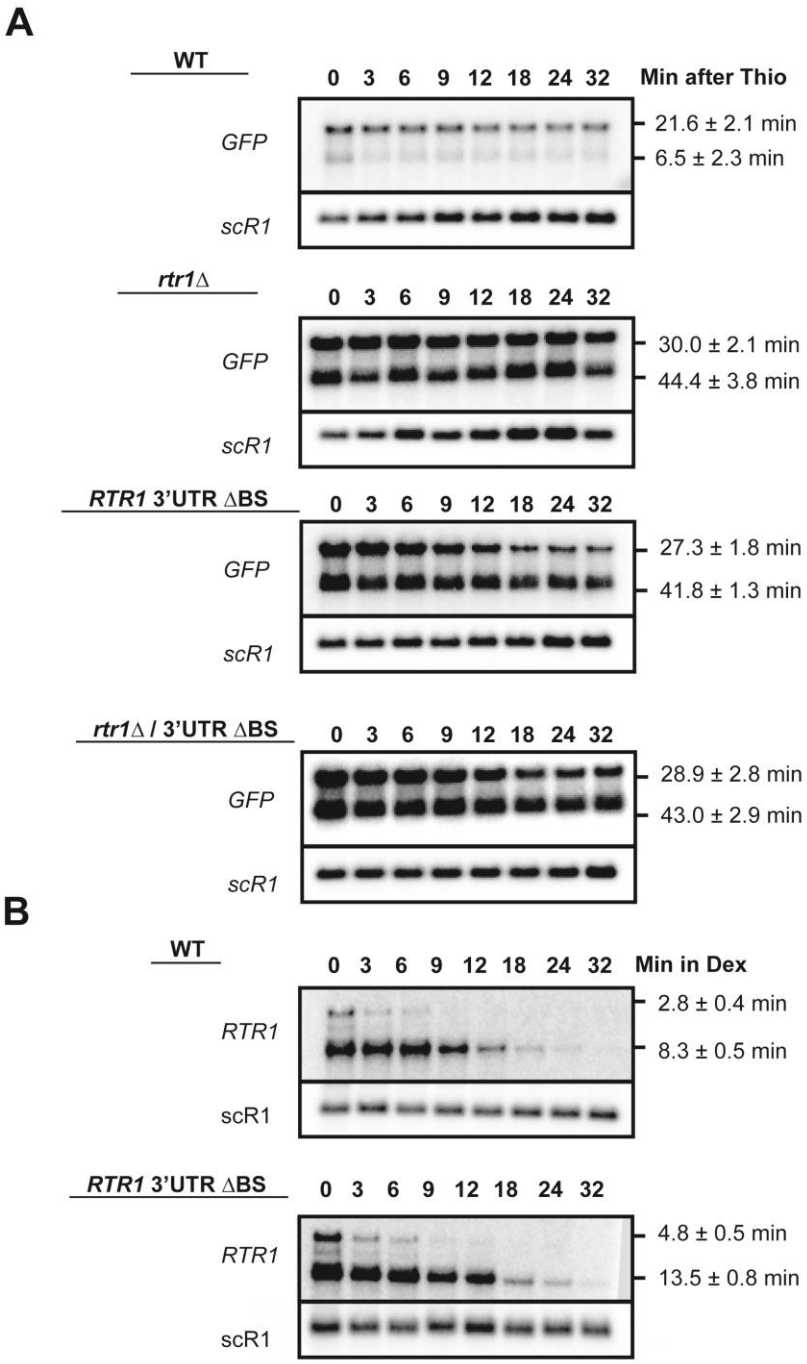

Figure 2. Transcription shut-off analysis of plasmid-borne or endogenous mRNAs. All calculated half-lives are the average of three independent biological replicates with standard deviation and shown at the right side of the blot. **(A)** Posttranscriptional stability of the *RTR1* containing mRNAs determined by addition of 3 μg/mL Thiolutin during log phase, OD 0.5. The WT or *rtr1*Δ strains were used with either the WT *RTR1* 3'UTR/TER plasmid or ΔBS *RTR1* 3'UTR/TER. Time points were harvested at the indicated times. **(B)** The GAL1

promoter was integrated into the *RTR1* locus upstream of the ORF in either the WT or ΔBS strains. Posttranscriptional stability of the endogenous *RTR1* transcripts expressed from the GAL1 promoter was subsequently determined by shifting the cultures from 2% Galactose to 4% Dextrose and harvesting samples at the indicated time points.

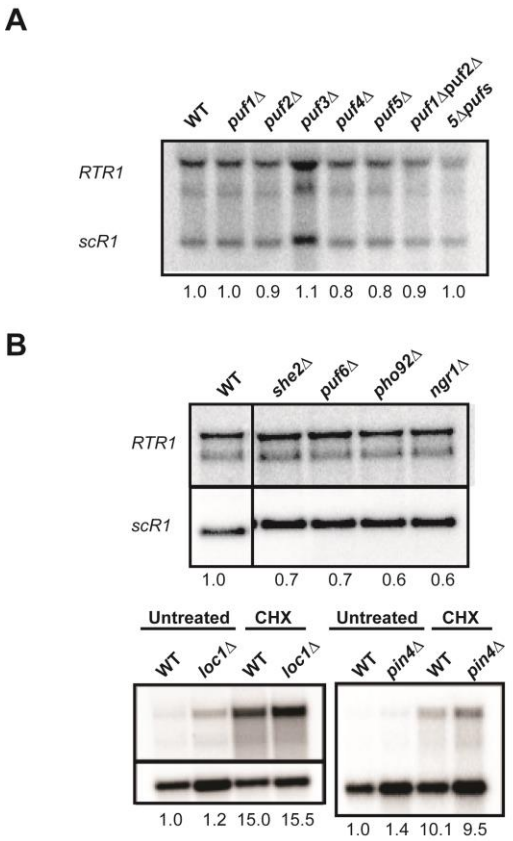

Figure 3. Steady-state analysis of RBP deletion strains by northern blotting. Representative northern blots of two independent biological replicates are shown. **(A)** *puf1*Δ, *puf2*Δ, *puf3*Δ, *puf4*Δ, *puf5*Δ, *puf1*Δ *puf2*Δ, or the *5*Δ*pufs* (quintuple deletion mutant of PUFs 1-5) were grown along with the isogenic wildtype strain in YPD and harvested in log phase at OD 0.5. Northern blot analysis was carried out with the *RTR1* ORF riboprobe. **(B)** The experiment was carried out exactly as in (A), except that, *loc1*Δ and *pin4*Δ were also subjected to CHX treatment for 20 minutes. All lanes shown in the left panel were from the same northern blot, but irrelevant lanes in between WT and *she2*Δ were omitted.

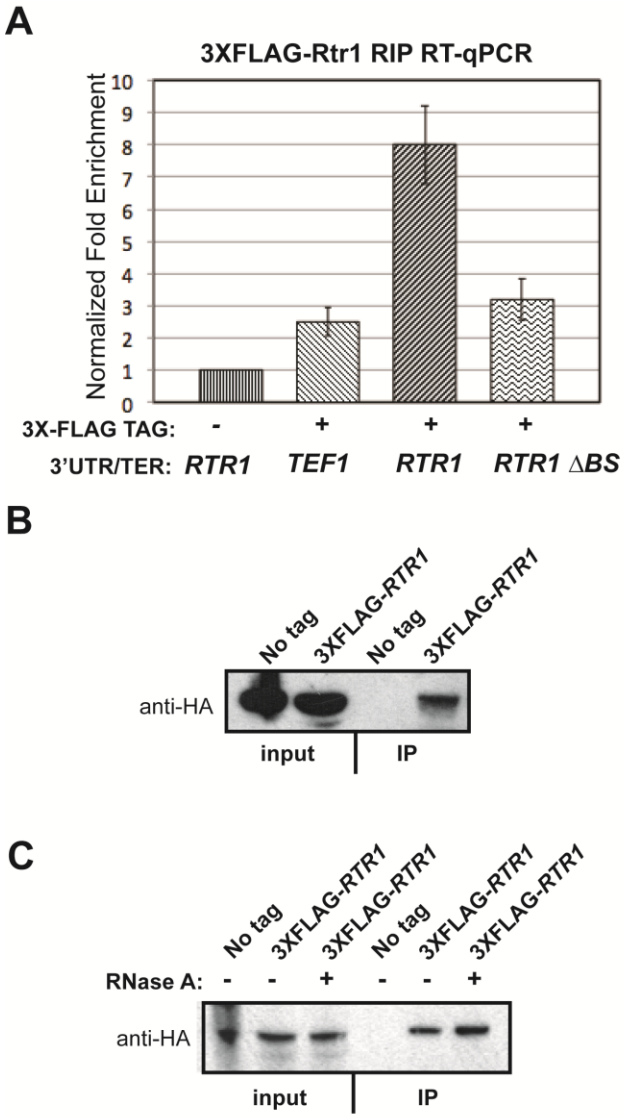

Figure 4. Association of 3X-FLAG tagged Rtr1p with the *RTR1* 3'UTR –containing *mRNP* complex and tagged Dhh1p. **(A)** RNA immunoprecipitation (RIP) assay performed using the endogenously tagged 3X-FLAG-*RTR1* strain. Cultures were grown in SD-TRP to maintain either the GFP-TEF1$_{3'UTR/TER}$, GFP-RTR1$_{3'UTR/TER}$, or *GFP-RTR1$_{3'UTR, \Delta BS}$ plasmids.* A WT strain with the WT GFP-RTR1$_{3'UTR/TER}$ plasmid was used as a negative control and for normalizing the fold enrichment of all other samples. A qPCR was performed on the reverse-transcribed RNA IP samples with the GFP-FAM Taqman assay. Each PCR reaction was

performed in triplicate and the bar graph displays the average and standard deviation for three independent biological replicates. **(B)** Co-immunoprecipitation assay performed utilizing the 3X-FLAG-*RTR1* strain and the tagged Dhh1p expressed from the BG1805 vector (Yeast ORF collection from Dharmacon). Lysed samples were immunoprecipitated with protein A sepharose beads in the presence of Protease 3C. Western blotting was performed with the anti-HA primary antibody to detect the tagged Dhh1. A representative western blot of three independent biological replicates is shown. **(C)** Co-IP assay performed the same as in (B), except, RNase A was added into the lysate in the indicated samples.

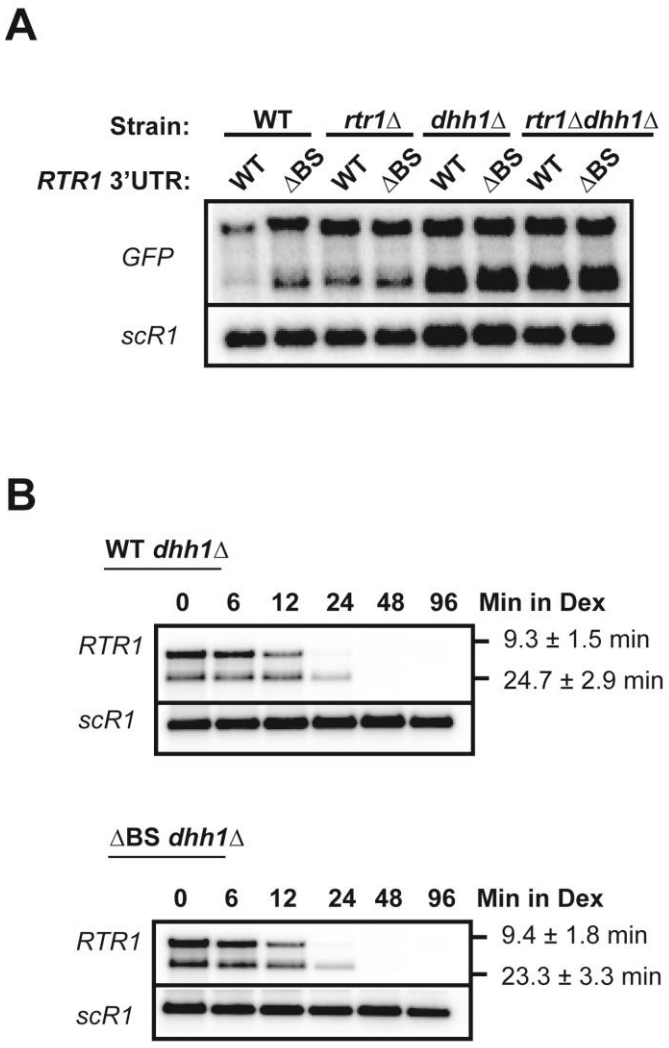

Figure 5. The impact of *DHH1* deletion on *RTR1* 3'UTR-containing mRNAs **(A)** Northern blot analysis of steady-state WT or ΔBS GFP-RTR1$_{3'UTR/TER}$ mRNAs in the WT, *rtr1*Δ, *dhh1*Δ, or *rtr1*Δ*dhh1*Δ background. **(B)** Transcription shut-off assay with the galactose-driven promoter. DHH1 was knocked out in either the GAL-RTR1 WT or GAL-RTR1 ΔBS strains. Posttranscriptional stability was determined by harvesting the samples at the indicated time points after shifting from 2% Galactose to 4% Dextrose. Calculated half-lives are the result of three independent biological replicates.

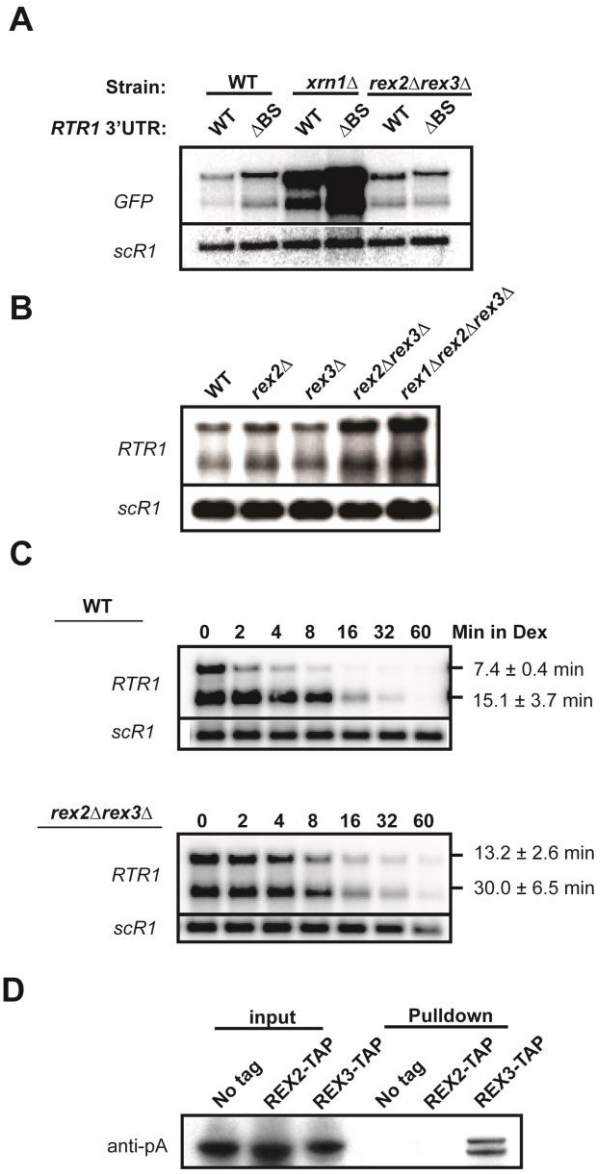

Figure 6. Testing the involvement of REX2 and REX3 in the Rtr1p autoregulation and degradation pathway by genetic and biochemical assays. **(A)** Northern blot analysis of steady-state WT or ΔBS GFP-RTR1$_{3'UTR/TER}$ mRNAs in the WT, *xrn1*Δ, or *rex2*Δ*rex3*Δ strains. Cultures were grown in SD-TRP and harvested during log phase at OD 0.4-0.5. A representative northern blot of three independent biological replicates is shown. **(B)** Northern blot analysis of steady-state *RTR1* mRNA levels. Cultures were grown in YPD and harvested during log phase at OD 0.4-0.5. A representative northern blot of three independent biological replicates is shown. **(C)** Posttranscriptional stability analysis of *RTR1* mRNAs

expressed from the GAL1 promoter in either the WT or *rex2*Δ*rex3*Δ background. Cultures were shifted from 2% Galactose to 4% Dextrose to turn off transcription from the GAL1 promoter. Calculated half-lives are the result of three independent biological replicates. **(D)** Pulldown assay performed to test the physical *in vivo* association of Rex2-TAP or Rex3-TAP with the tagged Dhh1p expressed from the BG1805 vector. Rex2-TAP, Rex3-TAP, or a "No tag" control were pulled down with calmodulin beads and tagged Dhh1p was detected with an anti-proteinA antibody. A representative western blot of three independent biological replicates is shown.

A

Name	Feature	Sequence
RTR1	3'UTR	TAATTCATCATCATA
XUT 4F-416	ncRNA	***ATCA***TCATCATCATA
MUT 278.1	ncRNA	***ATCA***TCATCATCATA
BMH2	5'UTR intron	***AT***ATTCATCATCA***A***A
IPT1	ORF	***AGT***TTCATCATCATA
CDC34	3'UTR	TAATTCATCATC***CC***A
YDR455C	Dubious ORF	***AAG***TTCATCATCAT***C***
GLT1	ORF	***GT***ATTCATCATCA***CC***
YDL172C	Dubious ORF	***ATC***TTCATCATCAT***C***
MSB1	ORF	***CG***ATTCATCATCAT***C***

B

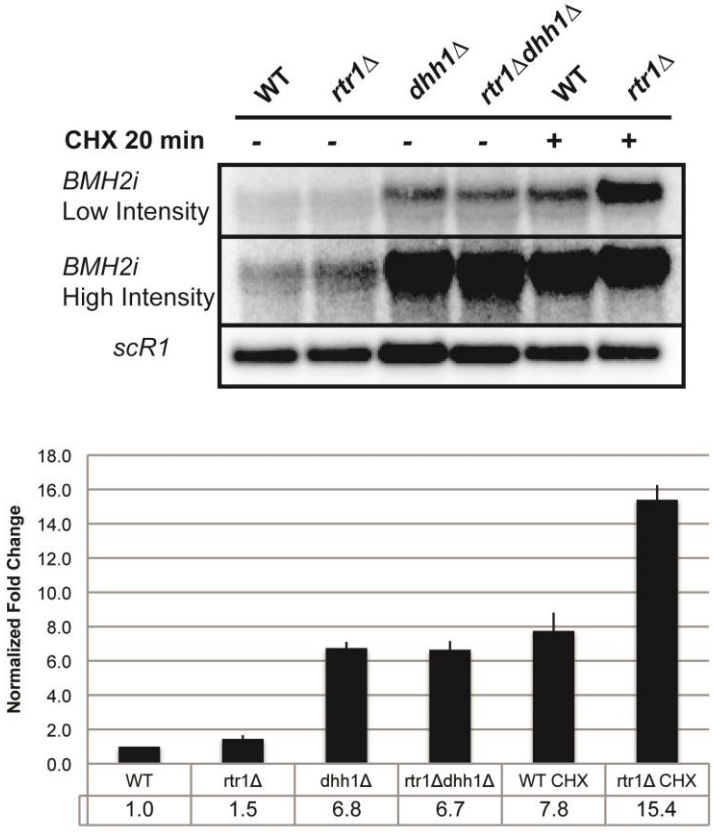

Figure 7. Potential RNAs targeted by Rtr1p-mediated decay **(A)** Hits for the BLAST search results for the *RTR1* 3'UTR cis element found within transcribed regions. Residues in the sequence that deviate from the *RTR1* element are bolded and italicized. **(B)** Northern blot analysis of steady-state *BMH2* pre-mRNAs in the trans mutants. An *in vitro* transcribed ^{32}P-radiolabeled riboprobe antisense to the *BMH2* 5'UTR intron was hybridized to the membrane. All samples are derived from cultures grown in YPD and harvested at log phase, OD 0.4-0.5.

WT and *rtr1*Δ cultures were also treated with 100 μg/mL CHX for 20 minutes and then harvested. The intensity of the autoradiogram was adjusted within the BioRad FX Quantity One software. The chart below shows the average quantitation of two independent biological replicates.

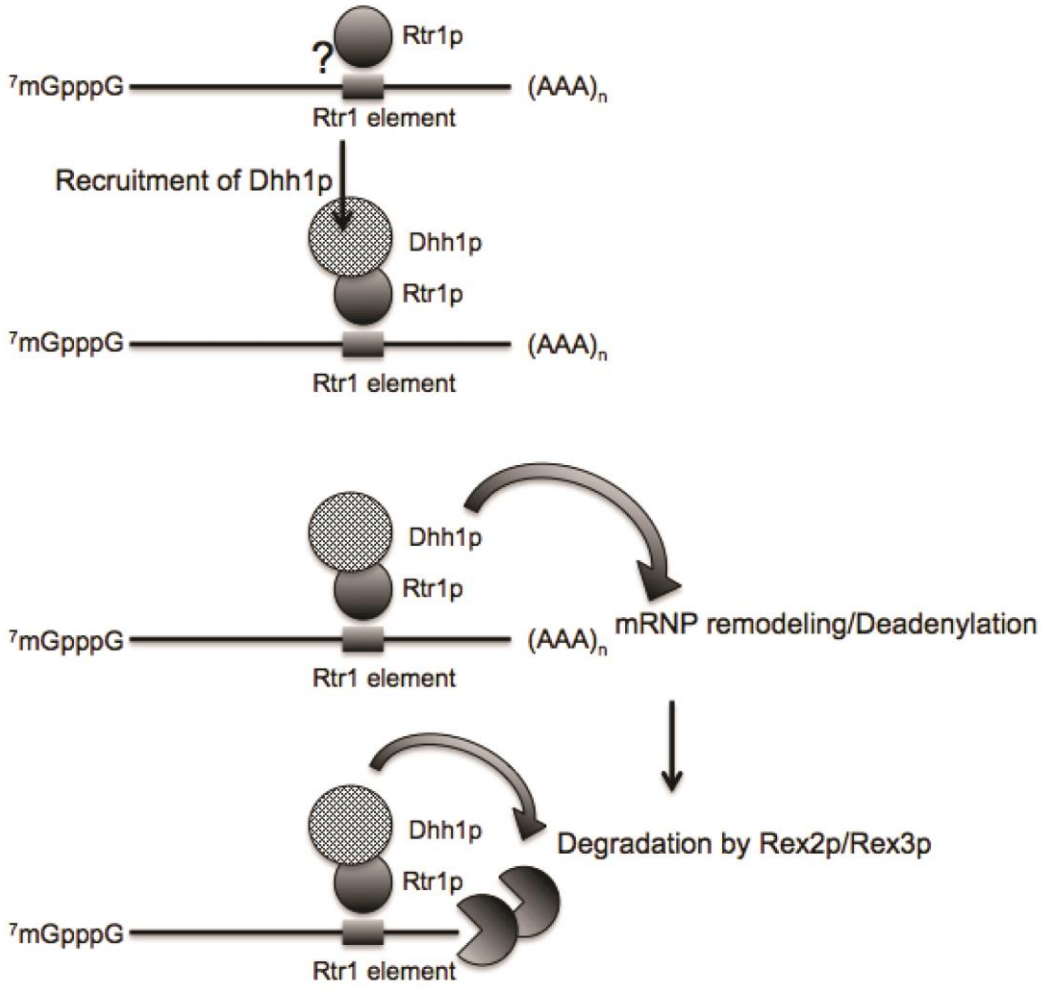

Figure 8. Model for Rtr1p-mediated mRNA decay. Depicted in the illustration is the proposed role of each factor involved in the pathway. An mRNA with the RBP binding element recruits the binding of Rtr1p to the mRNP. This event may occur co-transcriptionally given Rtr1p's association with the RNAP II CTD tail. The binding of Rtr1p to the mRNP recruits Dhh1p, which then may engage other degradation factors or serve to remodel the mRNP priming it for degradation. Dhh1p may also recruit deadenylases and ultimately, Rex3p. Rex3p would then digest the mRNA from the 3' end.

Supplementary Table 1. *S. cerevisiae* strains used in this study.

Background/Strain	Mutation	Source
BMA64-a	WT (derivative of W303)	Lab stock
BMA64-a	*upf1Δ*	Sayani and Chanfreau 2012
BMA64-a	*rrp6Δ*	Sayani and Chanfreau 2012
BMA64-a	*upf1Δrrp6Δ*	Sayani and Chanfreau 2012
BY4742	WT (Open Biosystems)	Lab stock
BMA64-a	*rex2Δ*	This study
BMA64-a	*rex3Δ*	This study
BMA64-a	*rex2Δrex3Δ*	This study
BMA64-a	*rex1Δrex2Δrex3Δ*	This study
yRP841	MATα *leu2-3,112, lys2, trp1-1, ura3-*	Olivas and Parker 2000
yRP1243	*puf1Δ*	Olivas and Parker 2000
yRP1237	*puf2Δ*	Olivas and Parker 2000
yRP1241	*puf3Δ*	Olivas and Parker 2000
yRP1245	*puf4Δ*	Olivas and Parker 2000
yRP1239	*puf5Δ*	Olivas and Parker 2000
yRP1290	*puf1Δpuf2Δ*	Olivas and Parker 2000
yRP1253	*5Δpufs*	Olivas and Parker 2000
BMA64-a	*rtr1*::CORE	This study
BMA64-a	RTR1 N-term CORE insertion	This study
BMA64-a	3X-FLAG-RTR1	This study
BMA64-a	*rtr1*::GFP	This study
BMA64-a	*xrn1*::TRP	This study
BMA64-a	RTR1-3'UTR::CORE insertion	This study
BMA64-a	RTR1-3'UTR-ΔBS	This study
BMA64-a	*dhh1*::KAN^R	This study
BMA64-a	*rtr1::*CORE *dhh1*::KAN^R	This study
BMA64-a	HIS3MX6-PGAL1-RTR1	This study
BMA64-a	RTR1-3'UTR-ΔBS HIS3MX6-	This study
BMA64-a	RTR1-3'UTR-ΔBS HIS3MX6-	This study
BMA64-a	rex2Δrex3Δ HIS3MX6-PGAL1-RTR1	This study
BMA64-a	dhh1::KAN^R HIS3MX6-PGAL1-RTR1	This study
REX2-TAP	S288C: (ATCC 201388: MATa his3Δ1	GE Dharmacon
REX3-TAP	S288C: (ATCC 201388: MATa his3Δ1	GE Dharmacon
BY4742	WT	GE Dharmacon
BY4742	*rrp6Δ*	GE Dharmacon
BY4742	*ski2Δ*	GE Dharmacon
BY4742	*she2Δ*	GE Dharmacon
BY4742	*puf6Δ*	GE Dharmacon
BY4742	*pho92Δ*	GE Dharmacon
BY4742	*ngr1Δ* (*rbp1Δ*)	GE Dharmacon
BY4742	*loc1Δ*	GE Dharmacon
BY4742	*pin4Δ*	GE Dharmacon

Supplementary Table 2. Oligonucleotides used in this study

Name	**Sequence**	**Purpose**
GFP-F	TGAGTAAAGGAGAAGAACTTTTCAC	PCR template for Riboprobe
GFP-T3-R	GGCTAAATTAACCCTCACTAAAGGTTTGTATAGTTCATCCATGCCA	PCR template for Riboprobe
RTR1-F	GATATTAAGGAAACGGCGTTAATCC	PCR template for Riboprobe
RTR1-T3-R	GGCTAAATTAACCCTCACTAAAGGCTGAATTTAGGTGCATTGATATAGC	PCR template for Riboprobe
BMH2-791UP-F	AGCTCCTTCCACAACCACCTTCATC	PCR template for Riboprobe
BMH2-290UP-T3-R	GGCTAAATTAACCCTCACTAAAGGATAACATTTGCCCCTTTCGACCGAC	PCR template for Riboprobe
scR1 probe	ATCCCGGCCGCCTCCATCAC	Oligoprobe for scR1
RTR1-3'RACE-BamHI	CGCCGCCGCGGATCCGACGCTGCAAGAAGAATCGTTCAC	3’RACE
RTR1-UP-INS-CORE-F	CGGCATCTTAGTTTGAAAAATTAGGACGAAGTTAACAAGAATAAGAAATG GAGCTCGTTTTCGACACTGG	Insertion of CORE at Rtr1 N-term
RTR1-UP-INS-CORE-R	TGCTTTTGGAAAGGGATTAACGCCGTTTCCTTAATATCTTCAATCGTCGC TCCTTACCATTAAGTTGATC	Insertion of CORE at Rtr1 N-term
GFP-Replace-RTR1-F	CATCGGCATCTTAGTTTGAAAAATTAGGACGAAGTTAACAAGAATAAGAAATGTCTTTAATTAACAGTAAAGGAG	Replacement of RTR1 ORF with GFP for downstream plasmid construction
GFP-Replace-RTR1-R	AATGAAACGTCCATAATCTGTTCTGAATTTAGGTGCATTGATATAGCCGGCTATTTGTATAGTTCATCCATGC	Replacement of RTR1 ORF with GFP for downstream plasmid construction
RTR1-UP-3xFLAG-F	GTTTGAAAAATTAGGACGAAGTTAACAAGAATAAGAAATGGACTACAAAGACCATGACGGTGATTATAA	RTR1 N-term 3xFLAG insertion

	AGAT CATGACATCGAT	
RTR1-UP-3xFLAG-R	AAGGGATTAACGCCGTTTCCTTAATATCTTCAATCGTCGCCTTGTCATCGTCATCCTTGTAATCGATGTCATGATCTTTATAATC	RTR1 N-term 3xFLAG insertion
XRN1-F1	ACTTGTAACAACAGCAGCAACAAATATATATCAGTACGGTCGGATCCCCCGGGTTAATTAA	XRN1 knockout
XRN1-R1	TAAAGTAACCTCGAATATACTTCGTTTTTAGTCGTATGTTGAATTCGAGCTCGTTTAAAC	XRN1 knockout
RTR1-GAL-F4	GACACATTGAGGAGCGAATTGAACAATTCATAAACATTCCGAATTCGAGCTCGTTTAAAC	PGAL1 promoter replacement at RTR1 locus
RTR1-GAL-R2	AAGGGATTAACGCCGTTTCCTTAATATCTTCAATCGTCGCCATTTTGAGATCCGGGTTTT	PGAL1 promoter replacement at RTR1 locus
DHH1-F1	ATCCCAGGCCTAAAATACGACAAGAAAGAAAATAGTAGTACGGATCCCCGGGTTAATTAA	DHH1 knockout
DHH1-R1	GCGTATCTCACCACAGTAGTTATTTTTTCTTAGATATTCTGAATTCGAGCTCGTTTAAAC	DHH1 knockout
REX2-CORE-INS-F	AAATGAAAAAAAAGAAAAGGAGCTTTCACAAATAAACAGAAGAGATCAAG GAGCTCGTTTTCGACACTGG	REX2::CORE knockout
REX2-CORE-INS-R	TGTGAAATATTTGAAAAATTTCACTTCTTTTTTCTTTTTTTTTTTCTACA TCCTTACCATTAAGTTGATC	REX2::CORE knockout
REX2-CORE-EX1	AAAGAAAAGGAGCTTTCACAAATAAACAGAAGAGATCAAGTGTAGAAAAAAAAAAAGAAAAAAGAAGTGAAATTTTTCAA	Excision of CORE from REX2 locus
REX2-CORE-EX2	TTGAAAAATTTCACTTCTTTTTTCTTTTTTTTTTCTACACTTGATCTCTTCTGTTTATTTGTGAAAGCTCCTTTTCTTT	Excision of CORE from REX2 locus
REX3-CORE-INS-F	GTGTTTCAGTATACATTCAGTTTGACTATATATCAAGAGAAAGCTTTAGTGAGCTCGTTTTCGACACTGG	REX3::CORE knockout
REX3-CORE-INS-R	TATGAAATGTAATAACTATATATGTCTGCTCAACTTTGAATATGATCACA TCCTTACCATTAAGTTGATC	REX3::CORE knockout

REX3-CORE-EX1	ATACATTCAGTTTGACTATATATC AAGAGAAAGCTTTAGTTGTGATC ATATTCAAAGTTGAGCAGACATA TATAGTTATT	Excision of CORE from REX3 locus
REX3-CORE-EX2	AATAACTATATATGTCTGCTCAAC TTTGAATATGATCACAACTAAAGC TTTCTCTTGATATATAGTCAAACT GAATGTAT	Excision of CORE from REX3 locus
REX1-CORE-INS-F	ACCAAGGATGACTGAGGAAGAAA ACAATAATAGACTATACTCAGGC AAACGAGCTCGTTTTCGACACTGG	REX3::CORE knockout
REX1-CORE-INS-R	ATATATATATATATATATATATAT ATATTTATATATTTATACACATAG AA TCCTTACCATTAAGTTGATC	REX3::CORE knockout
REX1-CORE-EX1	ACTGAGGAAGAAAACAATAATAG ACTATACTCAGGCAAACTTCTATG TGTATAAATATATAAATATATATA TATATATAT	Excision of CORE from REX3 locus
REX1-CORE-EX2	ATATATATATATATATATTTATAT ATTTATACACATAGAAGTTTGCCT GAGTATAGTCTATTATTGTTTTCT TCCTCAGT	Excision of CORE from REX3 locus

REFERENCES

Bouveret, E., Rigaut, G., Shevchenko, A., Wilm, M., & Séraphin, B. (2000). A Sm-like protein complex that participates in mRNA degradation. *The EMBO journal*, *19*(7), 1661-1671. DOI: 10.1093/emboj/19.7.1661

Braun, K. A., & Young, E. T. (2014). Coupling mRNA synthesis and decay. *Molecular and cellular biology*, *34*(22), 4078-4087. DOI: 10.1128/MCB.00535-14

Carroll, J. S., Munchel, S. E., & Weis, K. (2011). The DExD/H box ATPase Dhh1 functions in translational repression, mRNA decay, and processing body dynamics. *The Journal of cell biology*, *194*(4), 527-537. DOI: 10.1083/jcb.201007151

Castello, A., Fischer, B., Eichelbaum, K., Horos, R., Beckmann, B. M., Strein, C., ... & Hentze, M. W. (2012). Insights into RNA biology from an atlas of mammalian mRNA-binding proteins. *Cell*, *149*(6), 1393-1406. DOI: 10.1016/j.cell.2012.04.031

Chang, L. C., & Lee, F. J. S. (2012). The RNA helicase Dhh1p cooperates with Rbp1p to promote porin mRNA decay via its non-conserved C-terminal domain. *Nucleic acids research*, *40*(3), 1331-1344. DOI: 10.1093/nar/gkr803

Coller, J., & Parker, R. (2004). Eukaryotic mRNA decapping. *Annual review of biochemistry*, *73*(1), 861-890. DOI: 10.1146/annurev.biochem.73.011303.074032

Coller, J. M., Tucker, M., Sheth, U., Valencia-Sanchez, M. A., & Parker, R. (2001). The DEAD box helicase, Dhh1p, functions in mRNA decapping and interacts with both the decapping and deadenylase complexes. *RNA*, *7*(12), 1717-1727. DOI: 10.1017/S135583820101994X

Czaplinski, K., Ruiz-Echevarria, M. J., Paushkin, S. V., Han, X., Weng, Y., Perlick, H. A., ... & Peltz, S. W. (1998). The surveillance complex interacts with the translation release factors to enhance termination and degrade aberrant mRNAs. *Genes & development*, *12*(11), 1665-1677. DOI: 10.1101/gad.12.11.1665

Dahan, N., & Choder, M. (2013). The eukaryotic transcriptional machinery regulates mRNA translation and decay in the cytoplasm. *Biochimica et Biophysica Acta (BBA)-Gene Regulatory Mechanisms*, *1829*(1), 169-173. DOI: 10.1016/j.bbagrm.2012.08.004

Fischer, N., & Weis, K. (2002). The DEAD box protein Dhh1 stimulates the decapping enzyme Dcp1. *The EMBO Journal*, *21*(11), 2788-2797. DOI: 10.1093/emboj/21.11.2788

Freeberg, M. A., Han, T., Moresco, J. J., Kong, A., Yang, Y. C., Lu, Z. J., ... & Kim, J. K. (2013). Pervasive and dynamic protein binding sites of the mRNA transcriptome in Saccharomyces cerevisiae. Genome Biol, 14(2), R13. DOI: 10.1186/gb-2013-14-2-r13

García-Martínez, J., González-Candelas, F., & Pérez-Ortín, J. E. (2007). Common gene expression strategies revealed by genome-wide analysis in yeast. *Genome Biol*, *8*(10), R222. DOI: 10.1186/gb-2007-8-10-r222

Glisovic, T., Bachorik, J. L., Yong, J., & Dreyfuss, G. (2008). RNA-binding proteins and post-transcriptional gene regulation. *FEBS letters*, *582*(14), 1977-1986. DOI: 10.1016/j.febslet.2008.03.004

Goldstrohm, A. C., Hook, B. A., Seay, D. J., & Wickens, M. (2006). PUF proteins bind Pop2p to regulate messenger RNAs. *Nature structural & molecular biology*, *13*(6), 533-539. DOI: 10.1038/nsmb1100

Haimovich, G., Medina, D. A., Causse, S. Z., Garber, M., Millán-Zambrano, G., Barkai, O., ... & Choder, M. (2013). Gene expression is circular: factors for mRNA degradation also foster mRNA synthesis. *Cell*, *153*(5), 1000-1011. DOI: 10.1016/j.cell.2013.05.012

Hata, H., Mitsui, H., Liu, H., Bai, Y., Denis, C. L., Shimizu, Y., & Sakai, A. (1998). Dhh1p, a putative RNA helicase, associates with the general transcription factors Pop2p and Ccr4p from Saccharomyces cerevisiae. *Genetics*, *148*(2), 571-579.

Hogan, D. J., Riordan, D. P., Gerber, A. P., Herschlag, D., & Brown, P. O. (2008). Diverse RNA-binding proteins interact with functionally related sets of RNAs, suggesting an extensive regulatory system. *PLoS Biol*, *6*(10), e255. DOI: 10.1371/journal.pbio.0060255

Hsu, P. L., Yang, F., Smith-Kinnaman, W., Yang, W., Song, J. E., Mosley, A. L., & Varani, G. (2014). Rtr1 is a dual specificity phosphatase that dephosphorylates Tyr1 and Ser5 on the RNA polymerase II CTD. *Journal of molecular biology*, *426*(16), 2970-2981. DOI: 10.1016/j.jmb.2014.06.010

Hyun-Jun, K., Sook-Jin, J., Kyung-Nam, K., In-Joon, B., Miwha, C., Chang-Min, K., ... & Cheol-Won, Y. (2014). A novel protein, Pho92, has a conserved YTH domain and regulates phosphate metabolism by decreasing the mRNA stability of PHO4 in Saccharomyces cerevisiae. *Biochemical Journal*, *457*(3), 391-400.

Janga, S. C., & Mittal, N. (2011). Construction, structure and dynamics of post-transcriptional regulatory network directed by RNA-binding proteins. In *RNA Infrastructure and Networks* (pp. 103-117). Springer New York. DOI: 10.1007/978-1-4614-0332-6_7

Kawashima, T., Pellegrini, M., & Chanfreau, G. F. (2009). Nonsense-mediated mRNA decay mutes the splicing defects of spliceosome component mutations. *RNA*, *15*(12), 2236-2247. DOI: 10.1261/rna.1736809

Long, R. M., & McNally, M. T. (2003). mRNA decay: x (XRN1) marks the spot. *Molecular cell*, *11*(5), 1126-1128. DOI: 10.1016/S1097-2765(03)00198-9

Longtine, M. S., McKenzie III, A., Demarini, D. J., Shah, N. G., Wach, A., Brachat, A., ... & Pringle, J. R. (1998). Additional modules for versatile and economical PCR-based gene deletion and modification in Saccharomyces cerevisiae. *Yeast*, *14*(10), 953-961. DOI: 10.1002/(SICI)1097-0061(199807)14:10%3C953::AID-YEA293%3E3.0.CO;2-U

Maillet, L., & Collart, M. A. (2002). Interaction between Not1p, a component of the Ccr4-not complex, a global regulator of transcription, and Dhh1p, a putative RNA helicase. *Journal of Biological Chemistry*, *277*(4), 2835-2842. DOI: 10.1074/jbc.M107979200

Medina, D. A., Jordán-Pla, A., Millán-Zambrano, G., Chávez, S., Choder, M., & Pérez-Ortín, J. E. (2014). Cytoplasmic 5′-3′ exonuclease Xrn1p is also a genome-wide transcription factor in yeast. *Frontiers in genetics*, *5*. DOI: 10.3389/fgene.2014.00001

Neelamraju, Y., Hashemikhabir, S., & Janga, S. C. (2015). The human RBPome: From genes and proteins to human disease. *Journal of proteomics*. DOI: 10.1016/j.jprot.2015.04.031

Norbury, C. J. (2013). Cytoplasmic RNA: a case of the tail wagging the dog. *Nature Reviews Molecular Cell Biology*, *14*(10), 643-653. DOI: 10.1038/nrm3645

Pelechano, V., & Pérez-Ortín, J. E. (2008). The transcriptional inhibitor thiolutin blocks

mRNA degradation in yeast. *Yeast*, *25*(2), 85-92. DOI: 10.1002/yea.1548

Sayani, S., & Chanfreau, G. F. (2012). Sequential RNA degradation pathways provide a fail-safe mechanism to limit the accumulation of unspliced transcripts in Saccharomyces cerevisiae. *Rna*, *18*(8), 1563-1572. DOI: 10.1261/rna.033779.112

Sayani, S., Janis, M., Lee, C. Y., Toesca, I., & Chanfreau, G. F. (2008). Widespread impact of nonsense-mediated mRNA decay on the yeast intronome. *Molecular cell*, *31*(3), 360-370. DOI: 10.1016/j.molcel.2008.07.005

Scherrer, T., Mittal, N., Janga, S. C., & Gerber, A. P. (2010). A screen for RNA-binding proteins in yeast indicates dual functions for many enzymes. *PLoS One*,*5*(11), e15499. DOI: 10.1371/journal.pone.0015499

Smith-Kinnaman, W. R., Berna, M. J., Hunter, G. O., True, J. D., Hsu, P., Cabello, G. I., ... & Mosley, A. L. (2014). The interactome of the atypical phosphatase Rtr1 in Saccharomyces cerevisiae. *Molecular BioSystems*, *10*(7), 1730-1741. DOI: 10.1039/C4MB00109E

Storici, F., & Resnick, M. A. (2006). The delitto perfetto approach to in vivo site-directed mutagenesis and chromosome rearrangements with synthetic oligonucleotides in yeast. *Methods in enzymology*, *409*, 329-345. DOI: 10.1016/S0076-6879(05)09019-1

Sun, M., Schwalb, B., Schulz, D., Pirkl, N., Etzold, S., Larivière, L., ... & Cramer, P. (2012). Comparative dynamic transcriptome analysis (cDTA) reveals mutual feedback between mRNA synthesis and degradation. *Genome research*, *22*(7), 1350-1359. DOI: 10.1101/gr.130161.111

Sun, M., Schwalb, B., Pirkl, N., Maier, K. C., Schenk, A., Failmezger, H., ... & Cramer, P. (2013). Global analysis of eukaryotic mRNA degradation reveals Xrn1-dependent buffering of transcript levels. *Molecular cell*, *52*(1), 52-62. DOI: 10.1016/j.molcel.2013.09.010

Sweet, T., Kovalak, C., & Coller, J. (2012). The DEAD-box protein Dhh1 promotes decapping by slowing ribosome movement. *PLoS Biology, 10(6)* doi: 10.1371/journal.pbio.1001342

Tharun, S., He, W., Mayes, A. E., Lennertz, P., Beggs, J. D., & Parker, R. (2000). Yeast Sm-like proteins function in mRNA decapping and decay. *Nature*,*404*(6777), 515-518. DOI:

10.1038/35006676

Tsvetanova, N. G., Klass, D. M., Salzman, J., & Brown, P. O. (2010). Proteome-wide search reveals unexpected RNA-binding proteins in Saccharomyces cerevisiae. *PloS one*, *5*(9), e12671. DOI: 10.1371/journal.pone.0012671

Tucker, M., Staples, R. R., Valencia-Sanchez, M. A., Muhlrad, D., & Parker, R. (2002). Ccr4p is the catalytic subunit of a Ccr4p/Pop2p/Notp mRNA deadenylase complex in Saccharomyces cerevisiae. *The EMBO journal*, *21*(6), 1427-1436. DOI: 10.1093/emboj/21.6.1427

Van Dijk, E. L., Chen, C. L., d'Aubenton-Carafa, Y., Gourvennec, S., Kwapisz, M., Roche, V., ... & Morillon, A. (2011). XUTs are a class of Xrn1-sensitive antisense regulatory non-coding RNA in yeast. *Nature*, *475*(7354), 114-117. DOI: 10.1038/nature10118

van Hoof, A., Lennertz, P., & Parker, R. (2000). Three conserved members of the RNase D family have unique and overlapping functions in the processing of 5S, 5.8 S, U4, U5, RNase MRP and RNase P RNAs in yeast. *The EMBO journal*, *19*(6), 1357-1365. DOI: 10.1093/emboj/19.6.1357

Wahle, E., & Winkler, G. S. (2013). RNA decay machines: deadenylation by the Ccr4–not and Pan2–Pan3 complexes. *Biochimica et Biophysica Acta (BBA)-Gene Regulatory Mechanisms*, *1829*(6), 561-570. DOI: 10.1016/j.bbagrm.2013.01.003

Wilinski, D., Qiu, C., Lapointe, C. P., Nevil, M., Campbell, Z. T., Hall, T. M. T., & Wickens, M. (2015). RNA regulatory networks diversified through curvature of the PUF protein scaffold. *Nature communications*, *6*. DOI: 10.1038/ncomms9213

CHAPTER 3—Proteomic analysis of REX-interacting factors and transcriptomic analysis of REX exonuclease deletion

INTRODUCTION

Our previous results presented in chapter 2 demonstrated that the REX exonucleases have a function in mRNA degradation. This result in itself is surprising because a conserved and recognized function for RNase D type exonucleases such as the REX proteins in S.cerevisiae is to process ncRNAs typically by trimming the 3' ends (van Hoof et al., 2000). More broadly, RNase D exonucleases are members of the DEDD family of exonucleases which are characterized by a core that contains the invariant 4 amino acids for which this family is named (Zuo and Deutscher, 2001). These four acidic nucleotides bind two divalent metal ions required for their catalysis (Cudney et al., 1981; Steitz and Steitz, 1993). While structurally similar to oligoribonucleases, RNase D is unable to degrade short oligoribonucleotides due to the weak binding of smaller nucleic acids at the active site (Matos et al., 2011; Zuo et al., 2005). In *E. coli*, RNase D trims tRNAs that have an extra 30 nucleotides beyond the CCA sequence (Matos et al., 2011). RNase D also processes the 5S rRNA and other small structured RNAs in *E. coli* (Matos et a., 2011). Similarly in *S. cerevisiae,* Rex1p participates in the 3' end processing of tRNAs, a function that is redundant with the 3'-5' exonuclease, Rrrp6p, and the endonuclease, Trz1p (Copela et al., 2008; Skowronek et al., 2014). Rex2p was shown to function in processing the 3' ends of the RNase P and RNase MRP RNAs, the U4 and U5 snRNAs, and the 5S and 5.8S rRNA. In addition, Rex2p was found localized in the mitochondria, and a *rex2Δ* strain has a decreased rate of growth on nonfermentable carbon (van Hoof et al., 2000; Hanekamp and Thorsness, 1999), suggesting a role for Rex2p in mitochondrial RNA metabolism. Rex2p's mitochondrial function may be conserved since a human homolog, REXO2, also localizes to the mitochondria and is implicated in mitochondrial RNA metabolism (Bruni et al., 2013). Rex3p is required for the maturation of the RNase MRP RNA and is also functionally redundant with Rex1p and Rex2p in the

processing of the U5 snRNA and of the RNase P RNA (van Hoof et al., 2000). In addition to these classical and conserved substrates of the REX exonucleases and their homologs, characterization of a REX exonuclease homolog in *A. thaliana*, SDN1 showed that it targets microRNAs for degradation (Ramachandran and Chen, 2008). This work expands the array of targets degraded by REX exonuclease homologs and suggests that still other targets of the REX exonucleases may be unknown.

3' exonucleases differ by their level of exonucleolytic processivity . Highly processive 3' exonucleases are typified by having a clamp-like structure around their substrates (Ibrahim et al., 2008). Rrp6p, known to be involved in the processing of various ncRNAs and in the degradation of lncRNAs and mRNAs, is closely related in structure to RNase D exonucleases (Midtgaard et al., 2006). While Rrp6p has distributive exonuclease activity *in vitro*, its rate of degradation is vastly improved in the presence of the TRAMP complex (Callahan and Butler, 2010). This suggests that a distributive enzyme may increase processivity by interactions with additional factors. While *in vitro* studies of the REX exonucleases are lacking due to inherent difficulties in their purification (van Hoof, personal communication), biochemical and structural studies of their homologs suggest that they have a distributive mode of action (Zuo et al., 2005).

Our results suggest that REX exonucleases can act as initiators of mRNA decay or may themselves digest entire mRNAs perhaps in a distributive manner. Alternatively, it is possible that interacting factors may increase the processivity of the REX exonucleases. To gain insight into this matter and further our understanding of the Rex2p and Rex3p interactomes, we performed a TAP affinity purification of Rex2p and Rex3p followed by mass spectrometry sequencing of the associated peptides. Analysis of the mass spectrometry data suggests a high degree of interaction with transcription factors. Further experimens are

needed to clarify whether these interactions have a functional basis. Next, since we observed that Rex2p and Rex3p are necessary for the degradation of the *RTR1*-3'UTR and other mRNAs *in vivo*, we suspected that other targets of the REXs may be present within the yeast transcriptome. To test this hypothesis, we performed RNA-seq analysis of the *rex1Δrex2Δrex3Δ* strain to detect increases in abundances of mRNAs that might be indicative of potential REX targets. Our analysis of the RNA-seq data shows that the deletion of the REX exonucleases results in a global increase in transposable element transcripts, a decrease in ribosomal protein genes (RPGs) mRNAs, and also results in an increased abundance of unspliced pre-mRNAs. By performing transcription shut-off assays in a mutant background, we also observe that the observed half-life of the unspliced *RPL18B* transcript increases upon inactivation of the Rex proteins. These data give preliminary support to the hypothesis that the REX exonucleases function in a novel splicing quality control pathway and suggest that they might be involved in controlling levels of transcripts of transposable elements.

RESULTS

Rex2-TAP and Rex3-TAP mass spectrometry sequencing reveals highly probable physical interactions with histone acetyltransferase (HAT) complexes

Our previous coimmunoprecipitation analysis of REX2-TAP and REX3-TAP strains revealed that Rex3p reproducibly interacts with the 5'-3' DExD/H-box RNA helicase, Dhh1p, while Rex2-TAP did not interact with Dhh1p (Chapter2). To gain further insight into the mechanism by which Rex2p and Rex3p may degrade mRNA, we aimed at better defining their interactomes by performing a standard TAP purification followed by mass spectrometry sequencing of the co-precipitants (Kaiser et al., 2011).

Our TAP-MS analysis, performed in collaboration with the Wohlschelegel lab, revealed peptides belonging to 330 different proteins in the Rex2-TAP purification and Rex3-TAP analysis revealed potential interactions with 330 proteins as well. Unfiltered affinity purification and mass spectrometry data sets typically contain many nonspecifically binding proteins. We filtered these initial lists using the SAINT analysis tool available on the Contaminant Repository Affinity Purification database online (CRAPome.org) (Mellacheruvu et al., 2013). For each prey protein co-purifying with the bait, a SAINT score is assigned which gives a probability of a true interaction between two proteins, based on a normalization of the spectral counts to the length of the protein and the total number of spectra in the purification (Choi et al., 2011). While the SAINT algorithm utilizes the data sets of two or more independent bait proteins in an experiment to model false interactions, further "negative" controls are provided from the CRAPome database which allow for a more accurate estimation of the spectral count distribution for false interactions (Choi et al., 2011). We used a SAINT probability cutoff score of 0.75 to filter out any potentially nonspecifically

binding proteins from the analysis to reveal 86 highly probable interactions with Rex2p (Table 3.1) and 48 highly probable interactions with Rex3p (Table 3.2). Of these, 34 high probability interacting proteins were observed with both Rex2-TAP and Rex3-TAP (Table 3.3). While Dhh1p was below the cutoff score of 0.75 in the Rex3-TAP interacting proteins, spectral counts for Dhh1p were only observed in the Rex3-TAP purification and not Rex2-TAP in agreement with our previous co-immunoprecipitations.

Intriguingly, many members of the SAGA and ADA histone acetyltransferase (HAT) complexes and a couple of members of the NuA4 HAT complex were found to have highly probable interactions with both Rex2-TAP and Rex3-TAP (Figure 3.1). Consisting of Gcn5p, Ada2p, Hfi1p, Taf5p,Taf6p, Taf12p, Sgf73p, Spt3p, Spt7p, Ngg1p, and Spt20, the SAGA HAT complex is known to function in regulating many genes usually playing an activating role by opening chromatin and recruiting basal transcription factors (Jacobson et al., 2004). This result suggests that Rex2p and Rex3p may have additional roles in regulating transcription or that their interaction with the abundant SAGA, ADA, or NuA4 complexes may be utilized for their recruitment to the site of transcription in order to function in their roles in RNA processing or quality control.

In addition, many ribosomal proteins were found to copurify with Rex2-TAP and Rex3-TAP based on the unfiltered list. Though many of these RPGs were below the SAINT cutoff score of 0.75, a few, including Rpl24p, Rps29p, and Rps0p, were highly probable interactors of Rex2-TAP and/or Rex3-TAP. This led us to hypothesize that Rex2p and Rex3p may interact with either pre-ribosomes (consistent with their role in rRNA processing and ribosome biogenesis) or actively translating polysomes as constituents of mRNA surveillance pathways. To test these hypotheses, we performed sucrose gradient fractionation of cell extracts followed by western blotting with anti-pA to detect either Rex2-TAP or Rex3-TAP

in the individual fractions. This analysis revealed that both Rex2-TAP and Rex3-TAP were found in the free fractions showing that they do not cosediment with any larger complexes (Figure 3.2). Thus any mRNA quality control or gene regulation pathways involving Rex2p or Rex3p may take place in the cytosol or nucleus free of any large complexes. Alternatively, any potential interactions with larger complexes may be transient in nature or not strong enough to be seen co-sedimenting in the heavier fractions.

RNA-seq analysis of the *rex1Δrex2Δrex3Δ* strain shows global downregulation of RPGs

Our previous results presented in Chapter 2 revealed a new function for the REX exonucleases in the degradation of mRNA. We wished to determine whether the REX exonucleases may target other RNAs as well. To this end, we performed RNA-seq analysis of steady-state RNA extracted from the *rex1Δrex2Δrex3Δ* strain and the isogenic wildtype. We used two methods to sequence each of the replicates. PolyA+ RNAs were sequenced using the Illumina TruSeq mRNA Seq library prep kit or Ribozero RNAs were sequenced using the Illumina ScriptSeq Complete Gold library prep kit (See Figure 3.3). The Ribozero RNA contains total RNA depleted for the ribosomal RNAs and thus retains mRNAs which are degradation intermediates and have undergone deadenylation. The polyA+ RNA seq, however, will disproportionately represent mRNAs that have longer poly(A) tails. Given that 3'-5' exonucleases are expected to act downstream of deadenylation, the Ribozero RNA sequencing in theory provides a better representation of mRNAs that may accumulate in a deadenylated state in the *rex1Δrex2Δrex3Δ* mutant; however, a population of these deadenylated intermediates may still be sequenced in the polyA+ RNA sequencing if the poly(A) tail is not fully removed by cellular deadenylases. We thus primarily utilized the Ribozero RNA seq data to find genes upregulated or downregulated in the *rex1Δrex2Δrex3Δ*

strain due to a direct effect of the exonuclease activity of these strains and we used the PolyA+ RNA sequencing data to gauge indirect increases or decreases in steady-state mRNA levels due to the deletion of the REXs.

After performing differential gene expression analysis of the data sets, we used YeastMine (tool available from Saccharomyces Genome Database) to determine the gene ontologies associated with the list of exonic regions that increased or decreased greater than two fold in the *rex1Δrex2Δrex3Δ* strain over the wildtype (Table 3.4 and Table 3.5, respectively). From this analysis, we found that many transposable element genes have increased mRNA abundances in the *rex1Δrex2Δrex3Δ* strain compared to the wildtype suggesting that this strain may have a higher rate of transposition than wildtype (Table 3.4). The cause of this increase may be a lack of transcriptional repression of transposons or possibly a lack of degradation of RNAs transcribed from transposable elements.

The gene ontology analysis of the RNA-seq data also demonstrates that nearly all RPGs decrease by about two-fold in the *rex1Δrex2Δrex3Δ* strain (Table 3.5). Since we also found that Rex2p and Rex3p likely have physical associations with histone acetylase complexes, this result suggests that the REXs may have a role in promoting transcriptional activation of the RPGs. Consistent with this hypothesis, previous work from the Struhl lab has revealed that the NuA4 histone acetylase complex component Esa1 is recruited to RPG promoters and required for histone acetylation at those promoters (Reid et al., 2000). This further strengthens the hypothesis that Rex2p and Rex3p, and possibly Rex1p, may have roles outside of RNA degradation and processing in regulating transcriptional activation.

Evidence that REX exonucleases function in a novel splicing quality control pathway

In addition to our differential expression analysis of exonic regions, we also analyzed lncRNAs, intergenic regions, ncRNAs, 5'UTR regions, 3'UTR regions, and intronic regions. Most interestingly, we found that a large fraction of intron-containing genes show increased steady-state intronic signal in the *rex1Δrex2Δrex3Δ* strain. Importantly, not all introns were more abundant in the *rex1Δrex2Δrex3Δ* strain thus providing evidence that these introns are not simply more abundant due to a decrease in splicing efficiency. For example, the *NHP6B* or the *RPL18B* introns do not increase in steady-state abundance (Figure 3.4). In all, 236 out of 254 introns analyzed increased in abundance in the *rex1Δrex2Δrex3Δ* strain.

Our lab previously determined that unspliced mRNAs are to a large degree exported to the cytoplasm and then degraded by the NMD system (Sayani et al., 2008). Furthermore, many pre-mRNAs are also targeted by both the nuclear exosome and the NMD system (Sayani and Chanfreau, 2012). We analyzed strand-specific RNA-seq data from the *upf1Δ* mutant and compared the introns which accumulate in each of these mutant strains (Figure 3.5). A majority of introns increased in abundance in both the *upf1Δ* and *rex1Δrex2Δrex3Δ* mutants. 10 introns, like that of *NHP6B* (Figure 3.4), only increased in the *upf1Δ*, while 56 introns, like that of *ACT1* and *GOT1* (Figure 3.6), increased in only the *rex1Δrex2Δrex3Δ* strain. 8 introns did not show any changes in the steady-state levels including *RPL18B* (Figure 3.4) and *DBP2* (Figure 3.7). Previous work from our lab has demonstrated that the *RPL18B* unspliced species is largely degraded by the nuclear exosome component, Rrp6p (Sayani and Chanfreau, 2012). Likewise, comparison of our RNA-seq data of the *upf1Δ* and *rex1Δrex2Δrex3Δ* mutants to previously published *rrp6Δ* tilling array data (Xu et al., 2009) reveals that the *DBP2* pre-mRNA is affected by *RRP6* deletion as well but not *UPF1* or *REX* deletion.

Our lab previously discovered that the levels of unspliced precursors accumulate to a greater degree in a *upf1Δrrp6Δ* double mutant compared to single mutants, thereby demonstrating that both of these distinct pathways degrade some unspliced mRNAs, like *RPP1B* and *RPL18B*, to limit their accumulation (Sayani and Chanfreau, 2012). Given our RNA-seq data which showed that the REX mutants display increased abundances of unspliced precursors of transcripts distinct from the NMD system and the nuclear exosome, we wondered whether the REX exonucleases could be part of a distinct pathway that may degrade unspliced transcripts. To first address this, we generated a *upf1Δrex1Δrex2Δrex3Δ* strain to find if that strain would exhibit greater levels of unspliced transcripts than the *upf1Δ* or *rex1Δrex2Δrex3Δ* strains; this result would indicate that the NMD pathway is functionally distinct from a REX exonuclease-dependent degradation pathway. Indeed, we found that for all of the pre-mRNAs analyzed (*ACT1*, *RPS26B*, *RPS10A*, *RPL29*, *RPP1B*, *RPL31B*, and *RPL18B*), the accumulation of the intron-containing mRNA is higher in the *upf1ΔrexΔ* combinatorial mutant than the *upf1Δ* or *rexΔ* mutants alone (Figure 3.8). Consistent with previous results, the NMD system does not target the *ACT1* unspliced mRNA; but in absence of the REX exonucleases, the NMD system does contribute to the degradation of the *ACT1* pre-mRNA since the quadruple mutant displays a larger accumulation than the triple *rexΔ* mutant. A similar phenotype is observed for the *RPS26B* and *RPS10A* intron-containing mRNAs (Figure 3.8). Surprisingly, *RPL18B*, whose unspliced precursor is typically only detected to a large extent in an *rrp6Δ* background (Sayani and Chanfreau, 2012), appears to accumulate in the quadruple mutant suggesting that in addition to the nuclear exosome, the REX exonucleases and NMD may also cooperate to degrade a portion of the unspliced *RPL18B* transcripts.

To make certain that this increased accumulation of unspliced precursor observed for *RPL18B* and other pre-mRNAs is due to the exonuclease activity of the REXs and not due to

a splicing defect in the *rex1Δrex2Δrex3Δ* background, we analyzed the turnover rate of the pre-mRNAs in the same mutant backgrounds. To this end, we began constructing GAL promoter replacement strains for a few of the intron-containing genes tested in all of the mutant backgrounds. We successfully made the *GAL-RPL18B* strain in the *upf1Δ* and the *upf1Δrex1Δrex2Δrex3Δ* background. The half-life of the Gal promoter derived *RPL18B* pre-mRNA was determined to be 13 minutes in the *upf1Δ* strain while the half-life of that in the *upf1Δrex1Δrex2Δrex3Δ* strain was 30 minutes confirming that the increased abundance of the unspliced *RPL18B* observed in the combinatorial mutant was due to an increase in stability of the unspliced transcript when the REX exonucleases are deleted in the *upf1Δ* background (Figure 3.9). Because the unspliced *RPL18B* transcript does not accumulate in the *upf1Δ* background alone, this result implies that the REX exonucleases degrade the *RPL18B* pre-mRNA in the NMD null mutant. The increase of stability when the REXs are knocked out in the *upf1Δ* strain strongly suggests that they degrade unspliced mRNAs—at least when NMD is nonfunctional. Ongoing experiments are aimed at determining whether the same holds true in a wildtype context.

DISCUSSION

In this chapter, we presented two approaches that yielded novel insights into the function and potential mechanisms of the REX exonucleases. Our affinity purification and mass spectrometry sequencing of Rex2p/Rex3p interacting partners revealed associations with transcription factors. The RNA-seq analysis gave two important perspectives into the potential effect of the REX exonucleases on the transcriptome: the REXs may positively regulate RPG expression and the REXs could be involved in a novel quality control mechanism to limit the prevalence of unspliced transcripts. Given the data that the deletion of the REXs results in a dramatic decrease in global RPG expression and that the REXs interact with HAT complexes that regulate RPG expression, a tempting hypothesis is that the REXs may directly impact transcription of RPGs. Extensive RNAP II ChIP analysis of RNA Polymerase II and/or of the SAGA complex throughout RPGs in the REX mutants would give the most direct answer to this question. Second, more thorough determination of turnover rates of unspliced precursors will be performed to determine whether the REXs do in fact participate in the degradation of pre-mRNAs.

The observation that Rex2p and Rex3p both interact with HATs could be interpreted in different ways. One explanation for this interaction could be that the REXs recruit HATs to the site of RPGs and other genes in response to an increase in rRNA transcription and processing. It is known, for instance, that transcription of rRNA leads to the increased transcription of RPGs (ref). We observed that in the *rex1Δrex2Δrex3Δ* strain that RPGs are downregulated. This could be explained by the hypothesis that REXs recruit HATs to RP promoters. This attractive hypothesis invites the notion that transcriptional activation of RPGs may be linked to rRNA processing via the REXs. Changes in REX expression or possibly post-translational modifications could redirect the REXs to function as recruiters of

HATs to RP promoters and in a sense, act as co-activators. That an exonuclease can act as a transcription factor would not be entirely unforeseen as previous studies purport that Xrn1p acts as a transcription factor and reinitiates transcription of degraded mRNAs thus acting as a buffer for gene expression (Sun et al., 2013, Medina et al., 2014).

Another explanation for the interaction between the REXs and HATs could be that HATs recruit REXs to intron-containing genes to decrease the output of unspliced or aberrantly spliced transcripts.

Our findings presented in this chapter suggest that the REXs degrade unspliced mRNAs. If this is the case, it could also be possible that they are recruited to the site of transcription of intron-containing genes. This recruitment could be facilitated by HATs like the SAGA or NuA4 complex. Work from the Johnson lab has shown that *GCN5*-dependent HAT activity is a requirement for recruitment of the U2 snRNP components to the branchpoint (Gunderson and Johnson, 2009). It could also be that GCN5-dependent or other HAT activity is required for recruitment of the REXs to intron-containing genes. If this were the case, then we would expect that deletion of *GCN5* or another HAT may result in an increased stability of an unspliced pre-mRNA normally degraded by the REXs. Another informative experiment may be to test whether the localization of the REX exonucleases in the nucleus is required for their function in degrading unspliced transcripts. To test this, an anchor-away approach could be devised with the REX exonucleases whereby REXs would be rapidly re-localized to ribosomes upon rapamycin addition (Haruki et al., 2008). This experiment could be key in determining whether the interaction of the REXs with HATs and other transcription factors is related to their potential function in degradation of unspliced transcripts.

Finally, as 3'-5' exonucleases, the REXs would most likely need to be located at the 3' end of genes to function in a quality control pathway linked to transcription or mRNA

processing. However, significant gene looping occurs at highly transcribed gene units and thus the 5' end of an RPG may be quite proximal to its 3' end (O'Sullivan et al., 2004, Tan-Wong et al., 2012). Gene-looping thus may serve to recruit the REXs to the 3'end through their interaction with transcription factors localized to the promoter region. Alternatively, REX exonucleases could be present at the 3' termini of intron-containing genes independent of their interaction with transcription factors. These interactions could possibly be a consequence of their abundance and localization near transcription factors, though the likelihood of this scenario is in question since the TAP method is a double affinity purification which reveals stable interactions between proteins as opposed to single affinity purification which contain low level or dynamic interactions (Breikreutz et al., 2010).

Overall, our work expands upon a highly understudied group of exonucleases in *S. cerevisiaie*. We have demonstrated that REX exonucleases have a bona fide mRNA target operating in concert with other mRNA degradation factors to autoregulate the expression of *RTR1*. We have also shown that Rex2p and Rex3p interact with transcription factors and thus may play an even larger role in the regulation of gene expression. The RNA-seq data also serves to demonstrate that the deletion of the REX exonlucleases largely perturbs overall expression of many categories of genes and provides an impetus for the investigation of a novel splicing quality control pathway involving the REXs. We hope that this work will draw more attention to the REX exonucleases and encourage the undertaking of structural and biochemical characterizations that could provide more insight into the mechanism by which these enzymes may function.

FIGURES AND TABLES

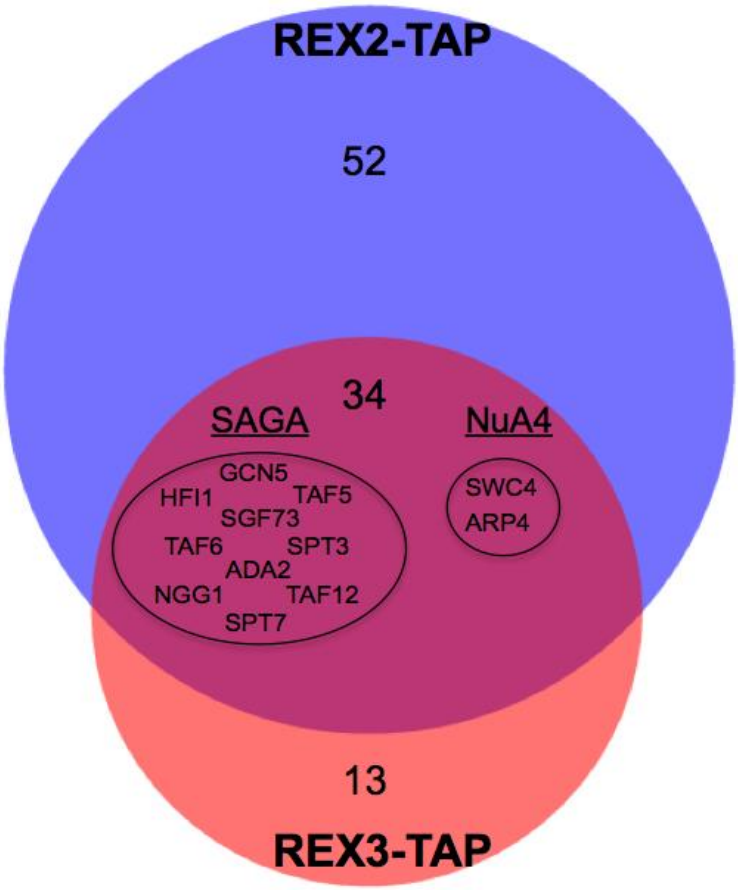

Fig. 3.1. Venn diagram of highly probable prey for Rex2-TAP and Rex3-TAP based on SAINT probability scores.
34 of proteins were common interactors of both Rex2p and Rex3p after filtering out less probable interactions using a SAINT cutoff score of 0.75. Members of the SAGA and NuA4 histone acetylase complex were highly represented among this list of common interactions with Rex2-TAP and Rex3-TAP. Venn diagram was produced using BioVenn.

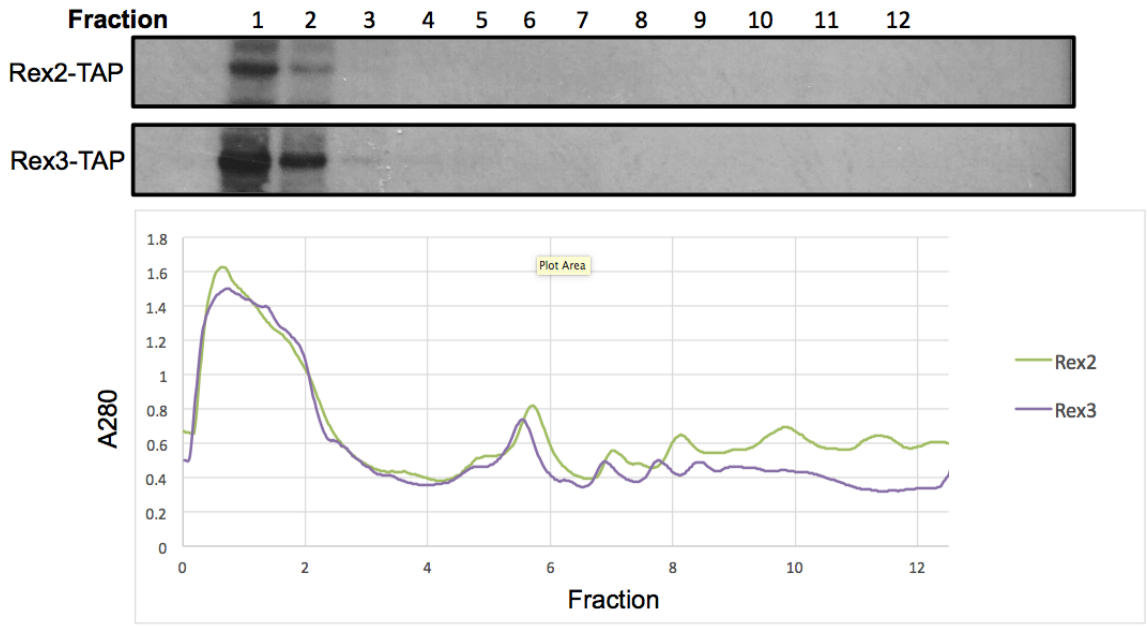

Fig. 3.2. Sucrose fractionation and western blot for Rex2-TAP and Rex3-TAP
Western blot with anti-pA detecting either Rex2-TAP or Rex3-TAP. After harvesting and lysing cells, equivalent OD units of the soluble fraction of the lysate was applied to a 15-50% sucrose gradient and the gradient was ulta-centrifuged at 37,000 RPM for 3.5 hours. Fractions were collected and the A280 trace during the fractionator run is shown below the western blots.

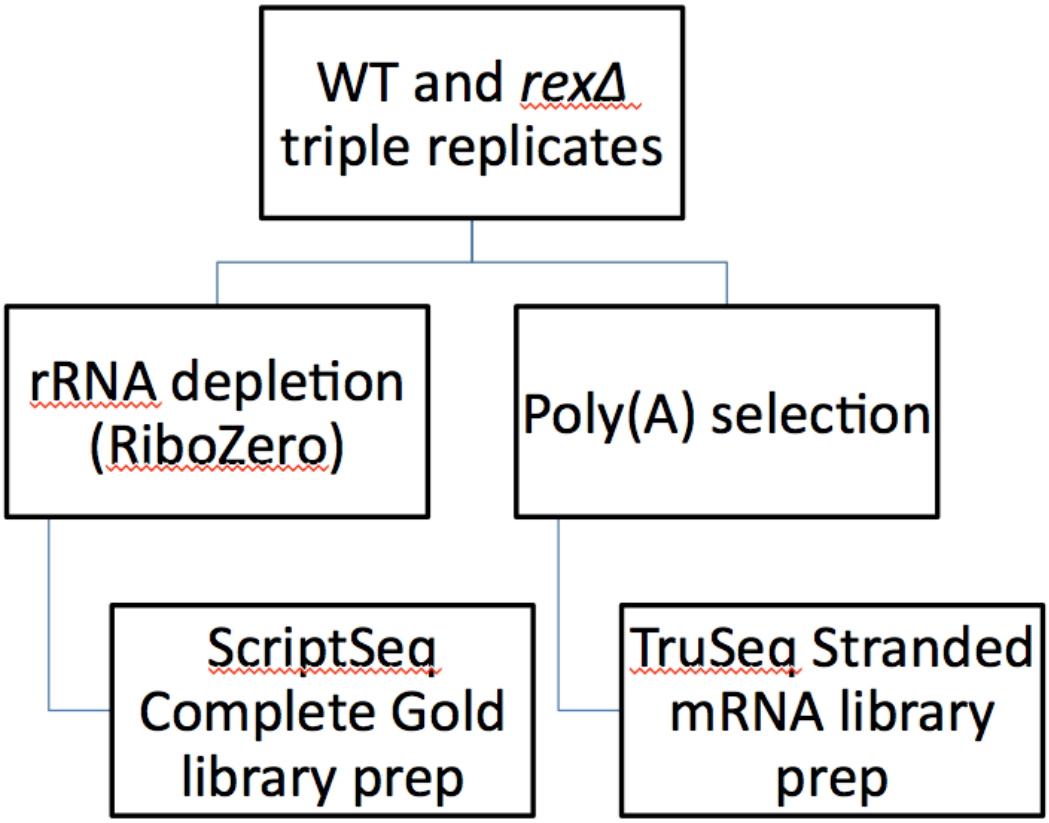

Fig. 3.3. Schematic of the REX RNA-seq experiment.
Three biological replicates from the WT and three biological replicates from the *rex1Δrex2Δrex3Δ* were harvested and RNA was extracted. These total RNA samples were then either rRNA depleted using the RiboZero rRNA Depletion kit or Poly(A) selected as part of the TruSeq Stranded mRNA library prep kit. The library prep kits were used to generate the libraries which had individual barcodes. All libaries were pooled together to allow for multiplex RNA-seq on one lane of the Illumina HiSeq2500.

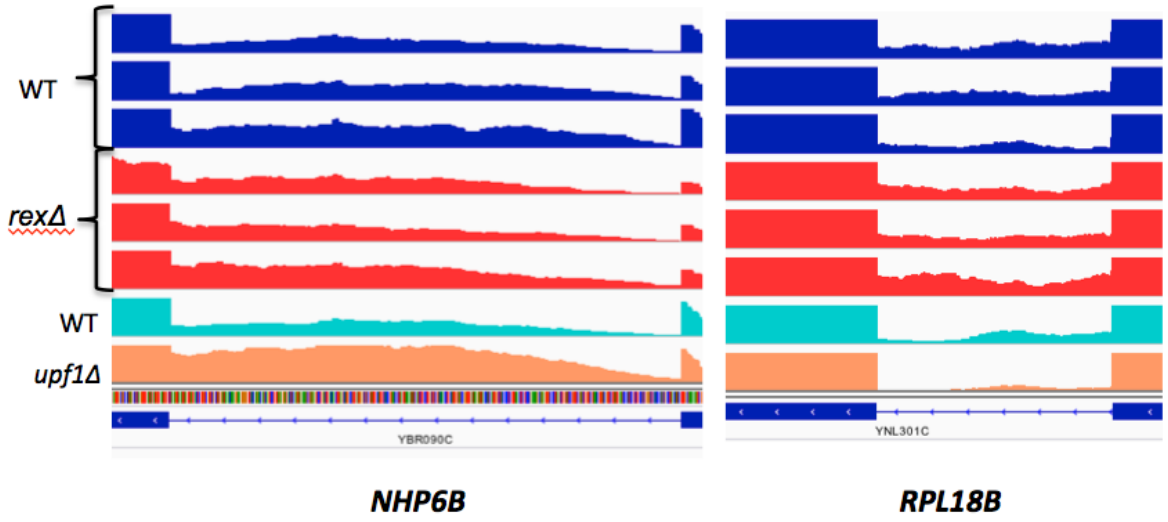

Fig. 3.4. Examples of intron-containing genes in which the steady-state level of intron-containing RNAs is about equivalent in the WT and *rex1Δrex2Δrex3Δ* strain.
Triple biological replicates of the WT strain are shown in blue, *rex1Δrex2Δrex3Δ* are shown in red. WT and *upf1Δ* from a different RNA-seq experiment are shown in green and orange, respectively.

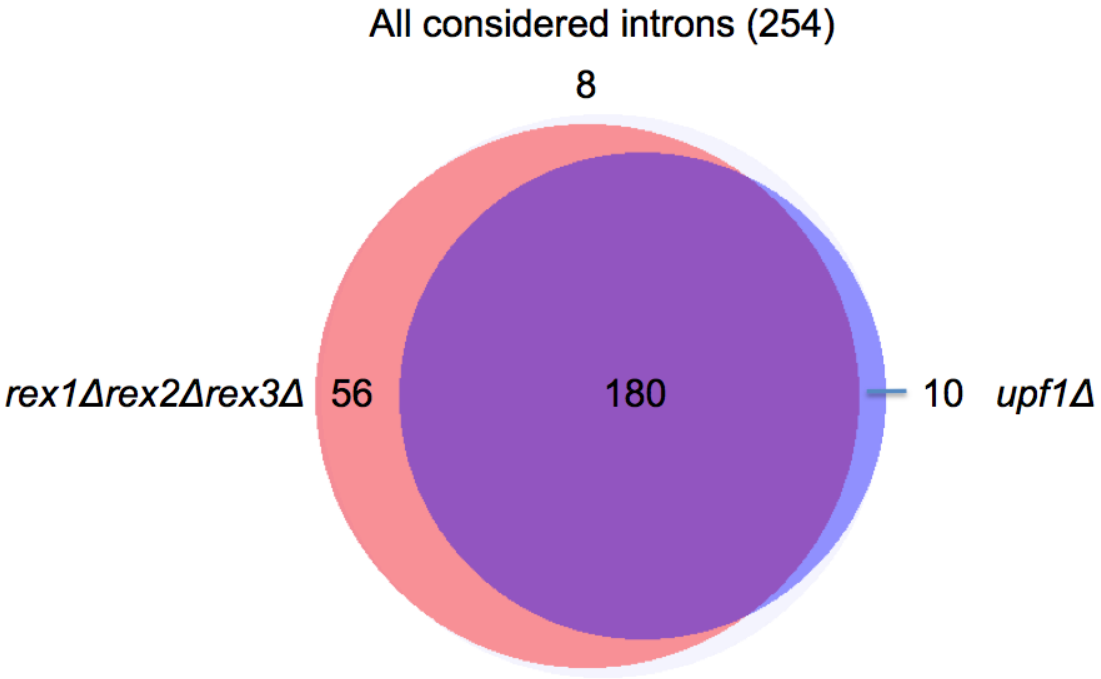

Fig. 3.5 Accumulation of introns based on RNA-seq read density.
254 introns in S. cerevisiae were analyzed for fold changes in the rex1Δrex2Δrex3Δ/WT or upf1Δ/WT. Only intronic regions with a fold change of 1.5 or higher were considered. Only 8 introns did not increase in either mutant strains. 56 introns increased in only the rex mutant and 10 increased in only the upf1 mutant. 180 introns increased in both mutant strains.

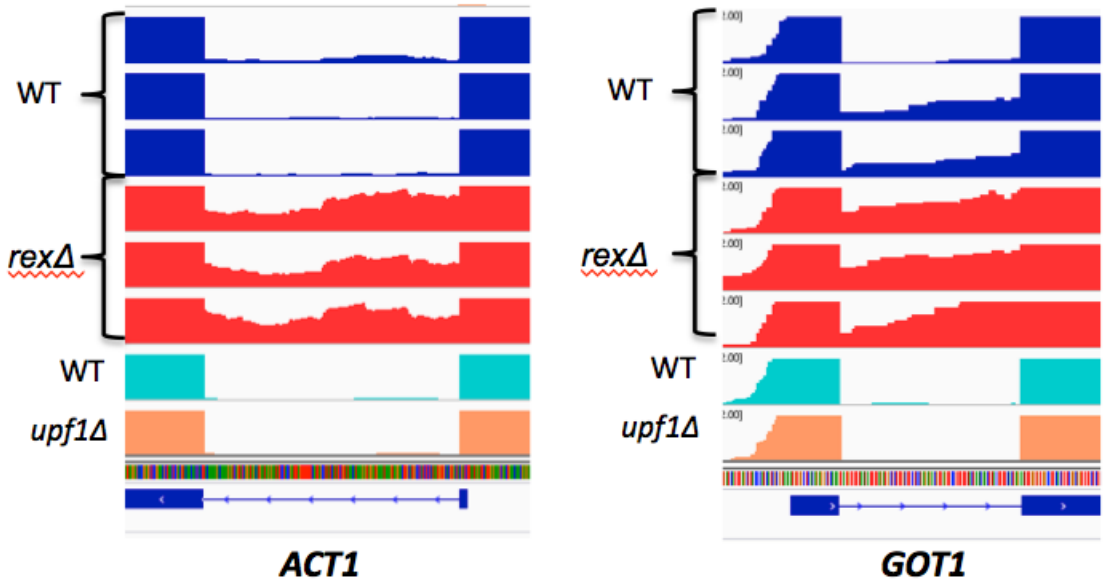

Fig. 3.6 Examples of intron-containing genes whose pre-mRNAs increase in abundance in the *rex1Δrex2Δrex3Δ* but not the *upf1Δ* strain.
Intron-containing *ACT1* and *GOT1* mRNAs do not substantially increase in the *upf1Δ* but increase in the *rex1Δrex2Δrex3Δ.* Triple biological replicates of the WT strain are shown in blue, *rex1Δrex2Δrex3Δ* are shown in red. WT and *upf1Δ* from a different RNA-seq experiment are shown in green and orange, respectively.
Fig. 3.1. Venn diagram of highly probable prey for Rex2-TAP and Rex3-TAP based on SAINT probability scores.

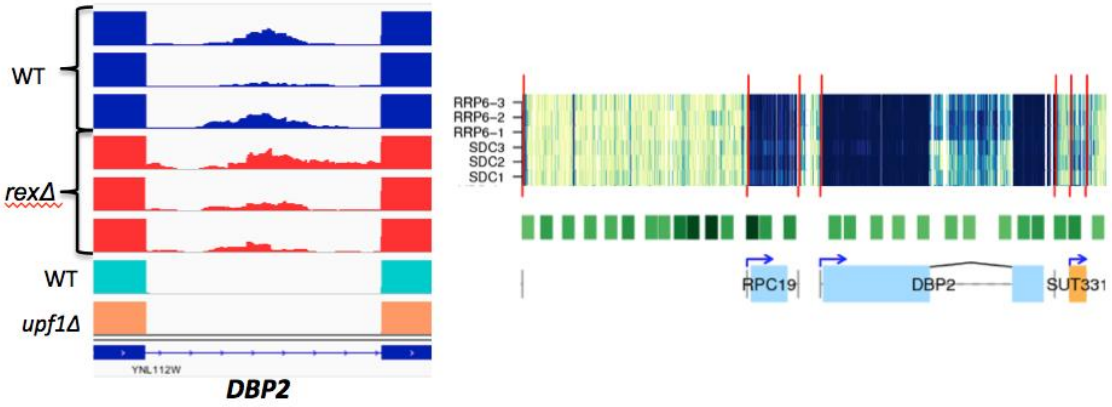

Fig. 3.7 Comparison of RNA-seq data of *upf1Δ* and *rex1Δrex2Δrex3Δ* to tilling array data with the *rrp6Δ* mutant (From Xu et al., 2009)
Intron-containing DBP2 mRNAs do not substantially increase in the *upf1Δ* or *rex1Δrex2Δrex3Δ*, but rather, the tiling array data show that there is an increase in the *rrp6Δ* mutant. Triple biological replicates of the WT strain are shown in blue, *rex1Δrex2Δrex3Δ* are shown in red. WT and *upf1Δ* from a different RNA-seq experiment are shown in green and orange, respectively.
.

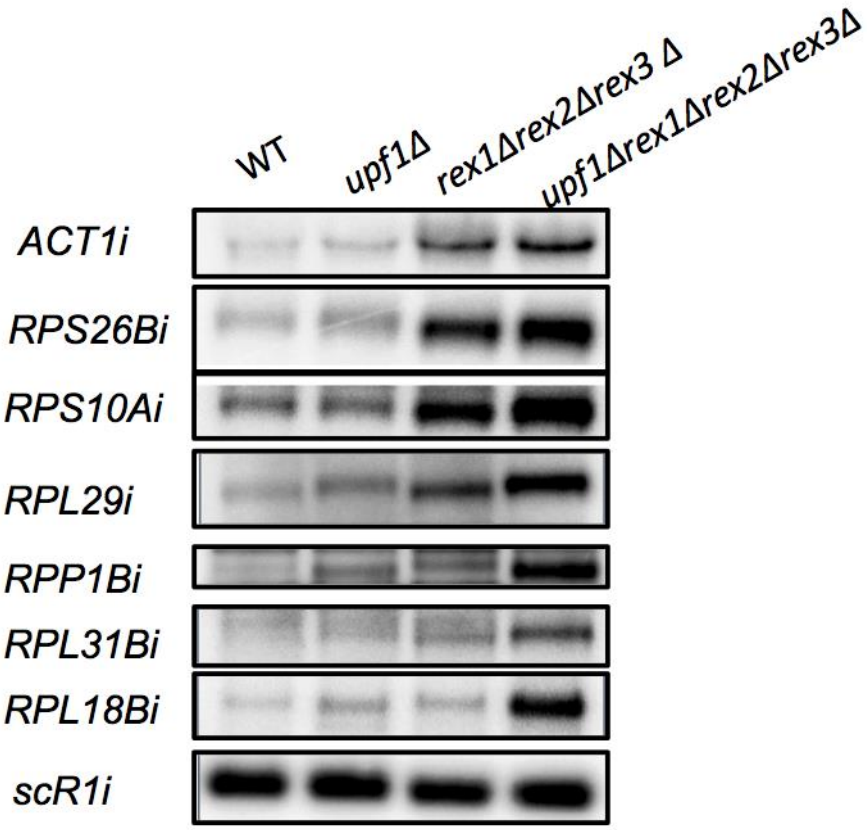

Fig. 3.8 Northern blot with various riboprobes directed against intronic regions with total RNA extracted from the WT, *upf1Δ*, *rex1Δrex2Δrex3 Δ*, and *upf1Δrex1Δrex2Δrex3Δ strains*
Riboprobes were designed to detect only the intron-containing RNAs

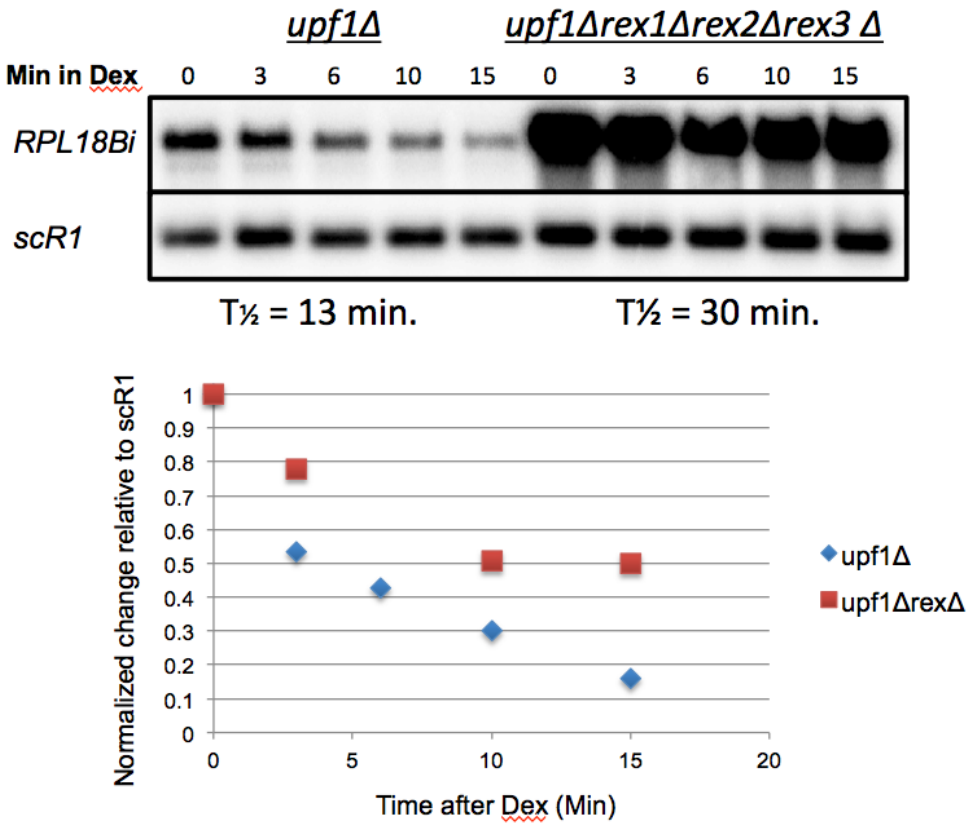

Fig. 3.9 Northern blot of the GAL-RPL18B transcription shut-off assay
The native *RPL18B* promoter was replaced with the Gal promoter for inducible expression of *RPL18B*. Cells were grown in galactose containing medium and switched to dextrose at OD=0.2 to shut off transcription from the Gal promoter. The indicated time points were taken. The chart beneath the blot shows the normalized quantitation of the bands in the blot relative to the scR1 signal at each time point.

Table 3.1. List of Prey co-purifying with Bait, Rex2p

For each Prey, the common gene name, the high-stringency fold change score, FC_B, and the SAINT probability score are given. All hits listed have a SAINT probability score of 0.75 or higher.

PREY	GENE	FC_B	SAINT
YFL024C	EPL1	8.52	1
YBL054W	TOD6	14.16	1
YJL168C	SET2	10.4	1
YGL013C	PDR1	12.28	1
YGL112C	TAF6	14.82	1
YGL066W	SGF73	17.92	1
YKR099W	BAS1	17.92	1
YLR410W	VIP1	4.71	1
YMR128W	ECM16	6.12	1
YDR483W	KRE2	12.28	1
YDR334W	SWR1	10.4	1
YLR033W	RSC58	8.52	1
YDR356W	SPC110	10.4	1
YPR056W	TFB4	8.52	1
YHR023W	MYO1	23.56	1
YLR059C	REX2	51.75	1
YGR252W	GCN5	8.52	1
YBR198C	TAF5	16.36	1
YOL088C	MPD2	10.4	1
YGR186W	TFG1	8.52	1

YPL254W	HFI1	10.4	1
YOR153W	PDR5	6.06	1
YIL022W	TIM44	16.04	1
YDR145W	TAF12	29.19	1
YLR005W	SSL1	11.02	1
YDR164C	SEC1	14.39	1
YDR289C	RTT103	25.44	1
YOL148C	SPT20	12.28	1
YGL150C	INO80	6.06	1
YDR176W	NGG1	14.16	1
YBR049C	REB1	10.4	1
YBR081C	SPT7	23.56	1
YDR448W	ADA2	12.71	1
YDR392W	SPT3	6.59	1
YDR359C	EAF1	17.92	1
YJL081C	ARP4	10.4	1
YAR002W	NUP60	6.64	0.99
YDL061C	RPS29B	6.64	0.99
YKL016C	ATP7	6.64	0.99
YBL103C	RTG3	6.64	0.99
YIL036W	CST6	6.64	0.99
YPR023C	EAF3	6.64	0.99
YMR005W	TAF4	6.64	0.99
YIL084C	SDS3	6.64	0.99
YOR344C	TYE7	6.64	0.99
YDR227W	SIR4	6.64	0.99
YGR002C	SWC4	6.64	0.99

YPL146C	NOP53	6.64	0.99
YIL130W	ASG1	6.64	0.99
YDR167W	TAF10	6.64	0.99
YOR116C	RPO31	6.63	0.99
YLR357W	RSC2	6.64	0.99
YPL047W	SGF11	6.64	0.99
YCR030C	SYP1	4.27	0.98
YDL132W	CDC53	4.35	0.98
YML057W	CMP2	4.76	0.97
YDR379W	RGA2	4.76	0.97
YML041C	VPS71	4.76	0.97
YJL176C	SWI3	4.76	0.97
YML123C	PHO84	4.76	0.97
YDR326C	YSP2	4.76	0.97
YMR236W	TAF9	4.76	0.97
YLR433C	CNA1	4.76	0.97
YJL041W	NSP1	4.76	0.97
YPL011C	TAF3	4.76	0.97
YHL025W	SNF6	4.76	0.97
YDR028C	REG1	4.76	0.97
YLR055C	SPT8	4.76	0.97
YOL016C	CMK2	4.76	0.97
YML015C	TAF11	4.76	0.97
YBR289W	SNF5	4.76	0.97
YIR006C	PAN1	7.82	0.96
YER088C	DOT6	6.63	0.95
YHR099W	TRA1	7.64	0.94

YIL126W	STH1	5.58	0.94
YLR096W	KIN2	3.66	0.92
YML010W	SPT5	5.62	0.86
YNR023W	SNF12	4	0.86
YCL037C	SRO9	3.44	0.86
YBL085W	BOI1	5.17	0.85
YOR332W	VMA4	4.23	0.84
YLR293C	GSP1	2.88	0.79
YOR185C	GSP2	2.88	0.79
YGR214W	RPS0A	3.81	0.79
YPL124W	SPC29	2.04	0.77
YPL049C	DIG1	2.47	0.75

Table 3.1. List of Prey co-purifying with Bait, Rex3p

For each Prey, the common gene name, the high-stringency fold change score, FC_B, and the SAINT probability score are given. All hits listed have a SAINT probability score of 0.75 or higher.

PREY	GENE	FC_B	SAINT
YDR483W	KRE2	8.61	1
YHR023W	MYO1	13.18	1
YLR107W	REX3	52.75	1
YBR198C	TAF5	14.81	1
YPL254W	HFI1	11.65	1
YIL022W	TIM44	8.61	1
YDR145W	TAF12	14.7	1
YLR005W	SSL1	5	1
YDR164C	SEC1	5	1
YBR081C	SPT7	11.65	1
YLR293C	GSP1	4.97	0.99
YOR185C	GSP2	4.97	0.99
YJL168C	SET2	5.57	0.99
YGL112C	TAF6	5.86	0.99
YKL016C	ATP7	5.57	0.99
YBL103C	RTG3	5.57	0.99
YGR252W	GCN5	5.57	0.99
YOL088C	MPD2	5.57	0.99
YLR185W	RPL37A	5.86	0.99
YDR289C	RTT103	5.57	0.99
YPL146C	NOP53	5.57	0.99
YDR176W	NGG1	5.57	0.99

YNL088W	TOP2	7.24	0.99
YPR165W	RHO1	3.63	0.98
YDR500C	RPL37B	3.69	0.98
YDR448W	ADA2	3.63	0.98
YBL054W	TOD6	4.04	0.97
YER126C	NSA2	4.04	0.97
YGL066W	SGF73	4.04	0.97
YKR099W	BAS1	4.04	0.97
YDL061C	RPS29B	4.04	0.97
YIL036W	CST6	4.04	0.97
YJL041W	NSP1	4.04	0.97
YGR002C	SWC4	4.04	0.97
YDR359C	EAF1	4.04	0.97
YJL081C	ARP4	4.04	0.97
YDR392W	SPT3	2.99	0.95
YMR128W	ECM16	2.42	0.93
YFL016C	MDJ1	5.23	0.91
YNR053C	NOG2	2.14	0.91
YPR043W	RPL43A	2.35	0.88
YJR094W-A	RPL43B	2.35	0.88
YOR207C	RET1	3.34	0.86
YML010W	SPT5	4.02	0.81
YGR214W	RPS0A	3.13	0.79
YBL022C	PIM1	3.1	0.78
YGL031C	RPL24A	2.17	0.77
YLR009W	RLP24	2.2	0.77

Table 3.3. List of prey which had a SAINT probability score of 0.75 or higher in both Rex2 and Rex3 TAP-MS data sets

Common Name
TOD6
SET2
TAF6
SGF73
BAS1
ECM16
KRE2
MYO1
GCN5
TAF5
MPD2
HFI1
TIM44
TAF12
SSL1
SEC1
RTT103
NGG1
SPT7
ADA2
SPT3
EAF1
ARP4

RPS29B
ATP7
RTG3
CST6
SWC4
NOP53
NSP1
SPT5
GSP1
GSP2
RPS0A

Table 3.4. Gene Ontology (GO) enrichment analysis of exonic regions which increase 2-fold or more in the *rex1Δrex2Δrex3Δ* strain relative to wildtype. The p-value listed for each GO term represents the significance of the occurrence of the GO term in the provided list versus all the genes in the *S. cerevisiae* annotation database.

Gene Ontology	P-value
transposition, RNA-mediated	9.17E-16
transposition	6.65E-15
mitochondrial translation	2.47E-11
mitochondrion organization	2.40E-10
viral process	1.34E-09
viral life cycle	1.34E-09
viral release from host cell	1.34E-09
symbiosis, encompassing mutualism through parasitism	1.34E-09
DNA integration	1.97E-09
interspecies interaction between organisms	3.25E-08
RNA-dependent DNA replication	3.32652E-05
DNA biosynthetic process	0.000256393
tRNA aminoacylation for mitochondrial protein translation	0.000306349
cellular response to extracellular stimulus	0.000589645
cellular response to external stimulus	0.000589645
single-organism cellular process	0.000807007
single-organism process	0.000807528
mitochondrial respiratory chain complex assembly	0.001755965
cellular response to nutrient levels	0.001878078
carbon catabolite regulation of transcription from RNA polymerase II promoter	0.004036741
cytochrome complex assembly	0.005963919
generation of precursor metabolites and energy	0.007476869

oxidation-reduction process	0.012648835
response to extracellular stimulus	0.014785589
carbon catabolite regulation of transcription	0.017518057
RNA phosphodiester bond hydrolysis, endonucleolytic	0.026208983
mitochondrial RNA metabolic process	0.031810763
response to external stimulus	0.03400497
response to nutrient levels	0.044210779

Table 3.5. Gene Ontology (GO) enrichment analysis of exonic regions which decrease 2-fold or more in the *rex1Δrex2Δrex3Δ* strain relative to wildtype. The p-value listed for each GO term represents the significance of the occurrence of the GO term in the provided list versus all the genes in the *S. cerevisiae* annotation database.

GO term	P-value
cytoplasmic translation	4.00E-35
organonitrogen compound metabolic process	1.03E-25
organonitrogen compound biosynthetic process	4.32E-20
translational elongation	1.66E-13
hydrogen ion transmembrane transport	1.89E-10
respiratory electron transport chain	5.73E-10
electron transport chain	2.60E-09
peptide metabolic process	3.23E-09
proton transport	4.10E-09
ATP synthesis coupled electron transport	5.25E-09
mitochondrial ATP synthesis coupled electron transport	5.25E-09
hydrogen transport	5.40E-09
translation	5.45E-09
peptide biosynthetic process	6.88E-09
amide biosynthetic process	8.97E-09
cellular amide metabolic process	1.60E-08
oxidative phosphorylation	2.31E-08
monovalent inorganic cation transport	4.88E-08
nucleoside triphosphate metabolic process	7.79E-08
purine nucleoside triphosphate metabolic process	8.74E-08
ribonucleoside triphosphate metabolic process	1.27E-07
ion transmembrane transport	1.94E-07
purine ribonucleoside metabolic process	3.74E-07

ribonucleoside metabolic process	4.19E-07
purine nucleoside metabolic process	4.34E-07
purine ribonucleoside triphosphate metabolic process	5.16E-07
nucleoside metabolic process	1.0887E-06
purine nucleoside monophosphate metabolic process	1.9176E-06
purine ribonucleoside monophosphate metabolic process	1.9176E-06
ATP metabolic process	2.0786E-06
glycosyl compound metabolic process	2.0825E-06
alpha-amino acid biosynthetic process	2.558E-06
nitrogen compound metabolic process	2.9481E-06
mitochondrial electron transport, cytochrome c to oxygen	3.7974E-06
inorganic cation transmembrane transport	4.1841E-06
purine-containing compound metabolic process	4.3842E-06
nucleoside monophosphate metabolic process	4.46E-06
inorganic ion transmembrane transport	4.6446E-06
alpha-amino acid metabolic process	4.9697E-06
cation transport	6.3603E-06
purine nucleotide metabolic process	8.6882E-06
cellular amino acid biosynthetic process	9.8915E-06
cellular respiration	1.1204E-05
organic acid biosynthetic process	1.1547E-05
carboxylic acid biosynthetic process	1.1547E-05
small molecule metabolic process	1.8641E-05
ribonucleoside monophosphate metabolic process	1.8783E-05
cation transmembrane transport	2.0784E-05
ribonucleotide metabolic process	2.3762E-05
purine ribonucleotide metabolic process	2.7722E-05

ribose phosphate metabolic process	4.3252E-05
ion transport	5.0734E-05
ribosome biogenesis	6.1541E-05
nucleobase-containing small molecule metabolic process	0.0001004
nucleotide metabolic process	0.00014762
methionine metabolic process	0.00015507
nucleoside phosphate metabolic process	0.00022638
methionine biosynthetic process	0.00036382
cellular amino acid metabolic process	0.00048074
cellular biosynthetic process	0.00067919
biosynthetic process	0.00076791
aerobic respiration	0.00081044
sulfur amino acid biosynthetic process	0.00083922
sulfur amino acid metabolic process	0.00087402
organic substance biosynthetic process	0.00173536
ribonucleoprotein complex biogenesis	0.00320001
energy derivation by oxidation of organic compounds	0.00511839
oxidation-reduction process	0.00687679
ribosomal small subunit biogenesis	0.00830545
transmembrane transport	0.01565909
small molecule biosynthetic process	0.01617852
aspartate family amino acid biosynthetic process	0.01770097
leucine metabolic process	0.02845112
oxoacid metabolic process	0.03343121
organic acid metabolic process	0.03663945
aspartate family amino acid metabolic process	0.03696538

REFERENCES

Breitkreutz, A., Choi, H., Sharom, J. R., Boucher, L., Neduva, V., Larsen, B., ... & Tyers, M. (2010). A global protein kinase and phosphatase interaction network in yeast. *Science*, *328*(5981), 1043-1046.

Bruni, F., Gramegna, P., Oliveira, J. M. A., Lightowlers, R. N., & Chrzanowska-Lightowlers, Z. M. A. (2013). REXO2 Is an Oligoribonuclease Active in Human Mitochondria. *PLOS ONE, 8(5),* e64670

Callahan, K. P., & Butler, J. S. (2010). TRAMP complex enhances RNA degradation by the nuclear exosome component Rrp6. *Journal of Biological Chemistry*, *285*(6), 3540-3547.

Choi, H., Larsen, B., Lin, Z. Y., Breitkreutz, A., Mellacheruvu, D., Fermin, D., ... & Nesvizhskii, A. I. (2011). SAINT: probabilistic scoring of affinity purification-mass spectrometry data. *Nature methods*, *8*(1), 70-73.

Copela, L. A., Fernandez, C. F., Sherrer, R. L., & Wolin, S. L. (2008). Competition between the Rex1 exonuclease and the La protein affects both Trf4p-mediated RNA quality control and pre-tRNA maturation. *Rna*, *14*(6), 1214-1227.

Cudny, H., Zaniewski, R., & Deutscher, M. P. (1981). Escherichia coli RNase D. Catalytic properties and substrate specificity. *Journal of Biological Chemistry*, *256*(11), 5633-5637.

Gunderson, F. Q., & Johnson, T. L. (2009). Acetylation by the transcriptional coactivator Gcn5 plays a novel role in co-transcriptional spliceosome assembly. *PLoS Genet*, *5*(10), e1000682-e1000682.

Hanekamp, T., & Thorsness, P. E. (1999). YNT20, a bypass suppressor of yme1 yme2, encodes a putative 3′-5′ exonuclease localized in mitochondria of Saccharomyces cerevisiae. *Current genetics*, *34*(6), 438-448.

Haruki, H., Nishikawa, J., & Laemmli, U. K. (2008). The anchor-away technique: rapid, conditional establishment of yeast mutant phenotypes.*Molecular cell*, *31*(6), 925-932.

Ibrahim, H., Wilusz, J., & Wilusz, C. J. (2008). RNA recognition by 3′-to-5′ exonucleases: the substrate perspective. *Biochimica et Biophysica Acta (BBA)-Gene Regulatory Mechanisms*, *1779*(4), 256-265.

Jacobson, S. J., Laurenson, P. M., & Pillus, L. (2003). Functional analyses of chromatin modifications in yeast. *Methods in enzymology*, *377*, 3-55.

Kaiser, P., Meierhofer, D., Wang, X., & Huang, L. (2008). Tandem affinity purification combined with mass spectrometry to identify components of protein complexes. In *Genomics Protocols* (pp. 309-326). Humana Press.

Matos, R. G., Pobre, V., Reis, F. P., Malecki, M., Andrade, J. M., & Arraiano, C. M. (2011). Structure and degradation mechanisms of 3′ to 5′ exoribonucleases. In *Ribonucleases* (pp. 193-222). Springer Berlin Heidelberg.

Medina, D. A., Jordán-Pla, A., Millán-Zambrano, G., Chávez, S., Choder, M., & Pérez-Ortín, J. E. (2014). Cytoplasmic 5′-3′ exonuclease Xrn1p is also a genome-wide transcription factor in yeast. *Frontiers in genetics*, *5*.

Mellacheruvu, D., Wright, Z., Couzens, A. L., Lambert, J. P., St-Denis, N. A., Li, T., ... & Nesvizhskii, A. I. (2013). The CRAPome: a contaminant repository for affinity purification-mass spectrometry data. *Nature methods*, *10*(8), 730-736.

Midtgaard, S. F., Assenholt, J., Jonstrup, A. T., Van, L. B., Jensen, T. H., & Brodersen, D. E. (2006). Structure of the nuclear exosome component Rrp6p reveals an interplay between the active site and the HRDC domain.*Proceedings of the National Academy of Sciences*, *103*(32), 11898-11903.

O'Sullivan, J. M., Tan-Wong, S. M., Morillon, A., Lee, B., Coles, J., Mellor, J., & Proudfoot, N. J. (2004). Gene loops juxtapose promoters and terminators in yeast. *Nature genetics*, *36*(9), 1014-1018.

Ramachandran, V., & Chen, X. (2008). Degradation of microRNAs by a family of exoribonucleases in Arabidopsis. *Science*, *321*(5895), 1490-1492.

Reid, J. L., Iyer, V. R., Brown, P. O., & Struhl, K. (2000). Coordinate regulation of yeast ribosomal protein genes is associated with targeted recruitment of Esa1 histone acetylase. *Molecular cell*, *6*(6), 1297-1307.

Sayani, S., Janis, M., Lee, C. Y., Toesca, I., & Chanfreau, G. F. (2008). Widespread impact of nonsense-mediated mRNA decay on the yeast intronome. *Molecular cell*, *31*(3), 360-370.

Sayani, S., & Chanfreau, G. F. (2012). Sequential RNA degradation pathways provide a fail-safe mechanism to limit the accumulation of unspliced transcripts in Saccharomyces cerevisiae. *RNA*, *18*(8), 1563-1572.

Skowronek, E., Grzechnik, P., Späth, B., Marchfelder, A., & Kufel, J. (2014). tRNA 3′ processing in yeast involves tRNase Z, Rex1, and Rrp6. *RNA*, *20*(1), 115-130.

Steitz, T. A., & Steitz, J. A. (1993). A general two-metal-ion mechanism for catalytic RNA. *Proceedings of the National Academy of Sciences*, *90*(14), 6498-6502.

Sun, M., Schwalb, B., Pirkl, N., Maier, K. C., Schenk, A., Failmezger, H., ... & Cramer, P. (2013). Global analysis of eukaryotic mRNA degradation reveals Xrn1-dependent buffering of transcript levels. *Molecular cell*, *52*(1), 52-62.

Tan-Wong, Sue Mei, et al. "Gene loops enhance transcriptional directionality."*Science* 338.6107 (2012): 671-675.

van Hoof, A., Lennertz, P., & Parker, R. (2000). Three conserved members of the RNase D family have unique and overlapping functions in the processing of 5S, 5.8 S, U4, U5, RNase MRP and RNase P RNAs in yeast. *The EMBO journal*, *19*(6), 1357-1365.

Xu, Z., Wei, W., Gagneur, J., Perocchi, F., Clauder-Münster, S., Camblong, J., ... & Steinmetz, L. M. (2009). Bidirectional promoters generate pervasive transcription in yeast. *Nature*, *457*(7232), 1033-1037.

Zuo, Y., & Deutscher, M. P. (2001). Exoribonuclease superfamilies: structural analysis and phylogenetic distribution. *Nucleic acids research*, *29*(5), 1017-1026.

Zuo, Y., Wang, Y., & Malhotra, A. (2005). Crystal structure of Escherichia coli RNase D, an exoribonuclease involved in structured RNA processing.*Structure*, *13*(7), 973-984.